

Founders: The National Academy of Sciences of Ukraine

The E.O. Paton Electric Welding Institute of the NAS of Ukraine, International Association «Welding»

Publisher: International Association «Welding»

Editor-in-Chief B.E. Paton

Editorial board:

Yu.S.Borisov V.F.Grabin
Yu.Ya.Gretskii A.Ya.Ishchenko
V.F.Khorunov
S.I.Kuchuk-Yatsenko
Yu.N.Lankin V.K.Lebedev
V.N.Lipodaev L.M.Lobanov
V.I.Makhnenko A.A.Mazur
L.P.Mojsov V.F.Moshkin
O.K.Nazarenko V.V.Peshkov
I.K.Pokhodnya I.A.Ryabtsev
V.K.Sheleg Yu.A.Sterenbogen
N.M.Voropai K.A.Yushchenko
V.N.Zamkov A.T.Zelnichenko

Promotion group:

V.N.Lipodaev, V.I.Lokteva
A.T.Zelnichenko (exec. director)

Translators:

S.A.Fomina, I.N.Kutianova,
T.K.Vasilenko

Editor

N.A.Dmitrieva

Electron galley:

I.V.Petushkov, T.Yu.Snegireva

Editorial and advertising offices:

E.O. Paton Electric Welding Institute,
International Association «Welding»,
11, Bozhenko str., 03680, Kyiv, Ukraine
Tel.: (38044) 227 67 57
Fax: (38044) 268 04 86
E-mail: journal@paton.kiev.ua
http://www.nas.gov.ua/pwj

State Registration Certificate
KV 4790 of 09.01.2001

Subscriptions:

\$460, 12 issues per year,
postage and packaging included.
Back issues available

All rights reserved.

This publication and each of the articles
contained herein are protected by copyright.
Permission to reproduce material contained in
this journal must be obtained in writing from
the Publisher.

Copies of individual articles may be obtained
from the Publisher.

CONTENTS

PRESSURE WELDING

Kuchuk-Yatsenko S.I. and Zyakhov I.V.

Mechanism of bimetal joints formation in friction
welding 2

Tretyak N.G. Friction stir welding of aluminium

alloys (Review) 10

Pismenny A.S. and Prokofiev A.S. Press welding

of pipes using activating materials 19

**Kuchuk-Yatsenko S.I., Kachinsky V.S. and
Ignatenko V.Yu.** Magnetically-impelled arc butt

welding of thick-walled pipes 24

Kireev L.S. and Zamkov V.N. Solid-state joining of
titanium to steel (Review) 29

**Kharchenko G.K., Falchenko Yu.V.,
Novomlins O.A. and Gorban V.F.** Vacuum

diffusion bonding of chromium to copper 36

**Markashova L.I., Arsenyuk V.V.,
Grigorenko G.M. and Berdnikova E.N.** Mass

transfer processes in pressure joining of dissimilar
metals 38

INDUSTRIAL

Korotynsky A.E. State-of-the-art, tendencies and
prospects of development of high-frequency welding
converters (Review) 44



Pressure welding has found wide application in different industries and is an integral part of the technological process in highly mechanised fabrication, providing a high and stable quality of welded joints.

Achievements of modern electronic industry and information science open up broad capabilities for developing new power sources and systems of control of the processes of pressure welding, which allow a highly accurate adjustment of parts heating and control of the process of deformation of the parts being welded. Considerable progress is also observed in the field of development of the systems of diagnostics and control of the quality of joints by the results of measurement of the main parameters, influencing the joint quality.

Much more interest has been shown over the last years to applying various processes of pressure welding to join difficult-to-weld, bimetal and dissimilar materials. In this case this welding process opens up unique possibilities for producing high-quality joints, as the welds do not have the cast metal structure, and there is less probability of formation in the joint zone of various intermetallic phases, which adversely affect the indices of mechanical properties of welded joints.

The proposed issue of the journal presents a range of articles devoted to investigation of the processes of pressure welding of various high-strength and dissimilar materials.

Editorial Board

MECHANISM OF BIMETAL JOINTS FORMATION IN FRICTION WELDING

S.I. KUCHUK-YATSENKO and I.V. ZYAKHOR

The E.O. Paton Electric Welding Institute, NASU, Kyiv, Ukraine

Features have been studied of contact interaction of copper and steel 12Kh18N10T with AD1 aluminium alloy in friction welding. Regularities of friction surface displacement in time and dependence of the displacement magnitude on process parameters have been established. Influence was studied of the initial and final stages of the welding process on the processes of mass transfer in the butt and kinetics of early stages of formation of the intermetallic interlayer in welding of copper to aluminium. A new process of friction welding with controlled deceleration of rotation has been developed.

Key words: *friction welding, bimetal joints, heating, forging, rotation deceleration, displacement of friction surface, mass transfer, intermetallic interlayer, dynamics of rotation deceleration*

The main feature of friction welding of dissimilar metals and alloys is asymmetry of the temperature and deformation fields. In this case displacement of the friction surface towards the billet with a lower shear resistance at the welding temperature is observed [1, 2]. This phenomenon has been studied mostly in friction welding of different classes of steels [3–5]. Displacement of friction surface means that welding has already occurred over the initial contact surface, and the joint in this case may be imperfect. Continuation of the heating stage promotes reducing the number of defects due to high-temperature deformation in the initial contact zone. However, in welding reactive metals in a dissimilar combination, increase of the heating time may lead to an irreversible change of the phase composition and structure of the metal in the joint zone, related to formation of a brittle intermetallic interlayer.

The aim of the work was to study the features of contact interaction and the associated displacement of

friction surface in friction welding of dissimilar metals and to determine the dependence of the structural and phase changes on the thermo-deformational cycle of welding at different stages of the process.

Investigations were conducted for such material combinations as copper–aluminium (commercial AD1 alloy), steel 12Kh18N10T–AD1 (billets of 25 mm diameter). End faces of the billets were processed without using lubrication directly prior to welding up to the 6–7th class of roughness (GOST 2789–73), and no degreasing with organic solvents was performed.

Displacement of friction surface was studied in keeping with a procedure, envisaging instant separation of the billets during heating without interruption of rotation. In this case, fracture of the formed joint ran over the surface, characterised by minimal shear resistance (friction surface). Determination of friction surface displacement was conducted by measuring the thickness of the metal layer, transferred from one billet onto the surface of the other, with successive mechanical removal of this layer with a step of 0.01 mm. Experiments were conducted with the following fixed values of process parameters: circumferential speed $v = 0.75, 1.5, 2.0, 2.5$ m/s; heating pressure $P_h = 25$ and 50 MPa; heating time $t_h = 0.2, 0.5, 1.0, 2.0$ and 3.0 s.

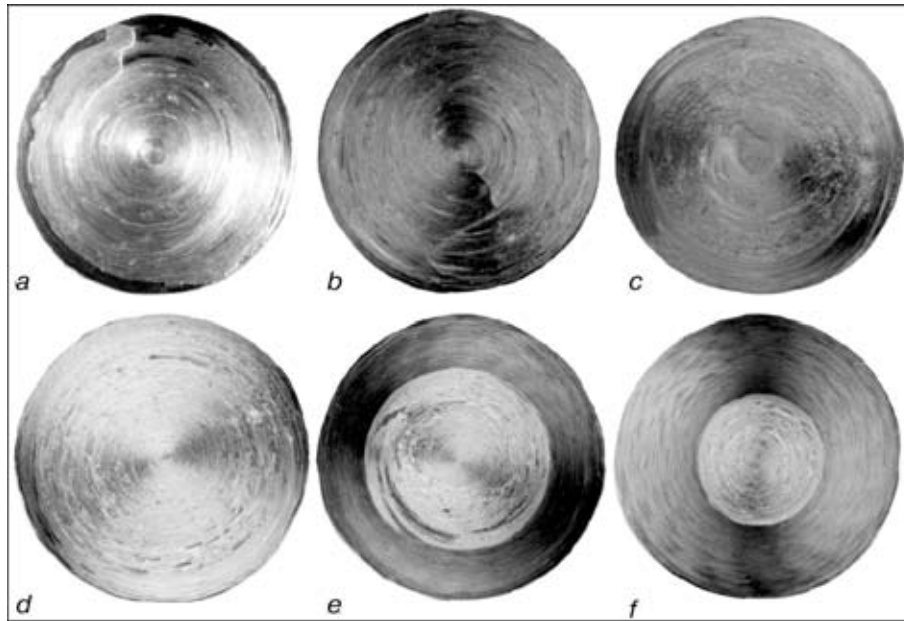


Figure 1. Surfaces of copper (*a-c*) and steel (*d-f*) billets after an instantaneous interruption of the process of their friction welding to aluminium AD1 after heating time 0.2 (*a*), 0.5 (*b*), 2.0 (*c*, *e*), 0.5 (*d*) and 3.0 s (*f*) at $P_h = 25$ MPa, $v = 0.75$ (*a-c*) and 2.0 m/s (*d-f*)

It is found that shifting of friction surface to one of the billets is observed in welding of the studied material combinations. However, the dynamics of change of displacement magnitude in time differs from that found in welding dissimilar steels [3–5]. Adhesion of the metal surfaces to each other and shifting of the friction surface to the aluminium billet occurs at the initial stages of the friction process, which is visually observed as aluminium spreading over a certain part of the section of a copper or steel billet. Displacement reaches a maximal value δ_{\max} after a certain time, which is followed by reverse displacement towards the initial contact and reaching the steady value of δ_{st} , which depends on the value of process parameters.

For a combination of materials copper–AD1 initial displacement is observed practically instantly after the surfaces of the rotating billets come into contact (Figure 1, *a-c*). At low values of circumferential speed and pressure ($v = 0.75$ m/s, $P_h = 25$ MPa), the magnitude of displacement at the initial stages of friction is considerable (Figure 2). Achievement of a steady-state value δ_{st} is observed after a time interval of more than 2.0 s. Value δ_{st} decreases with increase of pressure. At $v = 1.5$ m/s the displacement is significantly smaller, and reaches the steady-state value much faster, compared to $v = 0.75$ m/s. Further increase of rotation speed up to $v = 2.5$ m/s does not change the nature of the thermodeformational processes in the contact zone. For instance, it takes less, than 1.0 s to achieve the steady-state value of displacement δ_{st} . At interruption of the heating process after the above time the copper billet surface is covered by an extremely thin layer of aluminium, which is indicative of the completion of the process of adhesion of the surfaces being welded practically over the entire section.

Studying the dynamics of variation of the parameter of friction surface displacement over the billet section during heating for 12Kh18N10T–AD1 joints, it was found that displacement of the friction surface to the aluminium billet proceeds non-uniformly in different parts of the section being welded. Formation of an aluminium layer, transferred to steel, proceeds more intensively in a circular zone, located at a certain distance from the section centre. This distance decreases with the increase of the rotation speed and is equal to 0.4–0.7 of the billet radius in the studied range of parameter variation. Displacement of friction

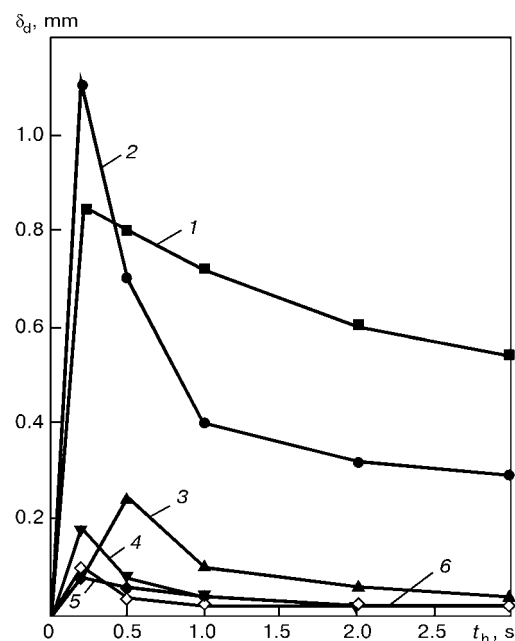


Figure 2. Dependence of the magnitude of displacement of friction surface δ_d on heating time t_h in welding of copper to aluminium: 1 – $v = 0.75$, $P_h = 25$; 2 – $v = 0.75$, $P_h = 50$; 3 – $v = 1.5$, $P_h = 25$; 4 – $v = 1.5$, $P_h = 50$; 5 – $v = 2.5$, $P_h = 25$; 6 – $v = 2.5$ m/s, $P_h = 50$ MPa



Table 1. Change in time of the magnitude of friction surface displacement δ_d maximal over the billet section for steel 12Kh18N10T–alloy AD1 joint

Rotation speed v , m/s	Heating pressure P_h , MPa	Heating time t_h , s				
		0.2	0.5	1.0	2.0	3.0
0.75	25	0.08	0.24	0.38	0.32	0.31
	50	0.16	0.34	0.28	0.26	0.20
1.5	25	0.12	0.20	0.14	0.08	0.06
	50	0.25	0.18	0.10	0.05	0.04
2.0	25	0.10	0.14	0.08	0.06	0.04
	50	0.10	0.07	0.05	0.03	< 0.02
2.5	25	0.06	0.05	0.03	0.02	< 0.02
	50	0.10	0.06	0.02	< 0.02	< 0.02

surface reaches the maximum magnitude in the above circular zone (Table 1). Reverse displacement of the friction surface initially proceeds in the peripheral regions of the section and then propagates to the central part (see Figure 1, $d-f$). Such a nature of the friction surface movement is, apparently, related to different intensity of heat evolution over the contact section, which is given by the dependence of the friction coefficient on time, rotation speed and pressure [6].

The obtained data on the change of displacement of friction surface in time are attributable to occurrence of two competing processes at the initial heating stage, namely strain hardening and thermally activated metal softening in the contact zone. The extreme nature of the change of friction moment in this period is indicative of the fact that the friction process is accompanied by in-depth pulling out, related to emergence and fracture of the sites of adhesion of the metals being welded.

Two circumstances are essential to emergence of in-depth pulling-out, namely formation of a strong bond between the two surfaces and presence of a negative gradient of mechanical properties [7, 8] through the depth from the contact surface. Meeting the above conditions is provided by appearance of adhesion bonding forces and work hardening of the surface layers of aluminium, i.e. formation in the contact zone of bonds with a strength higher than that of the more ductile metal (aluminium). As a result, at the initial stages of friction, the process of strain hardening prevails, and the surface with the minimal shear resistance (friction surface) shifts towards aluminium.

With the increase of heating time, the process of thermally activated softening predominates, the gradient of mechanical properties becomes positive and the friction surface shifts towards the surface of initial contact. As shown by the derived data, however, complete coincidence of these surfaces is not observed at transition to the steady-state friction process. An essential factor in this case is the strengthening impact of the harder copper (or steel) surface on the transferred layer of aluminium, resulting from manifestation of adhesion bonding forces. In the initial contact

zone the plasticised layer of aluminium is kind of strengthened, and at tangential displacement the rupture runs in-depth the layer.

Thus, the zone of maximal shear deformations is located at a certain distance from the initial contact surface, which distance is determined by the relationship of process parameters, namely the rotation speed and heating pressure. Reverse displacement of the friction surface results in development of a thin layer of plasticised metal (aluminium), which acts as a «lubricating material», and friction changes from dry to boundary friction. Achievement of the above stage coincides with lowering of the moment of friction in the butt. Interaction of the surfaces being welded during friction is focused in a certain volume of material with elasto-plastic properties. This material volume can be conditionally regarded as the «third body» [7].

To study the influence of displacement of the friction surface on the conditions of development of physical contact and activation of the surfaces being welded, processes of mass transfer in the butt were investigated, using the method of radioactive isotopes. Prior to welding the plane of one of the two billets being joined was electrolytically plated with a layer of radioactive isotope ^{63}Ni up to 1 μm thick. After welding the joint microsection was recorded on X-ray film and it was placed into a light-tight chamber. Exposure time was up to 200 h. Dependence of blackening density on isotope distribution in a specimen was determined by an autoradiogram in MF-4 micrometer. Obtained results (Figure 3) are indicative of the fact that in welding the isotope layer is not ousted completely into the flash, but remains in the butt, irrespective of which of the billets it has been deposited on prior to welding. Thus, no complete regeneration of the initial contact surface occurs during welding, and redistribution of the isotope layer over the billet section and depth is observed.

Maximum depth of isotope penetration is found at the distance of 0.4–0.7 of the billet radius and is between 110 and 140 μm . In the centre of the section the width of this zone is from 40 to 60 μm and on the periphery 30–50 μm . The above values are commensurate with the magnitude of displacement of friction surface at the heating stage, corresponding to the time of welding of the produced joints, which may be indicative of an interrelation of the isotope layer redistribution and friction surface displacements.

Obtained results account for numerous experimental data on the influence of the condition of the surfaces being welded on the quality of dissimilar metal welding. It is known [9] that disruption of the oxide and lubrication films is the necessary prerequisite for formation of valid metallic bonds of the two surfaces. Displacement of the friction surface from the initial contact surface and formation of a plasticised layer of aluminium leads to the layers of oxides or organic substances not being completely removed from the butt, but being redistributed in the joint zone, similar to ^{63}Ni isotope. In bend testing of joints, produced in welding billets after turning of end faces using a lu-

bricant (Figure 4, *a*, *b*) or with oxidized end faces (Figure 4, *c*, *d*), fracture proceeds, as a rule, in aluminium at 0.05–0.2 mm distance from the surface of the initial contact. Characteristic is the fact that variation of the welding mode parameters in a broad range does not provide sound joints of copper to aluminium through a layer of lubricant or a sufficiently thick oxide layer. In welding of billets with machined and degreased end faces a sound joint can only be produced in the case, if welding is performed not later than after a certain time. Therefore, there exists a boundary thickness of the oxide film, at which its mechanical disruption is possible, providing activation of the surfaces being welded.

Differences in the processes of contact interaction in friction welding of similar and dissimilar materials should be noted. For instance, by the data of [10] a layer of the isotope in friction welding of a similar combination of materials (low-carbon steel) at the initial period of heating is also redistributed over the billets section, but in further heating it is completely removed from the butt. This, probably, accounts for the negligible dependence of the quality of joints in similar materials on the condition of the surfaces being welded.

Conducted experiments lead to the conclusion that in friction welding of aluminium to copper and steel 12Kh18N10T at the final stage of the welding process (at forging) the joint is formed through a layer of plasticised metal along two different surfaces, namely surface of initial contact of the metals being welded and friction surface. Influence of process parameters on thermodeformational processes in the butt should be regarded in terms of optimisation of the conditions of physical contact development and activation of the surfaces being welded in the initial contact plane.

With any pressure welding processes the physical contact forms due to plastic deformation of the near-contact volumes of the materials being joined [11]. Therefore, preferable conditions are those, at which the displacement of friction surface is minimal.

Increase of circumferential velocity and heating pressure promotes lowering of the maximum and steady-state values of displacement and accelerates the process of reverse displacement of the friction surface. This, apparently, promotes activation of the surfaces being welded over the entire section of the billets. However, such a positive influence of increasing the values of the above process parameters on the deformation processes, proceeding in the butt, is lim-

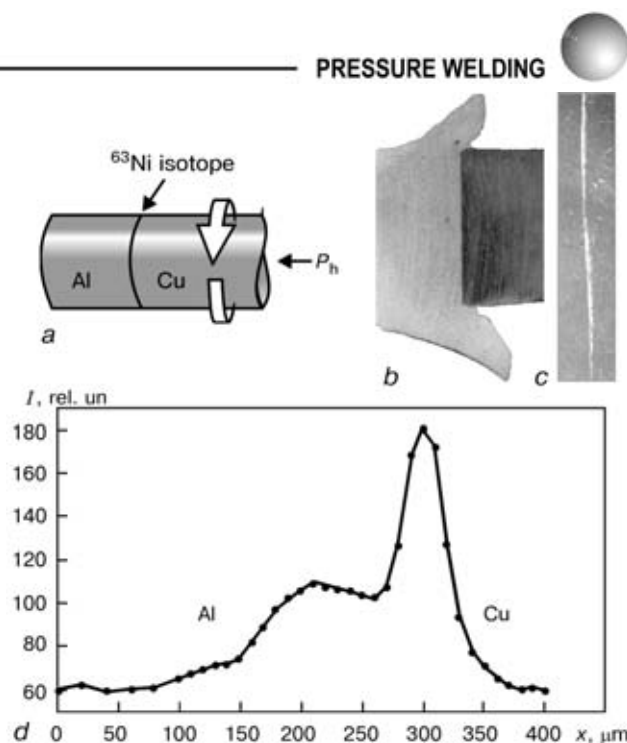


Figure 3. Studying mass transfer in friction welding of copper to aluminium, using ^{63}Ni isotope: *a* — schematic of conducting the tests; *b* — macrosection; *c* — autoradiogram of the joint; *d* — concentration profile of distribution of ^{63}Ni isotope; I — radiation intensity; x — depth of isotope penetration

ited by the ability of chemical interaction of the metals being welded.

It is known [1, 12–15], that increase of the rotation speed intensifies the process of formation of a brittle intermetallic interlayer in the butt. Therefore, a positive influence of increasing the rotation speed and heating pressure is, apparently, observed up to certain values and on condition of minimising the heating stage length. As the maximal intensity of shear deformation is found on the friction surface, and formation of the intermetallic interlayer proceeds over the surface of contact of the metals being welded, widening the zone of tangential deformation and involving into this zone the aluminium layer, transferred to the surface of the copper or steel billet, should be a priority at the final stage of the welding process. A criterion for correct selection of the magnitude and nature of change of the individual process parameters during welding may be the structure and phase composition of the joint zone, which are responsible for the mechanical and service properties of the bimetal transition pieces.

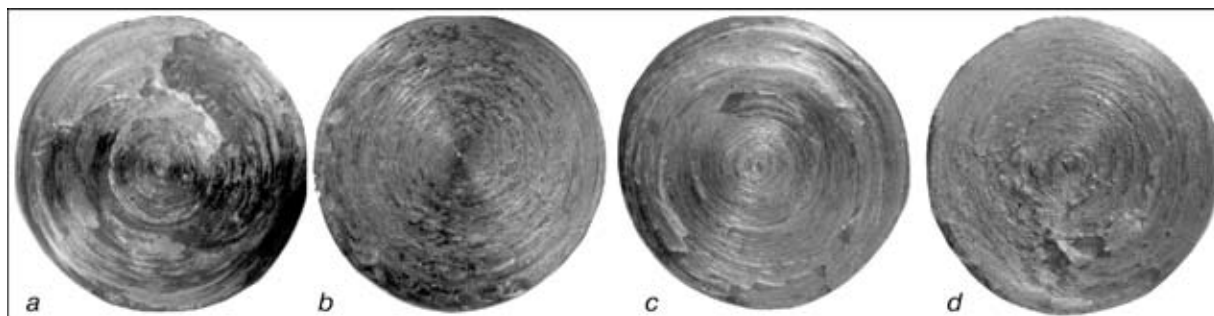


Figure 4. Surfaces of fractures from the side of the copper billet of joints of copper with aluminium, produced at turning, using lubrication 120 (*a*) and 0.5 h (*b*) before welding and turning without lubrication 120 (*c*) and 24 h (*d*) before welding

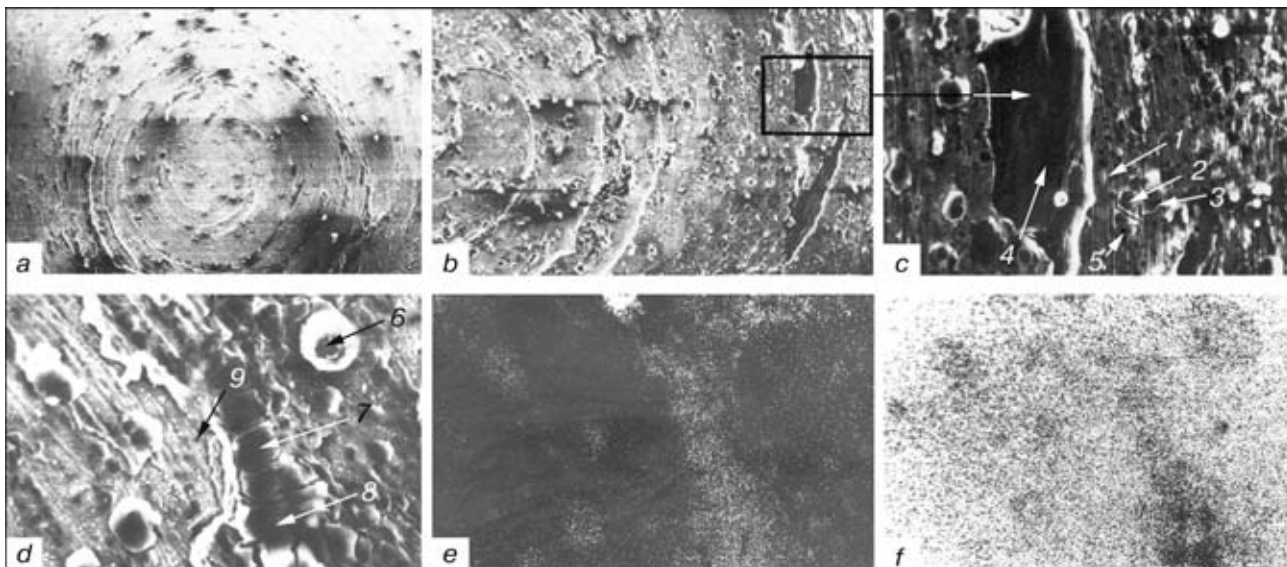


Figure 5. Surface of fracture from the side of the copper billet of a copper–aluminium joint, produced in mode 1: *a–c* — section centre ($\times 36$, $\times 150$, $\times 600$, respectively); *d* — peripheral part of the section ($\times 1200$); *e, f* — distribution maps of the peripheral part of the section on aluminium and copper, respectively ($\times 1200$)

Influence of the initial and final (deceleration and forging) stages of the welding process on the deformation processes in the butt, and formation of the structure and phase composition of a copper–aluminium joint were investigated. In order to study the mechanism of formation of a copper–aluminium joint at the early stages of contact interaction, mechanical testing by impact bending was conducted on joints, produced in the conventional welding process, characterized by fast deceleration of rotation (see Table 2, modes 1, 2). Value of heating time in mode 1 was approximately equal to achievement of the maximum value of displacement of friction surface. Fracture of specimens in mechanical testing proceeded over the surface of initial contact of copper with aluminium. Investigations of fractures were conducted, using electron microscopy analysis in SEM-515 system of Philips Company. The fracture surface from the side of the copper billet (Figure 5) reveals slip lines and individual dispersed particles of metal of stoichiometric composition, corresponding to solid solution of copper in aluminium and intermetallic compounds (mostly of CuAl_2 type, Table 3). Temperature measurements in welding copper to aluminium [13] show that at the initial stages of the friction process the rate of metal heating in the contact zone is about $10^3 \text{ }^\circ\text{C/s}$. It may be assumed that in individual points

of contact (in the places of formation and breaking up of friction bonds) the time to achieve the temperature of intermetallic phase formation may be equal to tens fractions of a second.

It is characteristic that particles of the above composition are found in different parts of the section (from central to peripheral part), differing greatly by the relative displacement rate and contact temperature. In other words, formation of intermetallic phases may be implemented in individual regions of the section already at the initial stages of contact interaction in a very short time interval.

Obtained results indicate that in friction welding the deformation impact on the metals being welded greatly increases the rate of diffusion processes running in the contact zone. Therefore, one of the main factors, influencing the formation and growth of the intermetallic interlayer is the length of the heating stage, and the conditions for minimising the thickness of this interlayer will be determined by the magnitude and rate of axial and shear deformation at the forging stage.

Considering the results of studying the movement of friction surface, it may be assumed that fast deceleration of rotation in welding in mode 1 allowed fixing the early stages of displacement of friction surface into the aluminium billet. Apparently, adhesion of the surfaces being welded was limited to individual regions of the billets section, and the processes of stress relaxation and heterodiffusion did not become well enough developed, which resulted in low mechanical properties of the joint.

Continuing the heating stage up to 0.8 s at a set rotation speed practically corresponds to completion of the process of reverse displacement of friction surface and formation in the contact zone of a thin layer of plasticised aluminium («third body»). Investigation of the microstructure of the joint produced at fast deceleration of rotation (see Table 2, mode 2), reveals the presence of an intermetallic interlayer, which is formed in contact of a plasticised aluminium layer with the copper billet surface (Figure 6, *a*). A

Table 2. Results of impact bend testing of joints of copper with aluminium ($P_h = 5 \text{ MPa}$, $P_f = 100 \text{ MPa}$, $v = 1.9 \text{ m/s}$)

Mode No.	Heating time, s	Upsetting in forging, mm	Upsetting speed in forging, mm/s	Bend angle α , deg	Remarks
1	0.4	1.5	1.9	2	Conventional welding
2	0.8	2.5	3.5	30	
3	0.4	5.8	9.8	90 (without fracture)	Welding with controlled deceleration of rotation
4	0.8	6.9	11.2	Same	

**Table 3.** Phase composition (%) of metal particles in different points of the surface of friction of copper and aluminium

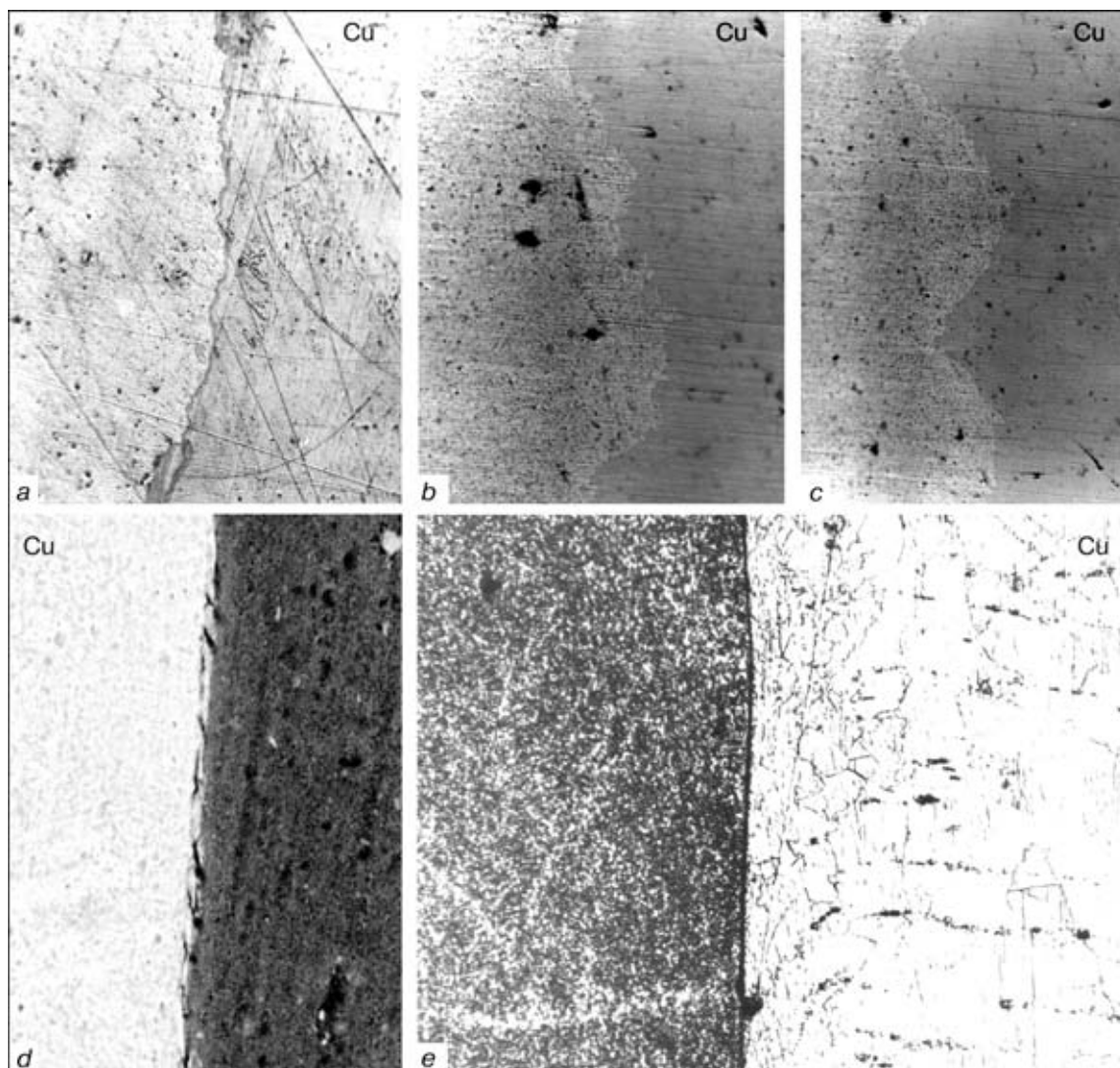
Point No.	1	2	3	4	5	6	7	8	9
Al	3.3	44.5	44.6	97.0	30.1	1.67	41.8	52.9	1.8
Cu	96.7	55.5	55.4	3.0	69.9	98.23	58.2	47.1	98.2

small magnitude and low rate of upsetting in forging, applied to non-rotating billets predominantly due to the radial component of deformation, is indicative of an absence of a sufficient temperature gradient in the joint zone.

Thus, formation of intermetallic interlayer in heating proceeds before the temperature gradient, required for forging, has been reached. The method, usually chosen to provide the required extent of joint plastic deformation of the metals being welded with the conventional process, is enhancement of the role of the thermal channel of activation of the surfaces being welded. For this purpose the heating time [14] is increased, this promoting achievement of the required temperature gradient, while inevitably leading, however, to a growth of the intermetallic interlayer. Partial ousting of this interlayer is achieved by a signifi-

cant increase of the forging pressure in combination with forced formation of the butt joint [14, 15]. It is problematic to provide a high stability of the indices of welded joint ductility with such an approach.

Analysis of the investigation results demonstrates, that formation of a continuous intermetallic interlayer in welding of bimetal joints can be prevented on condition of minimizing the duration of the heating stage and finding a method to intensify shear deformation over the surface of the initial contact at the forging stage. To intensify the deformation impact at the final stage of the process a method of friction welding with a controllable deceleration of rotation has been developed. Application of the forging force at the stage of rotation deceleration provides a simultaneous action of the axial and tangential components of deformation on the aluminium layer, transferred to the

**Figure 6.** Microstructure of the zone of copper-AD1 joint: *a* — mode 2 ($\times 400$); *b* — mode 3, section centre ($\times 500$); *c* — mode 3, peripheral section ($\times 1000$); *d, e* — mode 4 ($\times 950$ and $\times 200$, respectively)

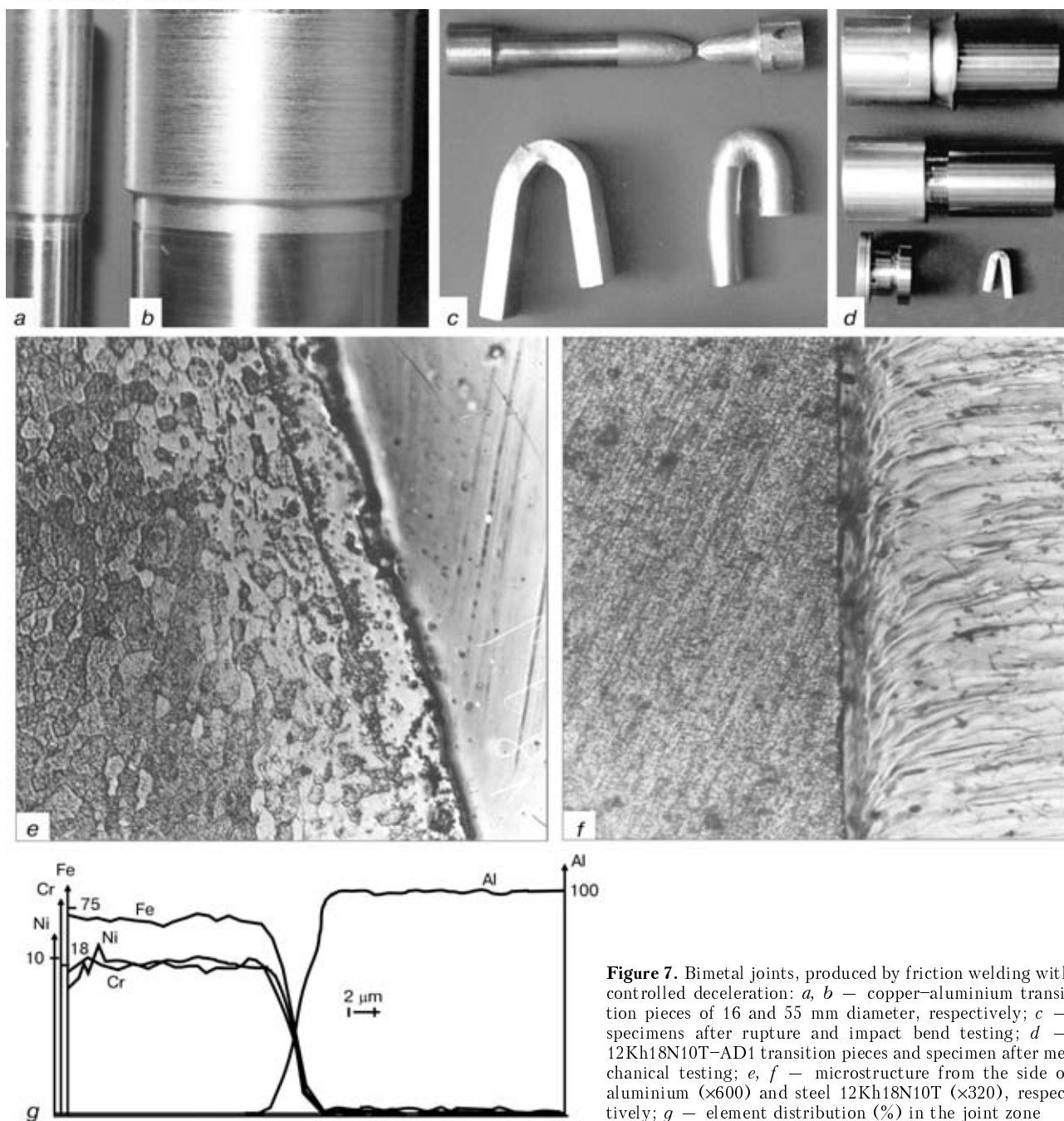


Figure 7. Bimetal joints, produced by friction welding with controlled deceleration: *a, b* — copper-aluminium transition pieces of 16 and 55 mm diameter, respectively; *c* — specimens after rupture and impact bend testing; *d* — 12Kh18N10T-AD1 transition pieces and specimen after mechanical testing; *e, f* — microstructure from the side of aluminium ($\times 600$) and steel 12Kh18N10T ($\times 320$), respectively; *g* — element distribution (%) in the joint zone

copper billet, and promotes intensification of shear deformation over the initial contact surface. The joint forms under the conditions, characterized by prevalence of the deformation channel of activation of the surfaces being welded.

It is known that the basic characteristic of the metal condition at high-temperature deformation is not the deformation, but its rate [11, 16]. Intensification of the diffusion processes at high-temperature plastic deformation is the consequence of increased distortion of the crystalline lattice and development of a large number of various defects of the crystalline lattice. Analysis of oscillograms of the friction process with controlled deceleration shows that an abrupt increase of upsetting speed (3 to 7 times compared to the heating stage) is found in the contact zone at the

deceleration stage, as a result of widening of the zone of tangential deformations. Upsetting, produced by the joint action of the compressive and tangential stresses, promotes intensification of shear deformation and activation of the diffusion processes over the surface of initial contact.

Microprobe analysis (Cameca SX-50 microanalyser), optical («Neophot-32») and scanning electron microscopy analysis (SEM-515 unit) were conducted to study the structure and phase composition of the joints, produced at programmed deceleration of rotation (see Table 2, modes 3 and 4). Optical microscopy was performed on angle unetched sections (angle of 11.5°), electronic microscopy on sections, made using ion polishing and etching in JEOL Ion Sputter JFC-1100 unit.



Diffusion of copper into aluminium to the depth of 3 μm is noted in the contact zone of the joint made in mode 3 (see Table 2). Formation of a solid solution of copper in aluminium of a variable composition is characteristic for the transition zone structure. No intermetallic layer is found in the butt, the joints having high indices of strength and ductility (see Figure 6, *b, c*). In mechanical rupture and impact bend testing no fracture is observed in the joint zone (Figure 7).

In the zone of the joint (see Table 2, mode 4), for which the heating time was approximately equal to achievement of the steady-state value of displacement of the friction surface, a diffusion zone up to 4 μm wide of the stoichiometric composition, corresponding to solid solution of copper in aluminium (see Table 2) and an interlayer of the composition of 19–40 % Cu and 60–80 % Al 1.3–2.0 μm wide are found from the aluminium side (see Figure 6, *d, e*). Fine-grained structure of copper and aluminium in the joint zone is indicative of the effect of dynamic forging, promoting refinement of the structure and increase of metal strength.

Thermal cycle of welding by the new technology is characterised by a high intensity and precise dosing of energy input into the butt, this promoting achievement of a high temperature gradient in the joint zone. This provides a high rate of cooling of the joint zone, allowing the forging time to be reduced 1.5 to 2 times, compared to the conventional process.

In joints of 12Kh18N10T–AD1, produced in welding with a controlled deceleration of rotation, the intermetallic interlayer is not found (Figure 7, *e–g*). The transition zone structure from the aluminium side reveals a zone of iron diffusion in aluminium 3 to 5 μm wide. A structure of fine-grained aluminium is further observed, the size of aluminium grain in the near-contact zone becoming smaller with the increase of pressure and reduction of the deceleration dynamics. A layer of steel 12Kh18N10T about 100 μm wide, which is adjacent to the joint line, is plastically deformed. Bending of δ -ferrite bands is observed in the near-contact region, which is indicative of intensive shear deformation in the contact zone during welding.

Optimisation of the parameters of the new process of friction welding is reduced to determination of a rational duration of the heating stage at a constant rotation speed and assigning the optimal dynamics of deceleration of rotation in the forging stage. A criterion of optimisation of the dynamics of deceleration of rotation in welding by the developed technology is provision of a certain rate of axial deformation with preservation of a high level of power of heat evolution in the contact zone.

CONCLUSION

At the initial moment of friction in welding of copper and steel 12Kh18N10T to aluminium, displacement of friction surface towards the aluminium billet is observed, its magnitude depending on the rotation speed and pressure in heating. At this stage of contact

interaction the prevailing processes are those of strain ageing, accompanied by formation of a zone of volume interaction in the form of solid solutions and dispersed phase precipitates of the metals being welded.

With the increase of heating time, the process of thermally activated softening prevails, and reverse displacement of the friction surface is observed. The magnitude of displacement reaches the steady-state value δ_{st} .

Interaction of the surfaces being welded at friction is concentrated in a certain volume of material (having elasto-plastic properties), which may be conditionally regarded as the «third body». Displacement of friction surface and formation of the «third body» predetermine the impossibility of complete ousting from the zone of initial contact of surface layers of materials and, therefore, the need for a thorough preparation of the surfaces being welded.

Main factors, influencing the formation of an intermetallic interlayer, are the duration of the heating stage, magnitude and rate of axial and shear deformation at the forging stage. In forging, provided by simultaneous action of the compressive and tangential stresses, an abrupt increase of upsetting speed is observed and intensification of shear deformation over the surface of initial contact is provided.

A new process of friction welding with a controllable deceleration of rotation has been developed, which allows in welding of bimetal joints limiting the intermetallic phase formation to its initial stages and producing joints with stable high indices of strength and ductility.

1. Lebedev, V.K., Chernenko, I.A. (1992) Friction welding. *Welding and Surfacing Rev.*, Vol. 4. Harwood A.P.
2. Lebedev, V.K., Mirgorod, Yu.A., Tsurul, I.A. (1993) Peculiarities of friction welding of Br.012 bronze with 40Kh steel through intermediate copper interlayer. *Avtomatch. Svarka*, **4**, 11–14.
3. Chernenko, I.A., Mirgorod, Yu.A., Simonov, V.I. et al. (1988) Friction welding of bimetallic shafts of axial-piston hydraulic machines. *Ibid.*, **3**, 46–48.
4. Fukakusa, K., Satoh, T. (1981) Travelling phenomena of rotational plane during friction welding. *J. JWS*, **10**, 7–12.
5. Mitelea, I., Bogdan, R. (1994) Mass transfer processes in case of dissimilar materials friction welding. *Sudura*, **2**, 1–4.
6. Lebedev, V.K., Chernenko, I.A. (1984) Distribution of power in friction welding joint. *Avtomatch. Svarka*, **12**, 23–25.
7. Kragelsky, I.V., Dobychin, M.N., Komalov, V.S. (1977) *Principles of calculation of friction and wear*. Moscow: Mashinostroenie.
8. Kragelsky, I.V. (1962) *Friction and wear*. Moscow: Mashgiz.
9. Gelman, A.S. (1970) *Principles of pressure welding*. Moscow: Mashinostroenie.
10. Lebedev, V.K., Kharchenko, G.K., Prodan, S.K. et al. (1979) Investigation of inertia friction welding process using radioactive isotopes. *Avtomatch. Svarka*, **8**, 74–75.
11. Karakozov, E.S. (1986) *Pressure welding of metals*. Moscow: Mashinostroenie.
12. Jessop, T.J., Nicholas, E.D., Dinsdale, W.O. (1978) Friction welding dissimilar metals. In: *Proc. of 4th Int. Conf. on Advances in Welding Processes*, Harrogate, May 9–11.
13. Zyakhov, I.V., Kuchuk-Yatsenko, S.I. (2001) Peculiarities of formation of friction welded joints between copper and aluminium. *The Paton Welding J.*, **9**, 24–29.
14. Shternin, L.A., Prokofiev, S.N. (1961) Friction welding of aluminium to steel and copper. *Svarochn. Proizvodstvo*, **11**, 30–32.
15. Nicholas, E.D. (1975) Friction welding of copper to aluminium. *Metal Constr.*, **3**, 135–141.
16. Larikov, L.N., Ryabov, V.R., Falchenko, V.M. (1975) *Diffusion processes in the solid phase in welding*. Moscow: Mashinostroenie.



FRICITION STIR WELDING OF ALUMINIUM ALLOYS (REVIEW)

N.G. TRETYAK

The E.O. Paton Electric Welding Institute, NASU, Kyiv, Ukraine

Considered are main principles of realisation of a new method for friction stir welding (FSW), allowing production of various joints in sheet billets. Designs of the tools for realisation of FSW, peculiarities of formation of the joints in different aluminium alloys, their properties and structure, application fields, equipment for FSW of various structures, quality control methods and methods for elimination of specific defects are described.

Key words: *aluminium alloys, friction stir welding, tools, applications, properties, structure, softening*

In December 1991, TWI, Great Britain, patented a new friction welding technique, which allowed butt and overlap joints to be produced in sheet blanks [1–3]. This technique was conditionally called friction stir welding (FSW), so as to distinguish it from the multitude of other existing friction welding processes [3–5]. Other names were also suggested, in particular in [3], it was recommended to call it a process with a higher reactivity (activation) on the interface.

With this technique the process of welding (Figure 1) proceeds as follows. A special rotating tool, consisting of a thicker part (shoulder) and protruding part (pin), in the butt area is brought into contact with the surface of blanks to be welded, which are fastened on a massive substrate, so that the pin would enter the blanks and the shoulder would touch their surface. Friction of the pin and the shoulder against a blank results in evolution of heat, which brings the metal surrounding the tool into a plasticised condition. Then the tool is imparted translational movement at the speed of welding, and the material of the blanks, moving from the heating to the cooling zone by-passes the pin to form a joint.

In terms of the nature of proceeding of the joining process, this technique has many features in common with pressing. Since aluminium alloys are favourable materials in this respect, FSW has been chiefly real-

ized for aluminium and its alloys. In the opinion of the developers, FSW technique has the following main advantages [6–10]:

- no fumes, noise or ultraviolet radiation are generated during welding;
- ability to produce welds without porosity in any aluminium alloy, including alloys, sensitive to porosity (Mg-, Li-containing alloys, etc.);
- absence of filler metal or shielding gas;
- no need to give any special profile to the edges or remove the oxide film before welding;
- ability to produce joints in all positions in space;
- welding process is ideally suited to automation;
- no high qualifications of the operator are required;
- relative simplicity of the equipment allows achieving high effectiveness of power utilization, as performance of single-pass welding of 12.5 mm aluminium alloy of 6000 series requires just 3 kW all in all;
- welding can be performed in strong magnetic fields, for instance, in joining busbars.

A low level of deformations and high reproducibility of the quality of welds, produced by FSW, promote an improvement of the existing welded structures of aluminium alloys. Thus the following technological capabilities are provided:

- welds may be produced in alloys, which cannot be made by fusion welding because of hot cracking susceptibility;
- higher level of strength can be achieved for heat-hardenable alloys;
- weld formation in the solid phase allows preserving the properties in metastable alloys, such as composites or alloys, produced by rapid solidification;
- large panels may be made, consisting of numerous small-sized sections, which it is practically impossible or not cost-effective to extrude or cast;
- light-weight extruded panels may be connected without distortions to produce superlarge structures of ships, flat-cars or heavy trucks;
- simpler semi-finished products, produced by casting or extrusion, may be joined to create hollow blanks;
- weldments with butt and overlap welds may be produced from blanks, made by various technologies (casting, extrusion, etc.);
- butt assembly does not require a very accurate fit-up of the edges, as for sheets of 1.6 mm thickness

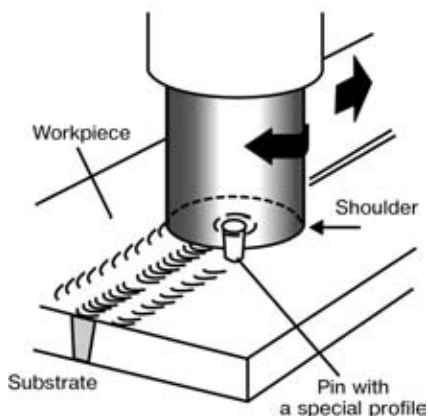


Figure 1. Schematic of FSW

© N.G. TRETYAK, 2002

the gap may up to 0.2 mm and for plates 12.7 mm thick up to 1.25 mm.

The following may be regarded as the disadvantages of FSW technique [6]:

- need for strong substrates, to which the blanks to be welded should be reliably fastened;
- formation at the end of the weld of a hole, equal to the pin size, which is to be filled using other methods, such as welding-in of special plugs by the friction process;
- application of run-on and run-off tabs to produce extended welds for the entire length of the blanks;
- limitations for application of the welding process in the portable variant, because of the need to fasten the blanks to the substrate;
- lower level of welding speed, compared to mechanized arc welding for some alloy grades.

Main parameters of FSW technique are [11] welding speed (tool displacement speed), tool rotation frequency, clamping force and tool displacement force, angle of tool inclination and its dimensions. In addition, friction conditions are taken into account, depending on the applied tool material and material being welded, as well as yield stress of the blank material at deformation temperature.

Since major FSW research is of a commercial nature and is funded through the so-called Group Sponsored Projects, technological information in publications is limited and chiefly relates to speeds of welding and tool rotation [11, 12]. Works [12, 13] give the values of welding speed and frequency of the working tool rotation (Figure 2), which allow producing sound joints for alloys of series 5000 and 6000. As is seen from Figure 2, alloys of 6000 series may be welded in a broader range of welding modes, than alloys of 5000 series.

Types of joints, produced by FSW, are characterized by a great diversity, namely these are the butt, fillet tee and overlap joints, traditional for arc welding (Figure 3), as well as all kinds of lock and slot (Figure 4) welds [14, 15].

Special attention in FSW development was given to design of the rotating tool, responsible for joint formation, which is confirmed by a great number of patents and publications. In [16] a tool was proposed, in which several planes were made along the pin length so, that it may have a cross-section in the form of a polygon and the plane may be coiled into a spiral strip on the pin surface. Other variants envisage making on the pin radial protrusions of an aerodynamic shape, transverse and longitudinal notches, protrusions of various length and shape on the pin end face,

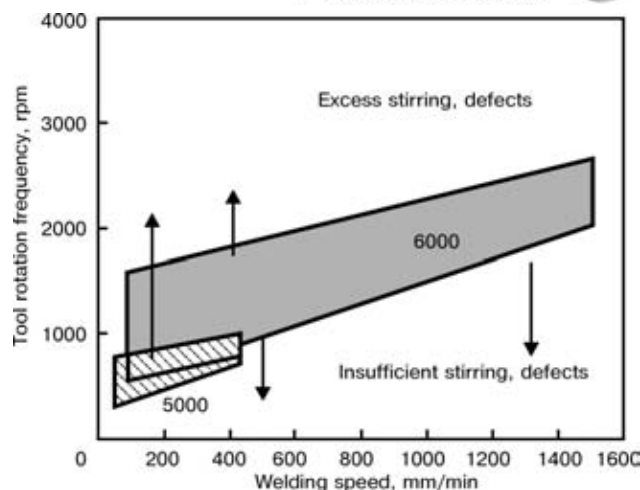


Figure 2. Ratio of welding speed and tool rotation frequency, producing sound joints in 5 mm aluminium alloys of 5000 and 6000 series

etc. Some of these tool variants are given in Figure 5. Authors of [17] developed a composite tool, in which the pin is inserted into the shoulder body and may be easily replaced by another (Figure 6). To intensify the flow of plasticised metal the shoulder is made in the form of a concave surface, and the pin has a threaded surface or, which is preferable, two or several protruding ribs. The tool, which simultaneously acts also as the substrate for the blanks being joined [18, 42], is called bobbin tool (Figure 7).

A design with pin length and shoulder diameter, controllable during welding, expands the technological capabilities of the working tool (Figure 8) [19]. This allows welding blanks of a variable cross-section at the weld end and avoid formation of a hole at the weld end, when circumferential welds are made. This was the basis to implement a programmable welding cycle, when a smooth transition to achievement of full penetration and completing the process without formation of a hole are provided by changing the pin length from zero up to a value, equal to the thickness of the blanks being welded.

For a reliable pressing of the shoulder to the surface of the blanks being welded and, thereby providing a constant thermal mode in the welding zone, a working tool design (Figure 9) with a mobile shoulder, which continuously is in a spring-loaded state with a specified force [20], was developed.

A design of the tool with cooling of its external side [21] by circulating a coolant (water) or blowing it with air was proposed to reduce metal sticking to the pin and remove excess heat in welding some high-

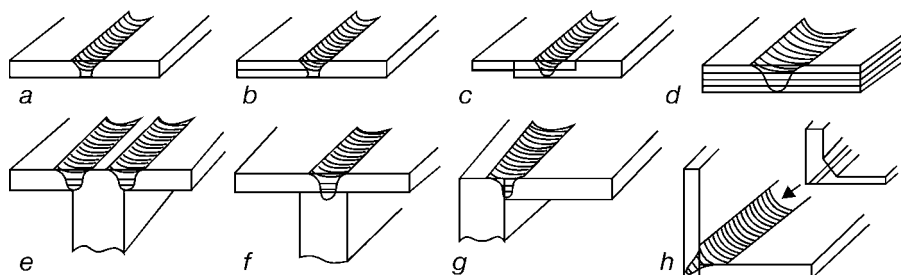


Figure 3. Types of the joints, made by FSW: *a* – butt; *b* – butt-overlap; *c* – overlap; *d* – multilayer overlap; *e* – two-pass tee; *f* – tee slot; *g*, *h* – fillet

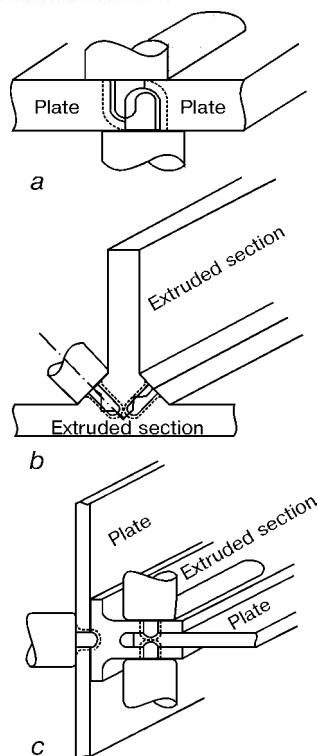


Figure 4. Variants of FSW joints of various semi-finished products: *a* – two-sided butt lock; *b* – fillet lock; *c* – slot joint

strength aluminium alloys (Figure 10, *a*). There also exist design variants, when the coolant is fed along channels, located inside the tool (Figure 10, *b*).

FSW of blanks of alloy 6082-T6 up to 50 mm thick in one pass and up to 75 mm thick from both sides became possible due to development of tools of Whorl™ and MX Triflute™ family [22, 23].

Profile of the developed Whorl™ working tool (Figure 11) is similar to a long conical sea shell in its outline. Despite some differences, the main design is developed so, that the pitch and angle of inclination of the profile are changed simultaneously, and thus the process of FSW of different aluminium alloys and thicknesses is optimized (Figure 12). The tool with MX Triflute trade mark (Figure 13) allows welding blanks of 6 to 50 mm thickness in one pass [23]. It has a pin in the form of a figure, limited by two parallel planes with three grooves and a special thread between them. Such a shape of the pin has a greater surface, compared to the cylindrical pin, and provides welding at a smaller (by about 70 %) amount of the displaced metal. Several concentric grooves are made in the shoulder to improve metal transfer.

TWI has recently developed a variant of FSW process, the so-called Skew-Stir technique [24], which uses a special A-Skew™ tool with a pin (Figure 14), which is fastened in a driven axle at a small angle so, that the intersection of the axes of the axle and the tool, which was called the focal point, may be located above, under or directly in the blank being welded, depending on material properties and mode parameters. A-Skew™ pin allows increasing the ratio of the dynamic to static volume, i.e. increases the volume of the metal plasticised during this time around the tool.

There is no doubt that information on new modifications of the tool may appear in the near future.

Properties of aluminium alloy joints, produced with FSW, are at a sufficiently high level. Studies [11, 17, 25, 26] give the results of mechanical testing of welded joints in extruded blanks of alloys of 5000, 6000 and 7000 series. For different thickness and welding conditions the strength of as-welded alloy AA6082-T6 is equal to 70 % of base metal strength. Artificial ageing after welding restores the strength up to 90 % of the initial value. In this case ductility indices are on the level of those of the base metal. Authors of [26] note that for alloy AA6082 in T6 condition before welding, relative elongation of the joints after welding and after artificial ageing is almost 2 times lower than that of the base metal. Proceeding from these considerations, it is recommended to use T4 mode of base metal heat treatment.

For alloy AA7108 the strength properties of the joints of metal 2–7 mm thick after welding and after artificial ageing are ≈ 86 and 94 % of base metal strength, respectively. According to [27], the coefficient of strength of welded joints for alloy 2014A-T6 is 80, that for alloy 7075-T7351 is 70 %.

Strength properties of the joints of alloys of 5000 series [25] in the range of thicknesses of 6–15 mm and welding speeds of 0.76–2.20 mm/s are between 303 and 344 MPa, which is much higher than for 6000 alloys.

Authors of [28] studied the mechanical properties of the joints of alloy 7075-T651, produced by FSW. It is found that the strength properties of the joints are inferior to those of the base metal, but are higher than similar properties, produced with other processes. Subsequent artificial ageing does not permit recovering the strength, and ductility properties decrease in this case. Joints fail in the HAZ in the area of a pronounced coarsening of the structure. Work [28] also gives the properties of a joint in the zone of the nugget. Specimens were cut out in the direction

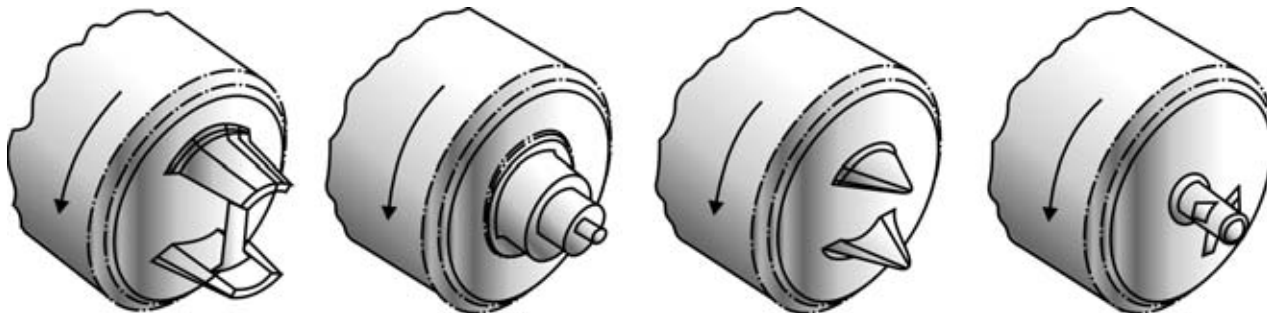


Figure 5. Variants of tool design for FSW

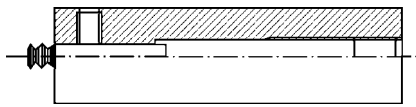


Figure 6. Design of a composite working tool

along the weld. It is found that the ductile properties after welding are on the level of those of the base metal, and strength indices are lower than those of the base metal, but higher than for the joints. Strength decrease in the nugget zone [28] is associated with refinement of thin strengthening particles and reduction of the number of dislocations.

Analysis of the data of fatigue testing of aluminium alloy joints, produced by FSW, demonstrated that their performance in many cases is higher than that of the joints, produced by fusion welding, and the scatter of values is smaller [7, 15, 29, 30]. Results of testing single-pass welded joints of 6 mm sheets of alloys 5083-0 and 2014-T6 (Figure 15) were higher and had smaller scatter of values than for two-pass joints, produced by TIG or MIG welding processes, which are specified by BS 8118 norms, class 35 and European recommendations B3 for joints, produced by fusion welding [15]. Fatigue properties of FSW joints in alloys 6082-T5 and 6005-T4 at cycle asymmetry factor R , equal to -1 [17], are close to those of the base metal, and are much higher than for other welding processes, in particular, MIG and plasma welding with through-thickness penetration.

It is known that microstructural features of the joints are dependent on the thermal cycle of welding. For this purpose, temperature fields at FSW were measured, using thermocouples [26]. As is seen from Figure 16, FSW is characterized by quite high temperature gradients, and heating temperature maximum of about $500\text{ }^{\circ}\text{C}$ exists for a very short time. Temperature interval of $200\text{--}300\text{ }^{\circ}\text{C}$, which determines the HAZ dimensions, is not more than several seconds either. This confirms the fact that the level of joint properties is higher at FSW due to a smaller degree of softening.

Close values of maximal temperatures on the level of $500\text{ }^{\circ}\text{C}$ are also recorded by other researchers [28, 31] in welding of alloy 7075-T651 and alloy 6N01 of Al-Si-Mg system.

Studies [32, 33] give the results of mathematical modelling of thermal processes in FSW, using traditional approaches to describe the temperature fields of moving heat sources, as well as the finite differences method. Derived equations allowed calculating with a certain accuracy the maximal temperature under the tool and thermal cycles in the HAZ metal, which correlate well with the experiment.

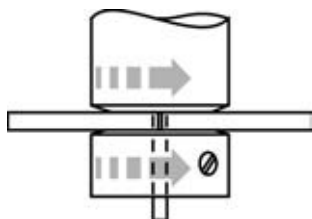


Figure 7. Schematic of the tool in the form of a bobbin (bobbin tool)

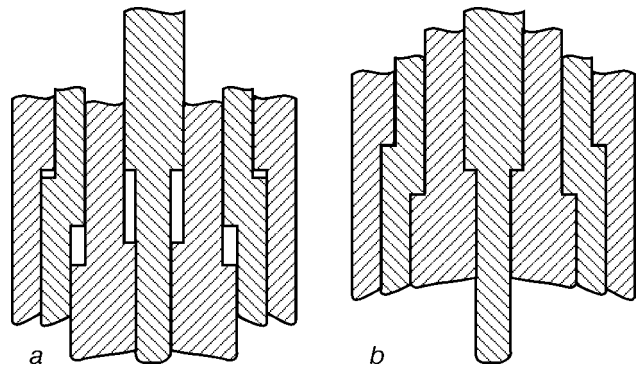


Figure 8. Schematics of the design of the working tool with a controllable length of the pin, minimal (a) and maximal (b) diameter of the shoulder

Comparison of hardness distribution in the joints of alloy 6N01, produced by MIG and FSW processes, demonstrated, that the degree of softening in the HAZ metal decreases markedly in FSW joints [31].

Hardness variation in butt joints of alloys 5083-0, 2014A-T6, 7075-T7351 (Figure 17) is characterized by an increase of the index in the nugget zone and presence of annealed sections in the HAZ metal for heat-hardenable alloys. Softening zone is equal to $\approx 30\text{ mm}$ to the side from the weld center.

Macrostructure of FSW welds has certain features, which are not typical for welds, produced by fusion welding processes, in particular TIG or MIG. The main difference is formation of a nugget in the joint center [34], which, irrespective of the alloy, contains the so-called annual rings (Figure 18), i.e. concentric oval rings, differing in their macrostructure.

As is seen from Figure 18, the shape of weld nugget is somewhat different, depending on the alloy. Adjacent to the nugget is a complex profile, which forms the weld upper part, and which is somewhat wider than the tool shoulder diameter. Nugget diameter is slightly greater than that of the tool pin, and it is, as a rule, located in the joint lower part. Significant

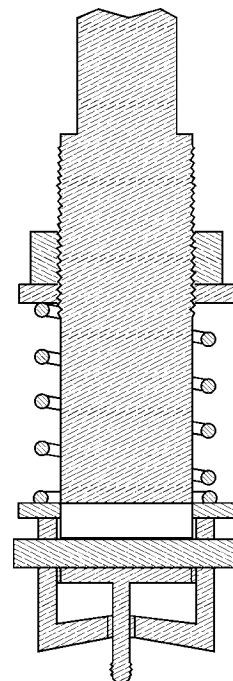


Figure 9. Working tool with spring-loaded shoulder

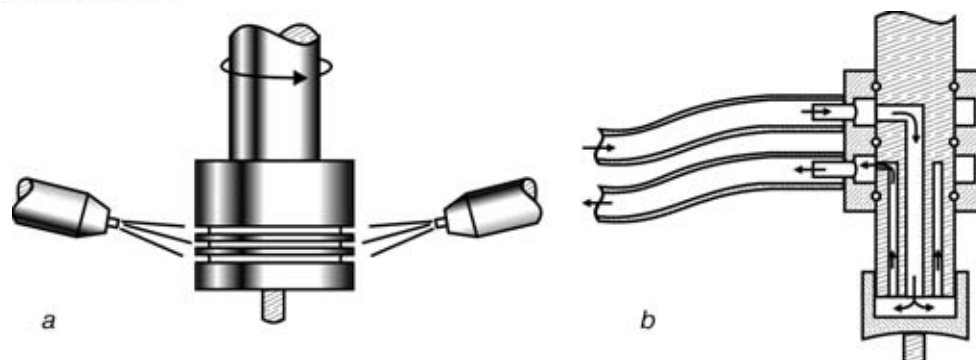


Figure 10. Schematics of working tool cooling with an external (a) and internal (b) feed of the coolant

changes of the macrostructure are observed directly at the nugget, which are due to a considerable plastic deformation of the metal and grain rotation through up to 90°, this eventually being manifested in lowering of hardness and mechanical properties [34].

Proceeding from microstructural studies of a large number of joints in various aluminium alloys, the author of [34] singles out four zones in the joint, which are schematically represented in Figure 19. Directly adjacent to zone *A* (base metal) is zone *B*, where the metal of the blanks remains undeformed, and changes its structure only under the impact of heating. By analogy to other arc processes this zone was called the heat-affected zone. Zone *C*, where the metal is exposed to considerable plastic deformations and heating, was called the zone of thermomechanical impact. And, finally, zone *D* is the joint nugget, where dynamic recrystallisation occurs.

Investigations, performed in [25, 34] on alloys of series 2000, 5000, 7000, demonstrated that the HAZ metal differs from the base metal by a higher etchability, hardness drop due to over-ageing, or reduced density of dislocations, or due to both these mechanisms. Bending of elongated base metal grains and their partial recrystallisation take place in the zone of thermomechanical impact. Ageing and annealing processes proceed in this zone under the impact of the thermal cycle, which results in a minimal hardness level. It should be noted, that some areas of zone *C* may be heated up to comparatively high temperatures, at which the strengthening phases may be dissolved.

Nugget microstructure consists of equiaxed grains, the dimension of which depends on the technology and alloy grade, usually being not greater than 10 µm. Hardness of this zone is noticeably lower than that of the base metal in the heat-hardened or work-hardened condition, although for alloy 5083 in the annealed condition, nugget hardness is somewhat higher than that of the base metal [25, 34].

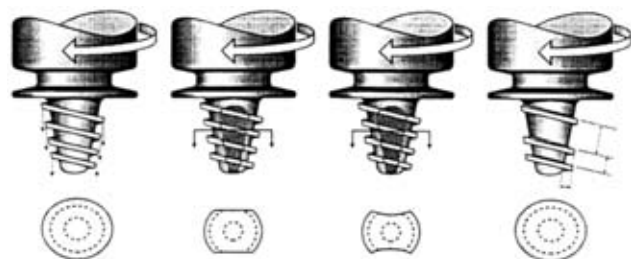


Figure 11. Variants of the design of the working tool with Whorl trade mark

Authors of [25] studied the microstructure and microhardness of the nugget in the places of the presence of the so-called annual rings and the adjacent regions for alloys AA5083 and AA6082, without, however, being able to find any differences.

Studies [28, 34, 35] give the results of electron microscopy investigations in alloys 7075-T6 and 2014-T6, characterizing the mechanisms of phase precipitations and their dimensions, grain crystallography and dislocation structure of the nugget. Authors note the need for further investigations to account for the phenomenon of the nugget structure formation in the welded joint center.

FSW equipment consists of the drives for tool rotation and its vertical displacement, drive of displacement in the direction of welding, as well as a device for fastening the assembled parts to be welded. FSW machines, as a rule, are of a specialized nature and are developed to suit certain dimensions and shape of the structure. The Table gives the parameters of FSW machines [36], developed at TWI.

A portable unit for FSW of blanks of sea vessel components of alloy AA5083 up to 5 mm thick was developed with TWI participation and is being successfully used at the Department of Engineering Mechanics of the University in Adelaide, Australia [37]. The machine may be transported and mounted by two operators, without using a crane, and allows welding butt welds with a curvature of the blanks being joined. The high quality of welded joints and absence of weld reinforcement allowed using the technology of explo-

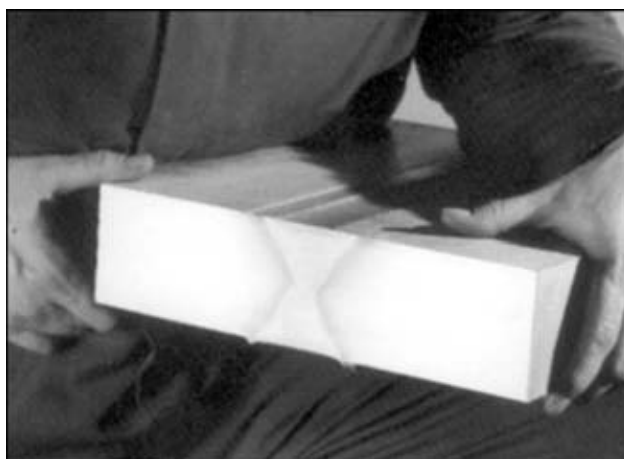


Figure 12. Macrostructure of a two-sided joint of plates of alloy 6082-T6 75 mm thick



Figure 13. Prototype of a tool with MX Triflute trade mark

sive forming to produce finished sections of the bottom of high-speed vessels.

ESAB Company, Sweden, is the main developer and manufacturer of industrial machines, having Super Stir trade mark. The first machine was supplied to Marine Aluminium Company, Norway [11, 38] for enlargement of extruded panels of ships and railway carriages (Figure 20). It allows welding blanks from 1.6 to 15.0 mm thick at their maximal dimensions of 16×6 m. Experience of such a machine operation demonstrated that working tool life is on average equal to 1–2 km and by April, 2000 about 200 km of welds without defects had been made.

Work [39] reports a sale by ESAB of two machines to a Swedish division of SAPA Company, which is a major European manufacturer of aluminium shaped sections. The first machine has two welding heads and is used for manufacture of parts of the rolling stock of railway and automotive transport. The second machine is designed for fabrication of sections of a large cross-section up to 14.5 m long and incorporates three welding heads, which allow simultaneous welding of two sides of the section or conducting welding of a butt from two sides.

ESAB is also successfully fulfilling a program on development and delivery of machines to Boeing Company, Huntington Beach, USA [27]. In the first stage machines for welding longitudinal butts of fuel tanks of «Delta» II and III missiles were supplied, which allow making welds up to 15.3 m long with fuel tank diameter from 2 to 6 m (Figure 21, a). Two more similar machines were purchased by Boeing for the factory in the city of Decatur, however the welding

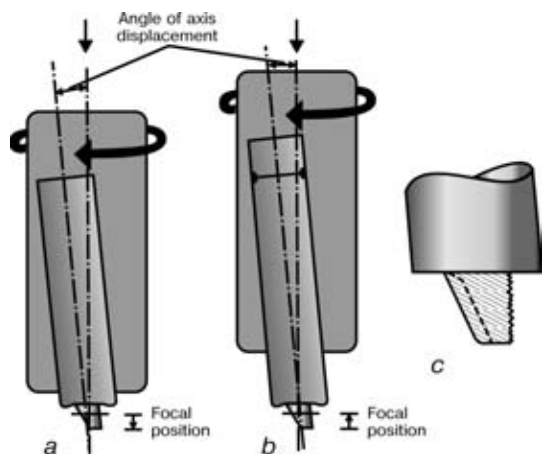


Figure 14. Principle of performance of a Skew-Stir variant of FSW process (a, b) and pin of A-Skew™ tool (c)

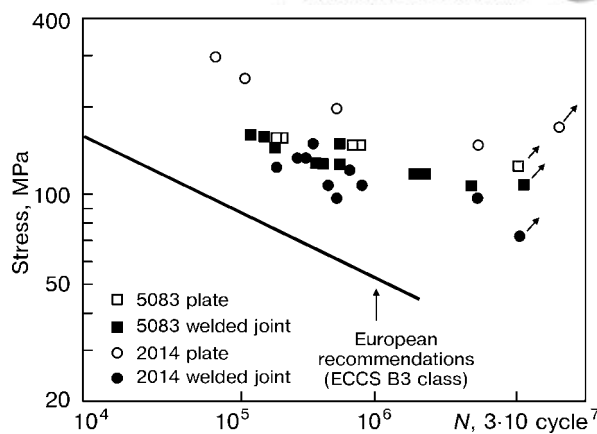


Figure 15. Fatigue properties of FSW butt joints in alloys 5083-0 and 2014-T6

process will be conducted in the vertical position to save floor space (Figure 21, b) [40]. Boeing spent \$15 mln for purchase of this equipment and conducting their own research. Boeing also purchased from ESAB machines for making circumferential welds and fitted a production line to manufacture fuel tanks for «Delta» family missiles, using FSW. All the tanks of 2.4 m diameter consist of three panels of alloy 2014-T6 with a waffle background 22.22 mm thick and are welded by three longitudinal welds (Figure 22).

The first prototype of a high-capacity industrial machine in Great Britain was developed and manufactured by Crawford Swift by an order from British Aerospace [41]. The machine, bearing Power Stir trade mark (Figure 23), in the next two years will be used in Fulton factory to fulfill a program, related to applying FSW for joining wing elements for a new generation of Airbus A3XX aircraft with passenger capacity of up to 550 persons.

The main areas of FSW application are ship-building (deck superstructures, partitions, hull elements); aerospace industry (elements of the fuselage, wings, fuel and cryogenic liquid tanks, missile bodies); railway transport (car bodies and base frames of metro cars); automotive industry (engine fastening components, wheel discs, car frames); electrical engineering (electric motor cases, current conduits, parabolic antennae, busbars); construction industry (aluminium bridges, aluminium pipelines, heat exchangers and conditioners); food industry (beer cans, packing), etc.

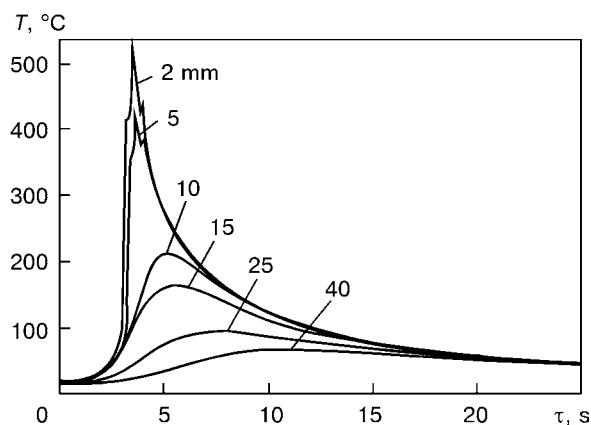


Figure 16. Thermal cycle in FSW of 4 mm alloy AA6063 at a speed of 0.5 m/min at different distances from weld centre

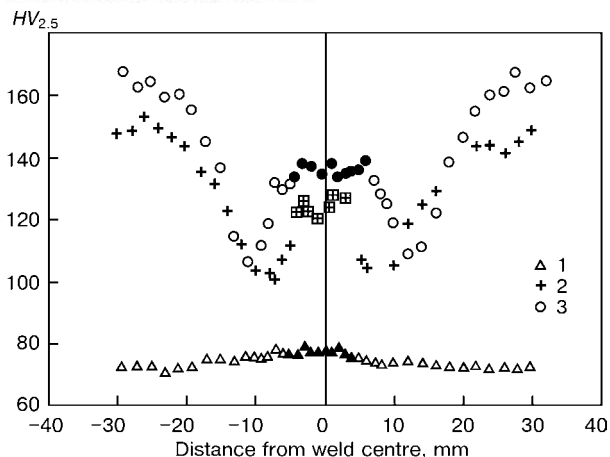


Figure 17. Hardness distribution in the cross-section of FSW joints in alloys 5083-0 (1), 2014A-T6 (2) and 7075-T7351 (3) 6.4 mm thick

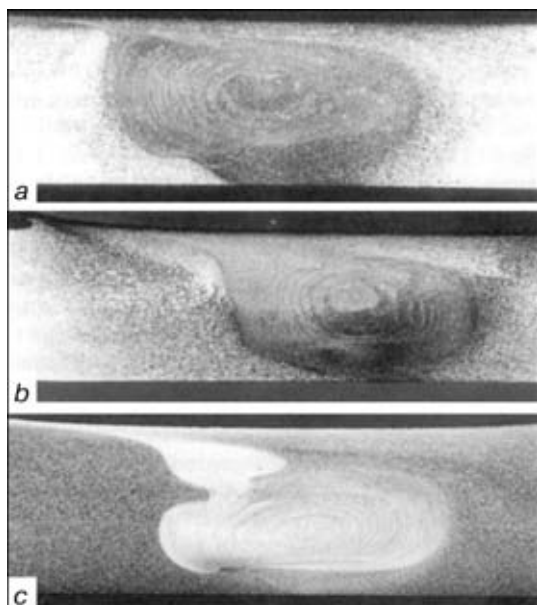


Figure 18. Macrostructure of FSW joints of 6.4 mm thick sheets: a – 7075-T7351; b – 2014-T6; c – 5083-H321 (×3.75)

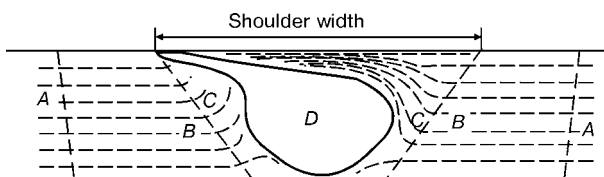


Figure 19. Schematic of the zones of a butt joint, made by FSW: A – base metal; B – HAZ; C – zone of thermomechanical impact; D – zone of dynamic recrystallization



Figure 20. ESAB Super Stir™ machine for welding extruded panels, supplied to Marine Aluminium, Norway

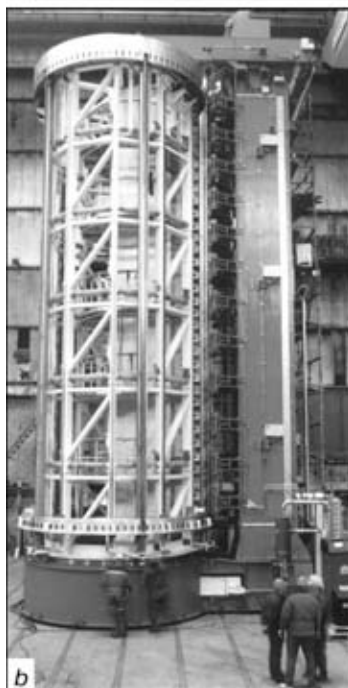


Figure 21. ESAB Super Stir™ machine in Boeing for welding shells of «Delta» missiles in the downhand (a) and vertical (b) position

[12, 13, 31, 36, 42]. This list may be continued infinitely. FSW application is particularly effective in manufacture of mass-produced parts [43]. Figure 24, a shows a car disc, consisting of a cast hub and rim, made by extrusion or rolling, and Figure 24, b shows a case of an electric motor, made of extruded blanks.

An example of successful application of FSW also was welding of railway carriages of extruded aluminium panels [12] by Hitachi Company, which has already made more than 200 pieces (Figure 25).

In the opinion of most of the researchers, the main specific defect of the joints, made by FSW, is lack-of-fusion in the weld root, which is called «kissing bonds». The main causes for this defect development are either a local thickening of the metal being welded, or disturbance of metal transfer into the root part of the joint. This defect, as a rule, has a very small size through the thickness, so that it is extremely difficult to detect it using X-ray inspection. A less expensive and more reliable method is the ultrasonic method [11, 12]. In some industrial machines of ESAB the UST equipment is mounted into the machine, and control is conducted simultaneously with the welding process [27].

The simplest control method is visual inspection, performed by the welding operator [11]. If possible,



Figure 22. Fragment of a fuel tank of «Delta» missile with FSW longitudinal weld

witness samples are cut out of the initial and final part of the blanks being welded, for instance, extruded panels. These samples are then used to make the sections and study the joint macrostructure. In some cases, the suspicious sections of the root part of the joints are controlled, using dye penetrant inspection.

The level of defectiveness of welds, produced by consumable-electrode arc welding, is by almost an order of magnitude higher than for FSW [27, 40]. This allows saving several hundred thousand dollars annually in repair of defective areas. More over, such a high quality of FSW welds allows eliminating 100 % control of welds, and applying selective statistical control [27] to save more money.

TWI specialists proposed applying the so-called identification sign on the root side of the joint [22] by engraving in the substrate a mirror reflection of required information on the manufacturer, time, date of welding, etc. During welding the weld metal fills the recesses in the substrate to form an appropriate word or sign. The extent of filling of the engraving in the substrate may also be used as a specific measure of the joint quality, particularly of its root part, where the defects form the most often. Improvement of metal stirring in the joint root part may be achieved by making the edge bevel from the reverse side of the plate (Figure 26, *a*), which improves filling of this region during its flow in the plasticised condition [44].

Elimination of defects in the weld root is promoted by application of grooved backing (Figure 26, *b*),

FSW machines developed by TWI

Machine type	Thickness welded, mm	Welding speed, m/min	Dimensions of welded blanks, m	Remarks
FW 20	1.2–12	2.6	–	Maximal frequency of tool rotation, 15000 rpm
FW 21	3–15	1.0	2.0×1.2	
FW 22	3–15	1.2	3.4×4.0	
FW 14	5–50 100 (from both sides)	1.0	–	Machine power 22 kW
FW 16	Small-sized mobile machine to demonstrate FSW process			

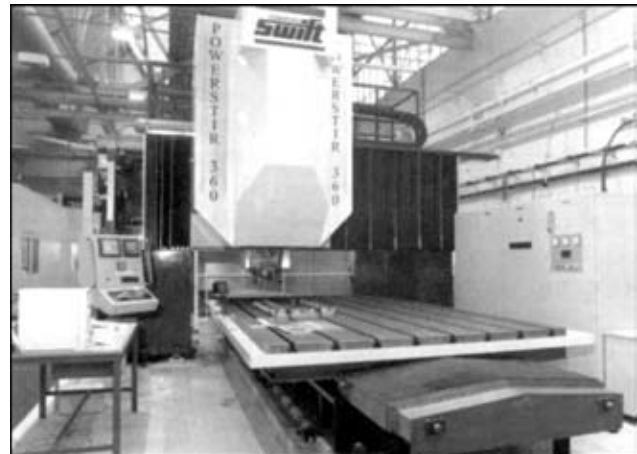


Figure 23. 60 kW Power Stir-360 machine of Crawford Swift, Great Britain

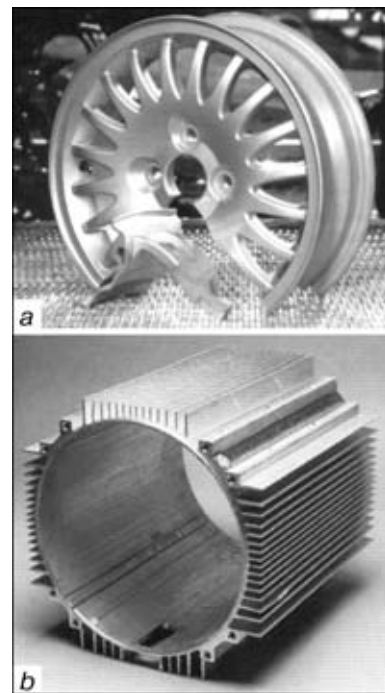


Figure 24. Car disc (*a*) and electric motor case (*b*), produced by FSW



Figure 25. Railway car, made by Hitachi, using FSW

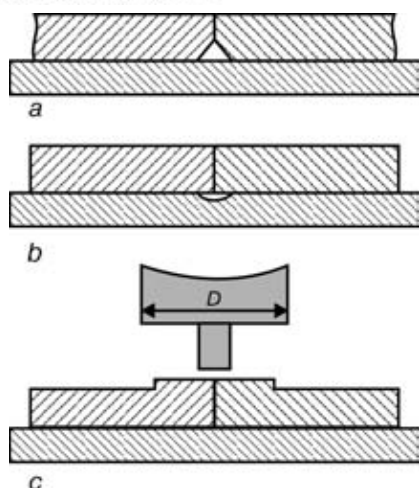


Figure 26. Preparation of edges to be welded with a root part bevel (a), making a groove in the substrate (b) and a local thickening in the welding zone (c)

into which the metal is pressed out, forming a small bead [45]. It is then removed by machining, providing a high quality of the joint root part.

One of the small drawbacks of FSW joints is a slight thinning of the metal in the joint zone due to contact of the tool shoulder and blank surface. This value is usually equal to 0.1–0.2 mm. In some cases, however, this may have an influence on joint strength. To eliminate this drawback, the recommendation is to introduce a thickening in the butt zone (Figure 26, c), of the width equal to the shoulder diameter. This method is particularly effective, in the opinion of its authors, when there is a gap in the butt [13].

Thus, materials of foreign publications are indicative of intensive development of FSW process for different aluminium alloys and widening of the fields of its application in industrial production in fabrication of a wide range of welded structures. Such advantages of FSW process, compared to other welding processes, as possibility of joining difficult-to-weld alloys, minimizing welding stresses and strains, absence of harmful evolutions or radiation, high level of the joint properties and process efficiency will ensure its wide acceptance in fabrication of critical structures for aircraft construction, ship-building, vehicle construction and aerospace engineering.

- Thomas, W.M., Nicholas, E.D., Needham, J.C. *Improvements relating to friction welding*. Eur. Pat. Spec. 0615480B1. Publ. 1995.
- Midling, O.T., Morley, E.J., Sandvik, A. *Friction stir welding*. Eur. Pat. 95907888.2. Publ. 1995.
- Shinoda, T., Endo, S. (1995) Recent development of friction welding of aluminium alloys and dissimilar materials. *J. Light Metal Weld. Constr.*, **7**, 19–26.
- Irving, B. (1993) Sparks begin to fly in nonconventional friction welding and surfacing. *Welding J.*, **5**, 37–40.
- (1997) Gas additions boost friction performances. *TWI Connect*, **9**, 3.
- Dawes, C.J. (1995) An introduction to friction stir welding and its development. *Welding & Metal Fabric.*, **1**, 13–16.
- Dawes, C.J., Thomas, W.M. (1996) Friction stir process welds aluminium alloys. *Welding J.*, **3**, 41–45.
- Dawes, C.J., Thomas, W.M. (1998) Trecie zvaranie hliníkových zliatin premiesaním rotujúcim nástrojom. *Zvaranie Svarovani*, **7**, 163–167.
- Thomas, W.M. et al. *Friction stir butt welding*. Pat. 9125978.8. GB 2306366 A. Publ. 05.07.97.
- Midling, O.T. (1994) Material flow behaviour and microstructural integrity of friction stir butt weldments. In: *Proc. of 4th Int. Conf. on Aluminium Alloys (ICAA4)*, Atlanta, 1994.
- Midling, O.T., Hval, M., Johansen, H.G. et al. (1998) Process optimisation of friction stir welding in fabrication of aluminium ship panels. In: *Proc. of 3rd Int. Forum on Aluminium Ships*, Haugesund, May 27–28, 1998.
- Okamura, H., Aota, K., Erumi, M. (2000) Friction stir welding of aluminium alloy and application to structure. *J. JILM*, **4**, 166–172.
- Okamura, H. (2000) Character of friction stir welding and application in Japan. *J. JWS*, **7**, 11–17.
- Dawes, C.J., Andrews, R.E. (1998) Friction stir welding of aluminium alloy 6–35 mm thick. In: *Proc. of Conf.*, Vasteras, Sweden, Nov. 18–19, 1998.
- Dawes, C.J., Thomas, W.M. (1995) Friction stir joining of aluminium alloys. *Bulletin TWI*, **6**, 124–127.
- Morris, T.W., Nicholas, E.D., Needham, J.C. et al. *Friction stir welding*. Pat. 2306366A UK, Int. Cl. B 23 K 20/12. Publ. 1997.
- Midling, O.T., Oosterkamp, L.D., Bersaas, J. (1998) Friction stir welding aluminium — process and applications. In: *Proc. of 7th Int. Conf. on Joints in Aluminium*, Cambridge, April 16, 1998.
- Dawes, C.J., Nicholas, E.D., Murch, M.G. et al. *Friction welding*. Pat. 5460317 GB, Int. Cl. B 23 K 20/12. Publ. 1995.
- Wykes, D.H. *Adjustable pin for friction stir welding tool*. Pat. 5697544 USA, Int. Cl. B 23 K 20/12. Publ. 1997.
- Colligan, K.J. *Friction stir welding tool for welding variable thickness work pieces*. Pat. 5718366 USA, Int. Cl. B 23 K 20/12. Publ. 1998.
- Colligan, K.J. *Friction stir welding with simultaneous cooling*. Pat. 5718366 EP 0810056 USA, Int. Cl. B 23 K 26/12. Publ. 1997.
- Thomas, W.M. (1998) Friction stir welding and related friction process characteristics. In: *Proc. of 7th Int. Conf. on Joints in Aluminium*, Cambridge, April 16, 1998.
- Thomas, W.M., Threadgill, P., Nicholas, E.D. et al. (2000) Tool technology. The heart of FSW. *TWI Connect*, **July/August**, 3.
- Thomas, W.M., Dolby, R., Johnson, K. (2001) Variation on a theme Skew-Stir™ technology. *Welding & Metal Fabric.*, **7**, 20–22.
- Karlsson, J., Karlsson, B., Larsson, H. et al. (1998) Microstructure and properties of friction stir welded aluminium alloys. In: *Proc. of 7th Int. Conf. on Joints in Aluminium*, Cambridge, April 16, 1998.
- Backlund, J., Norlin, A., Anderson, A. (1998) Friction stir welding — weld properties and manufacturing technique. *Ibid.*
- Johnsen, M.R. (1999) Friction stir welding takes off at Boeing. *Welding J.*, **2**, 35–39.
- Mahoney, M.W., Rhodes, C.G., Flintoff, J.G. et al. (1994) Properties of friction-stir-welded 7075 aluminium. *Metalurg. and Materials Trans.*, **6**, 1955.
- Hynds, P. (1999) Friction stir benefits include cost savings. *Speed at Sea*, **10**, 33–36.
- Larsson, H., Svensson, L.-E., Karlsson, L. (1997) Construcción naval avanzada con aluminio. *Rev. Soldadura*, **27**, 180–188.
- Kumagai, M., Tanaka, S. (2001) Application of friction stir welding to welded construction of aluminium alloys. *J. Light Metal Weld. Constr.*, **1**, 22–28.
- Frigaard, O., Grond, O., Miglin, O.T. (1998) Modelling of heat flow phenomena in friction stir welding of aluminium alloys. In: *Proc. of 7th Int. Conf. on Joints in Aluminium*, Cambridge, April 16, 1998.
- Russel, M.J., Shercliff, H.R. (1998) Analytical modelling of friction stir welding. *Ibid.*
- Threadgill, P. (1997) Friction stir welds in aluminium alloys — preliminary microstructural assessment. *TWI Bulletin*, **March/April**, 30–33.
- Rhodes, C.G., Mahoney, M.W., Bingel, W.H. et al. (1997) Effects of friction stir welding on microstructure of 7075 aluminium. *Scripta Materialia*, **36**, 69–75.
- Kallee, S., Nicholas, D. (1998) Causing a stir in the future. *Welding and Joining*, **2**, 18–21.
- Henderson, I. (1998) Exploiting friction stir welding in explosively formed aluminium boat hull construction. In: *Proc. of 7th INALCO-98 Int. Conf.*, Cambridge, 1998.
- Weman, K. (2000) Equipment for aluminium welding. *Seetsaren*, **2**, 11–13.
- (1999) Friction-Stir-Welding nun auch in der Massenproduktion von Aluminiumprofilen. *Schweißen Prüftechnik*, **9**, 135.
- Pekkari, B. (2000) Trends in joining and cutting within a sustainable world. *Bulletin TWI*, **March/April**.
- (2000) Heavy-duty machine for friction welding. *Metals Ind. News*, **17**, 10.
- Fukuda, T. (2000) Friction stir welding (FSW) process. *J. JWS*, **7**, 6–10.
- Johan, A.E., James, M.E., Terge, M.O. et al. *Two-piece wheel*. Pat. W 09715462 NO, Int. Cl. B 23 K 20/2. Publ. 05.01.97.
- Posen, Ch. *Friction stir welding total penetration technique*. Pat. 5611479 USA, Int. Cl. B 23 K 20/12. Publ. 1997.
- Colligan, K. *Weld root closure method for stir welds*. Pat. EP 0810054 USA, Int. Cl. B 23 K 20/12. Publ. 03.12.97.



PRESS WELDING OF PIPES USING ACTIVATING MATERIALS

A.S. PISMENNY and A.S. PROKOFIEV

The E.O. Paton Electric Welding Institute, NASU, Kyiv, Ukraine

Considered are capabilities of new technologies involving activating materials for induction butt welding of small- and medium-diameter pipes, producing of T-joints in thin-walled pipes and joining of pipes to flanges (brazing). Data on service properties of welded joints and results of laboratory and industrial tests of specimens and pipes produced by the above technologies using induction heating are reviewed.

Key words: *induction butt welding, brazing, activating materials, pipes, welds, T-joints, mechanical properties, induction heating*

Improvement in quality of butt welds in parts made by the fusion and flash welding methods is hampered in a number of cases by the factors which are associated with the effect of high temperatures on the initial structure of the material of billets. This may lead to deterioration in static and dynamic values of mechanical strength of the weld and adjoining zone. In addition, some welding methods may cause formation of flash, the removal of which is a very labour-consuming and difficult operation. Capillary brazing can be recommended in some cases for making joints to avoid the above drawbacks. However, its application has a number of limitations, such as the necessity to precisely prepare edges of a complex profile (which is not always expedient or possible) and decreased strength of brazing filler metals compared with strength of the base metal.

Results of the investigations conducted at the E.O. Paton Electric Welding Institute, aimed at improvement of quality of the joints in pipes and tubular pieces produced with no melting of the base metal led to the development of a promising method for providing the high-quality welded joints with strength equal to that of the base metal [1–4]. This method was called brazing. In its physical nature it is close to diffusion bonding involving micro evacuation of the joining zone, which is ensured by properties of the used activating material [4].

The brazing method consists of the following sequence of main technological operations: deposition of the activating material on the mating surfaces of the edges, heating of the weld zone to a melting temperature of the activating material and applying of the controlled amount of plastic deformation to the weld edges. Mixtures of a brazing filler metal with flux are usually used as the activating material. Normally, the activator is applied to the weld edges as in conventional brazing (in the form of inserted pieces or paste, by spraying, etc.) [5]. At the first stage of the process the molten activator wets and cleans the mating surfaces of the edges from oxides

and protects them from penetration of oxygen from the ambient atmosphere. The further operations are interrelated and determine to a substantial degree the result of the brazing process. Achievement of the required extent of plastic deformation of the weld edges is of a decisive importance in this case. It is determined by the temperature field parameters of the edges under a certain upsetting pressure.

As established for the butt joints in pipes, tensile strength and bending angle increase with increase in the extent of plastic deformation in the weld plane: $\epsilon = 100 H / \delta$ (H is the height of the weld convexity and δ is the pipe wall thickness), and reach their threshold values at $\epsilon \approx 40\%$ (Figure 1) [1–4, 6]. The same relationship is characteristic also of the impact toughness values of the welds [7]. This is associated with the fact that properties of welded joints are greatly affected by peculiarities of solidification of the weld metal under pressure and a small weld thickness (3–6 μm), leading to its contact strengthening [6, 7]. According to the metallography data, ≈ 30 –40 % of the joining zone cannot be visualised, and joining the billets occurs in the base metal. In addition, independently of chemical composition of the activator, the weld is enriched with the base metal elements, which also favours strengthening of the joint. Figure 2 shows dependence of chemical composition of the weld upon its thickness for billets of steel 20 and the activator based on the brazing filler metal of the PAN-3 type (TU 14-1-2991–80). The PAN-3 filler metal has the following chemical composition, %: Cu — base; Mn — 30.0–35.0; Ni — 7.0–10.0; Si — 1.5–5.0; P — ≤ 0.05 ; S — ≤ 0.04 ;

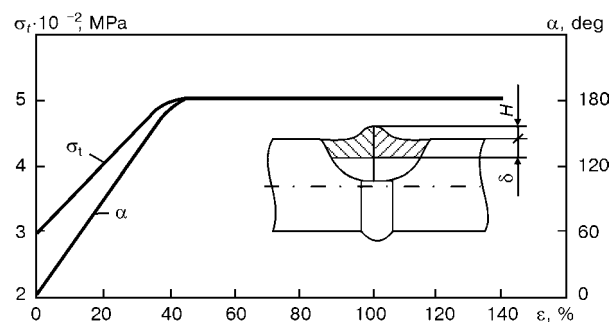


Figure 1. Dependence of strength σ_t and bending angle α of the joints upon the extent of plastic deformation ϵ in the weld plane

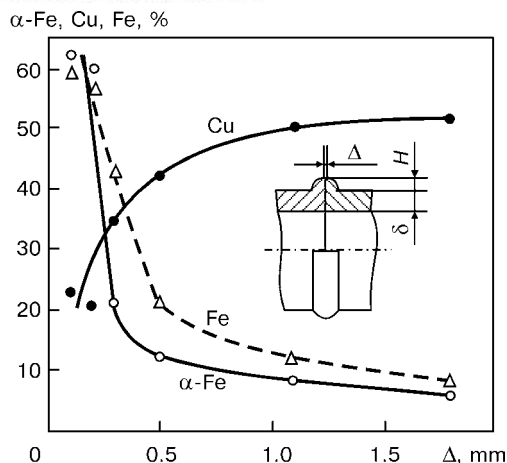


Figure 2. Dependence of chemical composition of the weld upon its thickness

Al — ≤ 1.5 ; Pb — ≤ 0.01 . The temperature field depends upon the energy and geometry parameters of the source of heating the weld edges.

As shown by the investigations, there are such relationships of parameters of the temperature field in the bulk of the pipe edges which do not lead to formation of an internal convexity of the weld [8, etc.]. Figure 3 shows specimens illustrating the character of formation of metal in the weld zone during braze welding.

The investigation results show that distribution of temperature along the pipe axis, providing the required character of deformation of the edges, can be sufficiently accurately described by the following expression [9]:

$$T(r_{\text{ex}}, z) = T_0 \exp(-2Dx^2), \quad (1)$$

where r_{ex} is the radius of the external pipe wall; T_0 is the temperature at the edges; $x = (z/r_{\text{ex}})$; z is the axial coordinate; $D = 0.2 (r_{\text{ex}}/z_0)^2$; and z_0 is the coordinate of the zone of zero deformation of the edges. This temperature distribution law holds in the case of heating the edges of cylindrical pieces using a circular inductor which encloses the butt joint. The vector potential of such an inductor at $r \leq R$ can be calculated from the following formula [10]:

$$A = \frac{\mu_0 R I}{4\pi a} \times \left\{ \frac{r}{R} \left(\arctg \frac{a+z}{0.4R} + \arctg \frac{a-z}{0.4R} \right) + \frac{1-r/R}{\sqrt{r/R}} \times \right. \\ \left. \times \left[\arctg \frac{a+z}{R-r} + \arctg \frac{a-z}{R-r} + \frac{a+z}{2R} \ln \left(1 + \left(\frac{R-r}{a-z} \right)^2 \right) \right] + \right. \\ \left. + \frac{a-z}{2R} \ln \left(1 + \left(\frac{R-r}{a-z} \right)^2 \right) \right\} \quad (2)$$

where R is the radius of the internal surface of the circular inductor; $2a$ is the axial line of the inductor; I is the inductor current; r and z are the axial coordinates of the observation point; and μ_0 is the magnetic permeability.

The temperature distribution law being known, it is possible to determine the proportional distribution

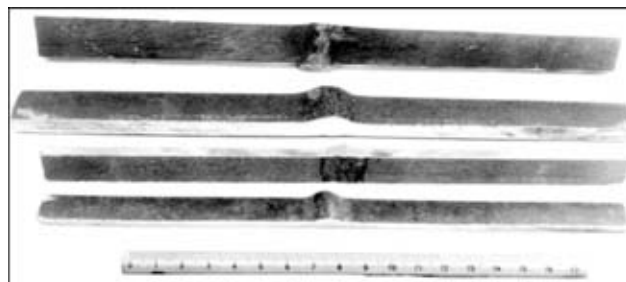


Figure 3. Specimens cut from steel pipes 325 mm in diameter with a wall thickness of 12 mm

of specific power along the surface of a billet, which allows the source data obtained to be related to the problem of development of an induction system and calculation of the heating conditions [9]. In addition to the desirable distribution of temperature along the pipe axis, it is necessary to ensure also the temperature field which would be sufficiently uniform over the surface area of the edges joined to guarantee simultaneity of melting of the filler metal over the entire surface area of the weld. Maximum non-uniformity of heating of the pipe edges should not be beyond the permissible limits of the operating temperature of the activator. It is about 50 °C for the majority of the filler metals used. This requirement is met by properly selecting frequency of the inductor current and duration of heating. To determine heating conditions and sizes of the inductor, it is necessary to harmonise geometrical sizes of the zone of joining the pipes and required parameters of the temperature field within the joint zone. Keeping to these parameters is required to perform the technological process, while the prerequisites here are the above threshold values of the extent of plastic deformation in the weld plane. Geometrical parameters of the zone of joining the pipes include the value of upsetting of pipe edges h_t , coordinate of the zone of zero deformation of edges z_0 and degree of plastic deformation of edges in the weld plane $\epsilon = H/\delta$ (Figure 4).

The degree of plastic deformation in the weld plane in induction welding should be $\epsilon = 0.2-0.5$, and in braze welding it should be not lower than 0.4 [9]. In practice, to ensure the consistent quality of the joints the process is performed at $\epsilon = 0.5$. Quality joining of smaller- and medium-diameter pipes (Figure 3) is characterised by the presence of a smooth outside bead of the forced out metal (convexity), whose geometrical characteristics (evaluated by processing the experimental results) have the following mean values: $h_y = 1.5\delta$ and $\delta_y = 0.5\delta$. Convexity of the weld with a sufficient degree of accuracy can be approximated by an assumption of an annular barrel [9] with a central hole the diameter of which is equal to the external diameter of pipe billets, $d_{\text{ex}} = 2r_{\text{ex}}$. Here the volume of the weld convexity (at one edge) is determined by the following expression:

$$V = 2.096 h_y H (d_{\text{ex}} + H). \quad (3)$$

Using the condition of equality of volumes of the weld convexity and deformed region of the pipe h_t long (upsetting allowance, see Figure 4), we find that



$$\frac{h_t}{h_y} = \frac{2}{3} \frac{H}{\delta} \frac{1 + H/d_{ex}}{1 - \delta/d_{ex}} \quad (4)$$

The calculations show that $h_t/h_y \approx 1/3$ at $d_y = 0.58\delta$. Given that $h_y = 1.5\delta$, we find the upsetting allowance equal to $h_t \approx 0.5\delta$. The total value of the upsetting allowance is $2h_t \approx \delta$, which is proved by the results obtained in induction pressure brazing and induction welding [9, etc.].

Therefore, the distance along the billet axis from the end to the zero deformation zone, which corresponds to a pipe wall temperature of about 700–750 °C under an upsetting pressure of 30–40 MPa, is

$$z_0 = h_y + h_t = 2\delta. \quad (5)$$

The data given serve as the basis for development of an inductor for heating the pipe ends [9] and statement of the work for selection or design of a welding machine.

Braze welding is performed using machines which provide clamping and aligning of pipes with the activator deposited on their ends, as well as regulated opposing deformation (upsetting) of the heated ends of the pipes.

A wide range of machines has been developed up to now, and machines of the types of P-127, P-130, P-139 (the latter is based on the K-584 flash butt welding machine) and P-145 are available. In addition, there is a small series of the P-144 machines for making butt joints of the pipe to pipe type. Available also is the P-134 machine for welding joints of the pipe to end fitting type (flanges, nipples, threaded tool joints, etc.), primarily for ship-building applications. The above machines allow joining of pipes with diameters ranging from 14 to 325 mm.

For the first time in the world practice the half-stands of the drill pipes 50×5 mm in diameter (low-alloyed steel) used for drilling exploratory wells were joined by braze welding of the casing pipe ends (with a diameter of 55×10 mm) [8]. Industrial tests of the half-stands of the drill pipes joined by braze welding were conducted on a selective string KPS-57/50 using cone-threaded joints. Experimental pipes with a total length of 400 m were located in the lower part of the string. Seven exploratory wells with an average depth of 700 m were drilled in the rock characterised by increased abrasiveness. Drilling was performed using a diamond-hard alloy tool 59 mm in diameter under the following conditions: rotation frequency of the drill shaft 200–500 rpm, axial load 7000 N, torque 300–500 N·m, and consumption of the flushing fluid 40–50 l/min. The wells were drilled for 16 months. No ruptures or fractures in the welds were observed during operation of the string and hoisting operations. The joints in the pipes produced by braze welding saved 180 sleeves during the test period. Wear resistance of the braze welded joints was 1.5–1.7 times higher than that of the sleeve joints [2].

The technology for braze welding of the oil production pipes was applied at the Neftekamsk Central

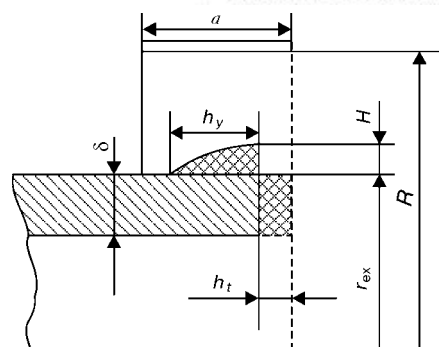


Figure 4. Schematic of the region of upsetting in butt high-frequency and braze welding of pipes

Base dealing with repair and rent of oil production and drilling equipment for the Company «Bashneft», and in Leninogorsk for the Oil and Gas Production Agency of the Company «Tatneft» [4]. In both cases the welding systems are located in workshops and are parts of the production lines for welding and insulation of two- and three-pipe sections. Working pressure in pipelines is up to 200 atm. Duration of the process proper is 10–35 s, depending upon the diameter and thickness of the pipe wall, as well as requirements for achieving the desirable character of the temperature field distribution in edges. The results of testing specimens cut from the test joints in pipes with a diameter of 89×5 mm, made from steel 20 with a standard tensile strength of 420 MPa (GOST 8731–74) and welded at the Neftekamsk Central Base of the Company «Bashneft», exhibited a mean tensile strength of 450 MPa and mean bending angle of 139°. The full-scale hydraulic tests of parts of the pipes containing circumferential welds were additionally conducted in application of the technology and equipment to generate the most comprehensive information about structural strength of the welded joints. To do it, hemispherical caps, one of which had a union for connecting the pump station to the hydraulic system, were welded to the pipe ends. The tests were conducted at a pressure of 36 MPa, which corresponded to 0.9 of the yield stress of metal in compliance with GOST 8731–74. The test results showed no fractures in the welds.

Pipelines with glass-enamel coatings on the walls are used or can be used for transportation of oil and oil products, chemical equipment, transportation of aggressive and radioactive fluids, in systems for supply of drinking and hot water to the population, in milk and food processing industry, environmentally safe sewage systems, heat pipelines etc., where their utilisation provides the required physical-chemical properties of pipelines and extension of service life 5 and more times. Widening of the application of the enameled pipelines is limited by the fact that no reliable method of joining the pipes, especially under field and erection conditions, has been available until recently.

One of the technical prerequisites for solving the integrated problem of manufacture of pipelines with an internal glass-enamel coating was the method of

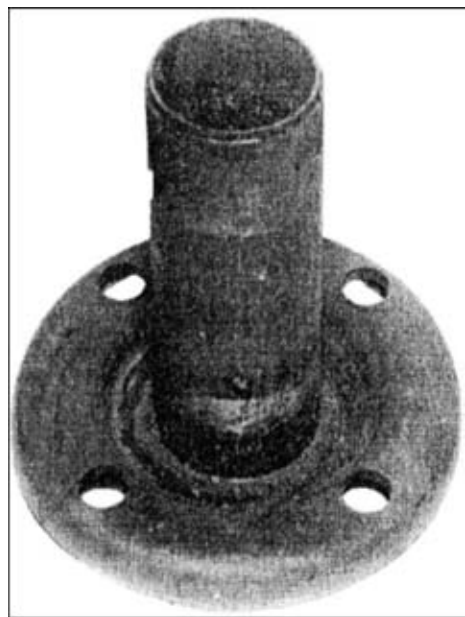


Figure 5. Sample of the joint in the 70x6 mm pipe with a flange (outside diameter 120 mm)

formation of joints in pipes with a glass-based coatings, which provided high-quality joining of the steel substrate to a coating. The braze welding method, which combines positive properties of pressure joining and brazing, allows simultaneous strong joining of pipes and internal coatings [11]. The equipment developed on its base makes it possible to solve the problems of welding pipe sections and pipelines under workshop, erection and field conditions. For example, in production of two- and three-pipe sections from the preliminarily enameled pipes by the braze welding method the production floor area and dimensions of equipment (necessary for performing the enameling operation) can be decreased 1.5–2 times, compared with traditional technologies of production of pipe sections, where the pipes are first welded into a section and then the section is enameled.

Tubular metal structures comprising flange joints are widely applied in making different-purpose pipelines, gas and other types of devices (gas, water, heat counters, etc.), in repair of old and assembly of new pipe supply lines in housing facilities, and installation of gas supply for domestic uses. However, the problem of their manufacture is still topical. As a rule, designs of pipelines provide for the use of the so-called intermediate (middle) fittings in the form of T-joints and four-way unions with welded flanges, which are manufactured using casting and forming followed by machining. In this case the material utilisation factor is very high, while labour consumption in the manufacture of fittings still has a reserve for reduction. Manufacture of flange joints in pipelines by the braze welding method allows the total weight of the pipeline systems and labour consumption to be reduced [12]. The process is performed by preliminarily preparing the end of the pipe to be joined to the flange, the preparation operation consisting of serrated turning of the outside diameter of the pipe. Then the flange

joint is assembled in clamps of the welding machine, and the brazing filler metal and flux are deposited onto the zone of joining. The flange to pipe joining zone is heated by an inductor [10], and the upsetting force is applied to the internal surface of the pipe joined with the flange connected to it to deform the weld zone using a conical punch. Formation of the weld zone of the flange joint depends upon the required deformation extent [12]. An example of joining by braze welding of the pipe with a diameter of 70x6 mm to the flange with an outside diameter of 120 mm is shown in Figure 5.

Tubular metal structures comprising T-joint elements are extensively applied in manufacture of bicycles and motorcycles, gas and other devices and pipelines. At the same time, the problem of ensuring strength and reliability of these tubular structures, including strength of a T-joint and its capability of preserving shape and service properties both under the effect of various external loads (static and dynamic) and loads caused by the effect of transported products, such as internal pressure, hydraulic shocks, etc., has an increasing topicality. One of the main ways of solving this problem is a rational selection of design of the T-joint, based on the strength and reliability criteria [13]. This is often accompanied by the requirement for ensuring a minimum cost of fabrication of a structure at its assigned strength. A serious challenge is minimisation of residual welding stresses in a location of the joint both in the main and branch pipes. Three types of the T-joints made by the braze welding technology (Figure 6) were developed in order to improve designs and methods for manufacture and welding of T-joints.

The T-joint shown in Figure 6, *a*, can be made with or without a hole (blind joint) in the main pipe. Designs shown in Figure 6, *b* and *c*, require that the hole be necessarily made in the main pipe. At the same time, in the design shown in Figure 6, *b*, the diameter of the hole in the main pipe is smaller than that in the branch pipe, while in the design shown in Figure 6, *c*, the diameter of the hole in the main pipe can be equal to or larger than that in the branch pipe. In all the three types of designs of the T-joints the branch pipe is machined by giving a saddle-type shape to the edge on the contour of its aligning with the main pipe. In the joint shown in Figure 6, *b*, the edges of the branch pipe are additionally machined to make a conical shape of the surface with an angle of 15–30°.

The braze welding process was used to make all the three types of the designs. The upsetting force was applied to the branch pipe, upsetting of edges of the branch pipe being within the limits of a double thickness of the pipe wall. In the first type of the joint (Figure 6, *a*) the branch pipe was deformed in upsetting outside the main pipe, enclosing it. This resulted in a blind T-joint.

In the second type of the T-joint (Figure 6, *b*) the joining was done on the conical surface formed in deformation of the branch pipe, which led to increase

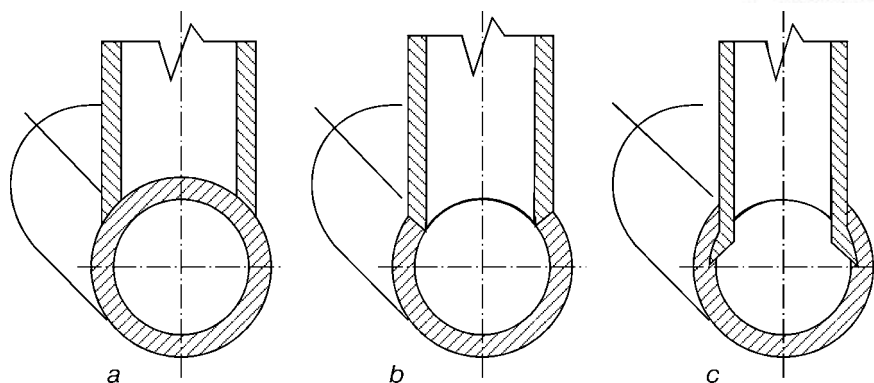


Figure 6. Designs of the T-joints made by the braze welding technology: *a* — by forming an external flange; *b* — with a conical shape of the external flange; *c* — by forming an internal flange

in the weld area and had a substantial effect on increase in strength of the joint. In this design of the T-joint the bore section of the main pipe was decreased in formation of the conical surface. Therefore, the use of such a joint in the pipeline with a diameter of the branch pipe close to that of the main pipe is inexpedient. It can be effectively used as a structural member of load-bearing metal structures, e.g. such as staircases, banisters, frames, etc.

To avoid the above drawback of joints with a design of the third type (Figure 6, *c*), the use was made of a special device introduced into the main pipe to flange the end of the branch pipe inside the main one directly during the braze welding process and produce the guaranteed bore section of the main pipe. In this case (like in the design shown in Figure 6, *b*) the surface area of the weld increases with formation of a flange located inside the main pipe from the end of the branch pipe. To avoid adhesion of the device which forms the flange, the working surface in the joining zone of the main pipe is covered with a chromium dioxide. Covering the working surface of the device is required for the third type of the joint in those cases where it is necessary to use the bore section of the main pipe. In other cases the inserted element introduced into the joining zone may not be removed to increase structural strength of the joints.

In all the three types of the joints the induction heating was used to make the joints, and the upsetting pressure was selected on the basis of being not less than 10 MPa. The welding process occurs like in the case of butt welding, the differences being caused by a spatial character of the edge metal flow in deformation of the weld zone. The inductor is developed on the basis of results of study [10].

The developed technology which involves braze welding makes it possible to produce all the three types of the T-joints by avoiding the labour-consuming preparatory operations of flanging the branch pipes, associated with forming, and the requirement for making capillary gaps between the weld edges. The above types of the T-joints made by this technology are characterised by improved performance. The new design of the T-joint (Figure 6) involves the increased-strength joints in thin-walled pipes of equal dimensions (diameter and wall thickness).

CONCLUSION

The braze welding method allows the quality butt joints to be produced on low-carbon steel casing and drill pipes intended for oil production. The method combines advantages of the brazing technology and press welding. Its benefits include ensuring full-strength joints of high ductility and toughness, avoiding the need for special edge preparation, providing a favourable shape of the weld (with a small convexity), prevention of formation of flash in internal cavities, possibility of using thin-walled pipes of equal dimensions (diameter and wall thickness) in structures with T-joints, and high corrosion resistance in sea water. The method of braze welding can be used to join parts operating at a temperature of 300–450 °C and higher.

The joints in pipes made by induction braze welding successfully passed the tests conducted under extreme conditions, in particular in drilling wells at the oil exploratory enterprise of Ukraine. The braze welding technology and equipment found application at the oil complex enterprises of the Russian Federation.

1. Lebedev, V.K., Tabelev, V.D., Pismenny, A.S. (1983) Butt pressure brazing of steel pipelines. *Avtomatich. Svarka*, **9**, 25–27.
2. Lebedev, V.K., Tabelev, V.D., Pismenny, A.S. et al. (1989) Brazing of tubes for exploration drilling. *Ibid.*, **5**, 28–30.
3. Pismenny, A.S., Shinlov, M.E., Buzhenetsky, A.I. (1995) Application of induction braze welding for joining pipes for petroleum products. *Ibid.*, **12**, 35–38.
4. Pismenny, A.S. (1998) Induction heating in welding and related technologies. *Ibid.*, **11**, 54–60.
5. Lebedev, V.K., Pismenny, A.S., Martynova, T.I. (1992) Experience of application of a composite brazing filler metal for pressure braze welding. *Ibid.*, **9/10**, 42–43.
6. Tabelev, V.D., Kareta, N.L., Panasencko, A.I. et al. (1985) Structure and phase composition of welds made by capillary and pressure brazing. *Ibid.*, **11**, 26–28.
7. Lebedev, V.K., Tabelev, V.D., Pismenny, A.S. (1993) Impact toughness of butt joints brazed with plastic deformation of base metal. *Ibid.*, **8**, 29–31.
8. Lebedev, V.K., Pismenny, A.S., Kasatkin, O.G. et al. (1990) Physical simulation of upsetting in butt welding or braze welding of pipes. *Ibid.*, **8**, 17–20.
9. Pismenny, A.S. (1990) Synthesis of induction systems for butt welding and brazing of pipes. *Ibid.*, **5**, 11–15.
10. Pismenny, A.S., Prokofiev, A.S., Shinlov, M.E. (1999) Synthesis of induction systems for brazing of flange joints in pipes with a preset distribution of power in the weld zone. *Ibid.*, **8**, 17–21.
11. Pismenny, A.S., Shinlov, M.E., Safronova, E.A. (1998) Some peculiarities of induction butt braze welding of pipes enameled on the inside. *Ibid.*, **10**, 32–37.
12. Prokofiev, A.S., Pismenny, A.S. (2000) Technology of braze welding of flanges to tubes. *The Paton Welding J.*, **5**, 48–50.
13. Prokofiev, A.S., Pismenny, A.S., Bondarev, V.A. (2001) Induction braze-welding of no-accessory T-joints in pipes. *Ibid.*, **4**, 43–47.



MAGNETICALLY-IMPELLED ARC BUTT WELDING OF THICK-WALLED PIPES

S.I. KUCHUK-YATSENKO, V.S. KACHINSKY and V.Yu. IGNATENKO

The E.O. Paton Electric Welding Institute, NASU, Kyiv, Ukraine

The new method of a magnetically-impelled arc butt (MIAB) welding of pipes with a wall thickness exceeding the sizes of active spots of arc column, has been developed. Results of MIAB welding of low-alloyed steel pipes with up to 16 mm wall thickness are presented. Welding equipment for welding thick-walled pipes was subjected to modification.

Key words: magnetically-impelled arc butt welding, heating of pipe edges, joint formation, thick-walled pipes

In world practice different methods of welding are used for welding pipelines, such as manual arc covered-electrode welding, shielded-gas welding, submerged-arc welding, flash butt welding. One of the high-efficient processes, which has found a wide application in construction of small-diameter (up to 100 mm) pipelines with up to 6 mm wall thickness, is the magnetically-impelled arc butt (MIAB) welding [1–4].

The principle of MIAB process consists in that the arc is moved in a gap between edges of parts being welded under the action of external control magnetic field created by magnetic systems. In the above-mentioned method of welding the welding current is changed by a special program. At certain conditions the linear rate of arc movement reaches 200 m/s. Owing to a relatively high rate of welding arc movement, its heat energy is redistributed along the entire surface of the part edges. This results in a relatively uniform heating of the pipe edges welded. The welded joint is formed in compression and combined plastic deformation of edges of pipes welded. The MIAB welding is performed in air without use of shielded gases.

Welding current and arc voltage, which depend on an arc gap length, are the most important technological parameters of the MIAB welding. The gap between edges of pipes welded is usually from 1.5 up to 2.8 mm and belongs to the setting parameters which define arc voltage, energy consumption, mobility of the moving arc.

Technology and equipment, developed at the E.O. Paton Electric Welding Institute, for MIAB welding thick-walled pipes found a wide spreading in welding low-carbon and low-alloyed steel parts in

various branches of industry and construction. Technical characteristics of a range of machines for MIAB welding of pipes are given in Table 1.

Machines MD-102 and MD-103 (Figure 1, *a*) can be used in mobile pipe welding complexes for welding small-diameter pipelines. Clamping, unclamping and upsetting of pipes are realized according to a preset cycle using clamping and upsetting mechanisms [5].

Machine K-872 (Figure 1, *b*) is designed for MIAB welding of different-purpose pipelines in the field conditions. It has a suspended tong-type head, being featured by a separate clamping of pipes being welded [6].

The high efficiency of MIAB welding of thick-walled pipes promoted the widening of fields of its application. One of the new trends in MIAB welding application became the conductance of research and experimental works in welding of thick-walled pipes. For this purpose the welding equipment was subjected to modification.

Known process for welding thick-walled pipes occurred to be unacceptable, because one of the conditions of uniform and stable heating of edges welded is the comparability of pipe wall thickness and sizes of arc column active spots. Figure 2, *a* shows the traces of arc column active spots on internal edges of pipes after their heating in MIAB welding. These traces are smaller than the cross-section of pipe edges. The welding process was instable, with short-circuits. Due to the effect of welding arc magnetic field and existing of a high gradient of external magnetic field induction in the initial moment of heating the arc is forced out from the gap and moved along the internal edges of pipes. In this case the arc column is bent towards the pipe geometric axis. During flashing of inner edges of pipes the arc gap in the place of arc burning is increased, the gradient of distribution of magnetic field induction in the arc gap is decreased and the welding arc is shifted to the external edges of pipes. The large thickness of pipe wall ($\delta = 8$ mm) prevents a stable arc movement to the area of high values of the control magnetic field induction. Non-uniform movement of the welding arc in the area of low values of the control magnetic field induction leads to a non-uniform heating of pipe edges, to metal melting and its flowing out.

The present work gives the results of research works, carried out at the PWI, on the process of MIAB welding of pipes with up to 16 mm wall thickness. The aim of investigations was to find the methods

Table 1. Technical characteristics of machines for MIAB welding

Parameter	MD-102	MD-103	K-872
Diameter of pipes, mm	25–60	57–114	76–219
Pipe wall thickness, mm	2.0–8.0	2.0–10.0	2.5–16.0
Efficiency, weld/h	120	70	20
Time of welding, s	2.5–14	14–22	12–100
Consumed power, kV·A	45	60	150
Mass, kg	440	950	2000

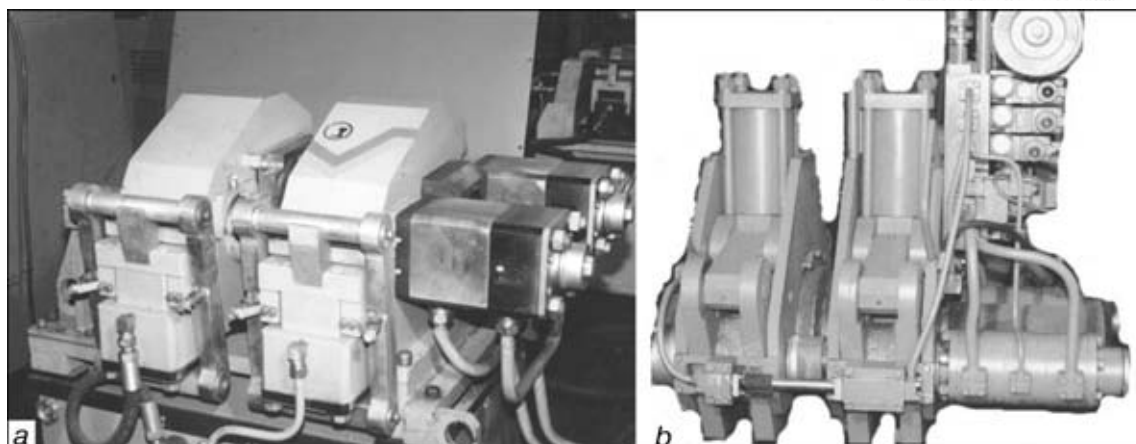


Figure 1. Welding machines of MD-103 (a) and K-872 (b) types

of control which will make it possible to move the arc continuously along the entire area of pipe edge cross-section. It was determined that after arc exciting it is necessary to shift the welding arc to the external edges of pipe to the region of maximum values of magnetic induction and to make it to move there. And this should be realized by creation of an optimum distribution of magnetic field induction in the arc gap. Here, a relative uniform distribution of welding arc heat energy in pipe edges is occurred. At a concentrated heat energy evolution the more uniform heating of pipe edges welded is occurred than in arc movement along the internal edges of the pipes.

Figure 2, *b* shows the traces of arc active spots formed on external edges of the thick-walled pipes after their heating using MIAB welding. Under the effect of external magnetic field the cathode flow of plasma, shifted with respect to opposite anode flow, is moved. The cathode flow of plasma forms anode spot after reaching the anode and then it is shifted. Anode and cathode spots are trying to be arranged opposite each other.

The trace, left by the arc on the edges of pipes after shifting to them, acquires different shapes that is due to change in values and direction of induction that can be due to the change in values and direction of induction of the control magnetic field, electrical and heat processes in places of arc burning, as well as roughness of treatment of the pipe edge surface.

The excited welding arc, controlled by a magnetic field, is shifted to external edges of thick-walled pipes towards the region of maximum values of the magnetic field induction. Here, it begins to move, providing heating of thick-wall pipe surfaces being welded. The welding arc column is bent, here, towards the side opposite to the pipe geometric axis. Owing to the welding arc movement along the external edges of thick-walled pipes their relatively uniform heating is occurred.

The as-welded samples (Figure 2) were cut along the axial line and their surface was subjected to metallographic examination. As the results showed during MIAB welding the microstructure of recrystallizing region in HAZ in the vicinity of external edges of pipes represents a ferritic-pearlitic mixture with a dominating pearlite (Figure 3, *a*). Overheating region is located in HAZ in the vicinity of internal edges.

Its metal is characterized by a coarse-dispersed structure, in which pearlite is dominating. Regions of bainite and ferrite are also observed (mainly in the form of a network, partially in the form of needles of Widmannstätten structure) (Figure 3, *b*).

Microstructure of metal of a molten layer on external and internal edges of pipes is differed noticeably. On the internal edges it represents a ferritic-pearlitic mixture with a dominating pearlite. Ferrite is located in the form of hypoeutectoid precipitations along the boundaries of crystallites and ferrite oriented by Widmannstätten. Content of ferrite in microstructure of external edges is higher than that of pearlite, whose mass fraction is rather small.

During arc movement along external edges of thick-walled pipes the overheating region is located in HAZ in the vicinity of external edges of the pipes (Figure 4, *a*). Microstructure of its metal represents a ferritic network along the boundaries of former grains of austenite, the presence of ferrite, oriented by Widmannstätten, pearlite and a negligible content of bainite is observed. HAZ in the vicinity of internal edges (Figure 4, *b*) is beginning by a region of recrystallizing which is characterized by a fine-dispersed ferritic-pearlitic structure with coarse grains. Microstructure of a molten layer metal on the internal edges

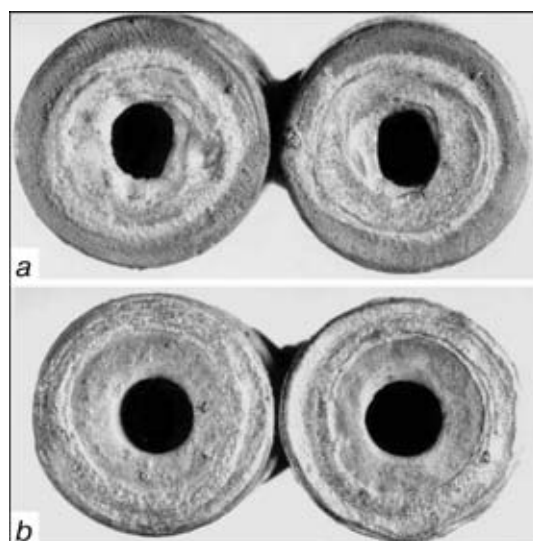


Figure 2. Traces remained by welding arc in movement along internal (a) and external (b) edges of thick-walled pipes ($\delta = 8$ mm)

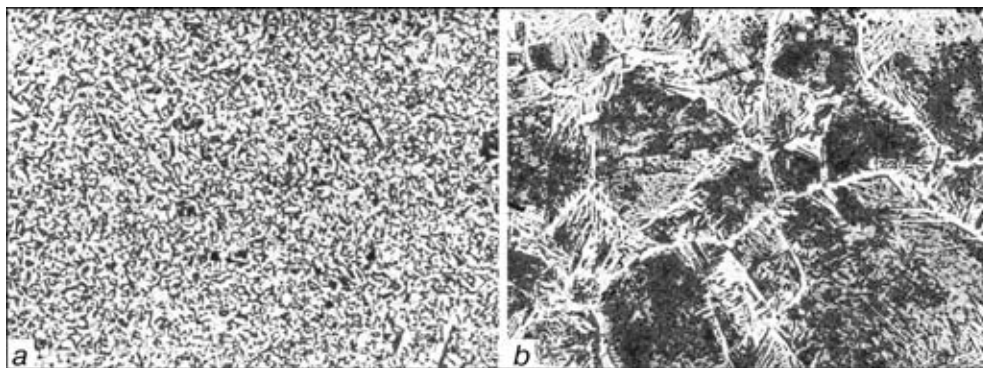


Figure 3. Microstructure of HAZ metal, obtained in arc movement along the internal edges of pipe: *a* — region of recrystallization in the vicinity of external edges; *b* — region of overheating with a coarse-dispersed structure, located on internal edges of pipes ($\times 180$)

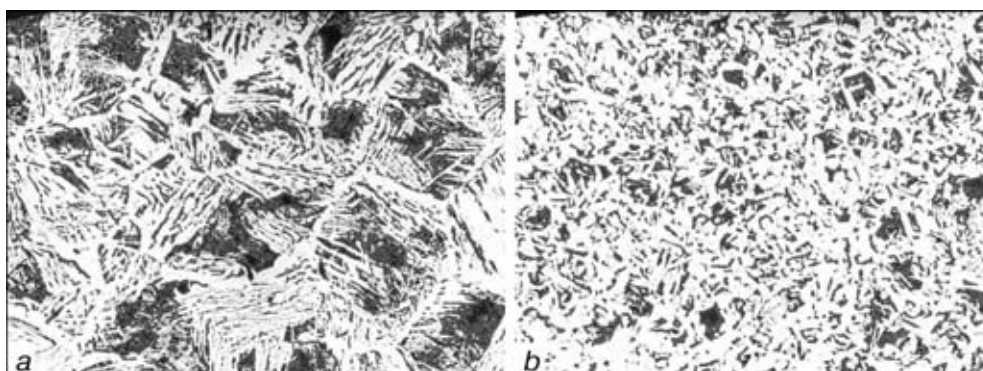


Figure 4. Microstructure of HAZ metal, obtained in arc movement along the external edges of pipes: *a* — region of overheating in the vicinity of external edges; *b* — region of recrystallization with coarse grains, located on internal edges of pipes ($\times 180$)

represents a ferritic-pearlitic mixture in which ferrite is located in the form of precipitations of a hypoeutectoid type and needles of the Widmannstätten structure.

On the external pipe edges the structure of a molten layer metal is differed from that above-described. It represents a ferritic-pearlitic mixture with a dominating ferrite. The larger mass fraction of ferrite is precipitated along the boundaries of crystallites in a hypoeutectoid region.

As a result of comparison of known and new methods of MIAB welding the effect of a long action of welding arc on separate heating surface regions of thick-walled pipes was proved.

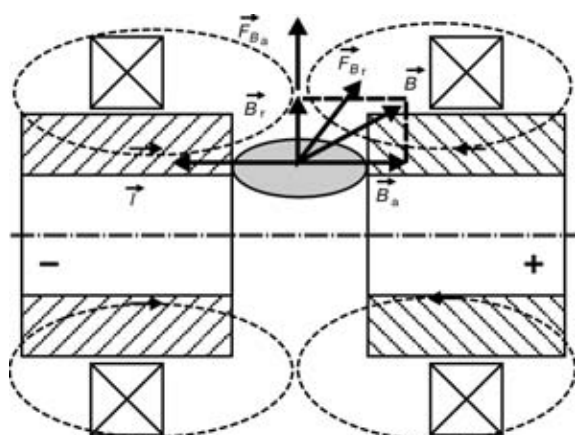


Figure 5. Action of forces determining nature of welding arc movement in MIAB welding; I — arc current component; B — magnetic field inductance; P_{Br} , P_{Ba} — radial and axial components of surface magnetic inductance, respectively; F_{Br} , F_{Ba} — forces affecting radial and axial arc movement along the pipe edges, respectively

At a known MIAB welding process a region of overheating is formed in the vicinity of internal edges after heating, occupying up to 70 % of surface area of the pipe edge section heated. The structure of its metal has a ferrite oriented by Widmannstätten and possesses a decreased deformability. After upsetting the overheating region remains in a central part of the welded joint, thus deteriorating its quality. The use of the known MIAB welding process cannot provide quality welded joints, if the size of arc active spots is smaller than the area of the pipe section welded.

With the new process of MIAB welding the microstructure similar to the above-mentioned is formed on the external edges of pipes. The overheating region occupies up to 30 % area of pipe edge section being heated in the vicinity of external edges. After upsetting the overheating region is removed from the joint zone that favors the weld formation.

The principle of the new MIAB welding process is shown schematically in Figure 5. The edges are

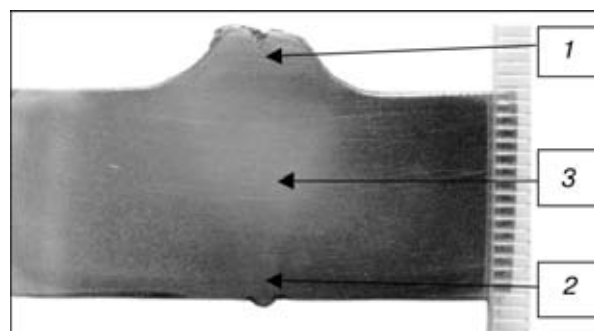


Figure 6. Macrosection of welded joint of pipe ($\delta = 16$ mm): 1-3 — regions which were used for metallographic examination

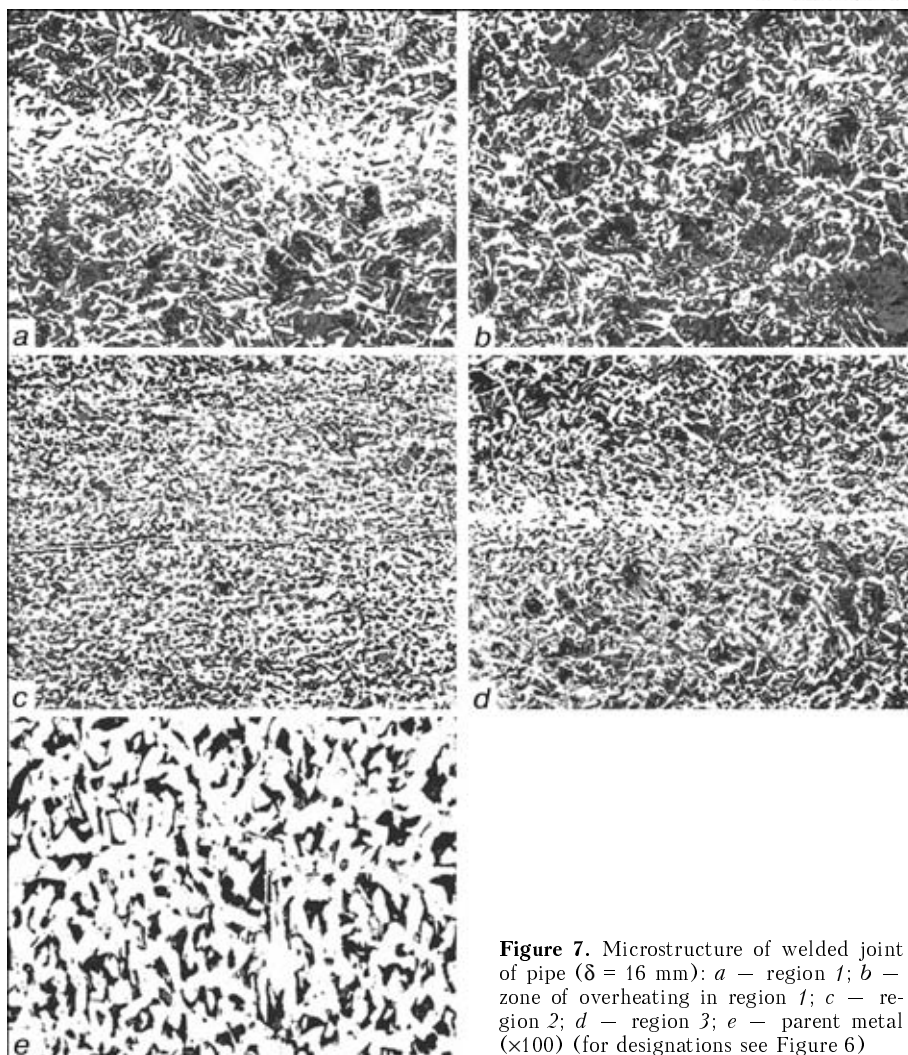


Figure 7. Microstructure of welded joint of pipe ($\delta = 16$ mm): *a* — region 1; *b* — zone of overheating in region 1; *c* — region 2; *d* — region 3; *e* — parent metal ($\times 100$) (for designations see Figure 6)

heated in welding arc movement along the external edges towards the increased values of a radial component \vec{B}_r of control magnetic field induction, thus providing stable movement of the welding arc.

When the heating, corresponding to that required for plastic deformation of pipes, is reached the forces F_{B_s} , F_{B_r} and values of welding current are changed, thus leading to the welding arc scanning along the pipe edge surface. Then upsetting is performed. The investigations resulted in the solution of the main problem: the development of a method with help of which it is possible to move the arc over the entire area of cross section of the pipes.

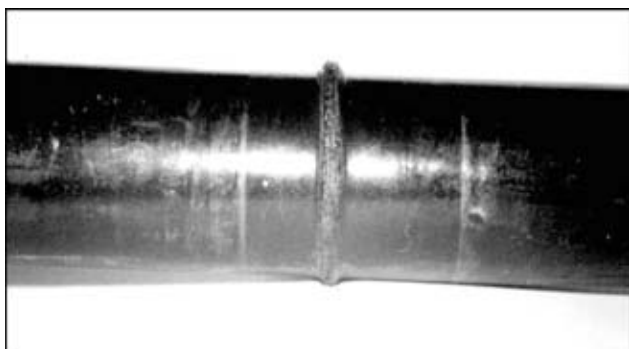


Figure 8. Welded joint of 76x16 pipe (time of welding is 104 s)

As was above-stated, the formation of welded joints of thick-walled pipes in MIAB welding, the same as in other methods of press welding, is occurred at a combined deformation of abutted surfaces of parts heated up to the plastic state. The uniform heating of pipe edges is main, but not sufficient condition for the formation of quality welded joint. In MIAB welding the shielding gases are not, as a rule, used. This leads to the oxidation of pipe edges with air oxygen

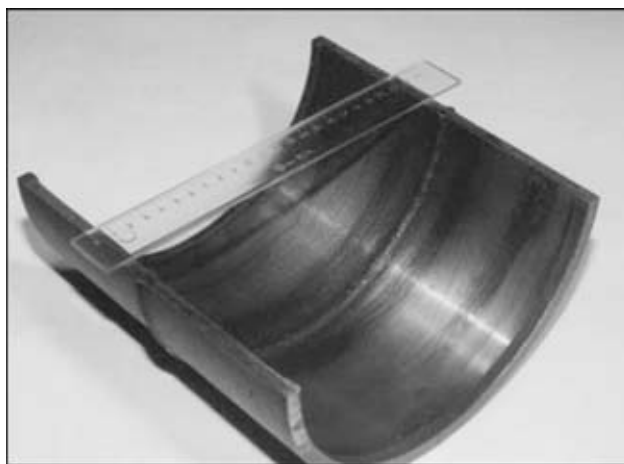


Figure 9. Section of welded joint of 219x8 mm pipe (time of welding is 38 s)

**Table 2.** Mechanical properties of welded joints of thick-walled pipes

Steel grade	Pipe size, mm	σ_t , MPa		KCV, J/cm ²		$\sigma_{0.2}$, MPa
		Parent metal	Welded joint	Parent metal	Welded joint	
St.20	89×12	488–509	488–509	92–100	78–86	290
		502	502	97	82	
	108×8	488–509	486–506	90–100	76–92	305
		502	500	95	84	
St.35	219×8	488–509	488–509	92–100	79–94	295
		502	502	97	85	
	76×16	538–565	538–565	56–64	37–54	345
		551	551	60	44	

Note. In numerator the minimum and maximum values of results obtained at static tensile and impact bend tests are shown, in denominator the mean values are shown.

and to the formation of oxides during the welding process. The removal of oxides is an obligatory condition which should be fulfilled in use of all the types of press welding.

It was established experimentally, that at controllable arc column movement along the pipe edges being welded ($\delta = 16$ mm) it is managed to provide the required frequency of arc movement for keeping melt in a molten state. Oxides together with a molten metal are forced out from the joint zone during the plastic deformation of the pipe edges. The use of the new process makes it possible to produce the welded joints with a minimum inner flash (Figure 6).

Metallographic examination of the steel 35 76×16 mm pipe welded joint was performed after etching in 4 % solution of HNO₃ in alcohol. The microstructure was examined in optical microscope «Neophot-32» at ×100 and ×180.

Hardness of HAZ metal was measured in LECO hardometer at 10, 100 and 1000 g loading. Metallographic measurements were made in different areas of the welded joint (see 1–3 in Figure 6). Microstructure of the welded joint in region 1 represents a ferritic-pearlitic mixture with a dominating ferrite component, a small part of the ferrite is oriented by Widmannstätten (Figure 7, *a*). Width of the welded joint line at the given region is 0.126 mm, hardness is HV₁₀₀ 151–165. HAZ consists of several clearly expressed regions of overheating (3.906 mm width), as well as complete and partial recrystallization (2.268 and 1.638 mm, respectively).

Metal structure of overheating region represents a ferritic-pearlitic mixture with a dominating pearlitic component. Pearlite is precipitated in the form of grains fringed in edges by ferritic precipitations. Most part of the ferrite is oriented by Widmannstätten. Metal of overheating zone (Figure 7, *b*) has hardness HV₁₀₀ 181–199, grain size corresponds to 6, more seldom to 5 mark (GOST 5639–82).

Metal of complete recrystallization region has a ferritic-pearlitic fine-dispersed (mark 10) structure and hardness HV₂₀₀ 170. Metal of partial recrystallization region is characterized by a ferritic-pearlitic structure with a grain size corresponding to mark 7.

At the region 2 (Figure 7, *c*) the microstructure of metal of the welded joint line is ferritic, its width is 0.01 mm, metal hardness is HV₁₀ 201–205. The HAZ consists of regions of complete and partial recrystallization, there is no region of overheating. The width of complete recrystallization region is 1.008, while that of partial recrystallization is 2.394 mm. Microstructure of metal of complete recrystallization region represents a fine-dispersed ferritic-pearlitic mixture with a grain size corresponding to 9–10 marks, metal hardness is HV₁₀₀ 199–220. At the region of a partial recrystallization the presence of ferrite + pearlite with a grain size corresponding to 7–8 marks is observed, metal hardness is HV₁₀₀ 181–196.

Microstructure in region 3 is transitional. Width of welded joint line is 0.0252 mm (Figure 7, *d*). Microstructure of region 3 is ferritic, metal hardness is HV₁₀₀ 192–202. HAZ consists of regions of overheating, and also complete and partial recrystallization. Microstructure of this region of 1.386 mm width is characterized by the finer size of the metal grain, approximately 8 mark. It is ferritic-pearlitic, the most part of the ferrite is oriented by Widmannstätten, metal hardness is HV₁₀₀ 182–199. Microstructure of parent metal is ferritic-pearlitic, grain size corresponds to 7–8 mark, hardness is HV₁₀₀₀ 192 (Figure 7, *e*).

As a result of investigations made using the advanced welding equipment the new method of MIAB welding has been developed for pipes with 16 mm wall thickness (Figures 8 and 9). Mechanical properties of welded joints of pipes are presented in Table 2. Stability of producing quality joints is reached by control of main technological condition parameters directly in the process of welding.

1. Ganovski, F.J. (1974) The magnetarc welding process. *Weld. Met. Fabric.*, **June**, 206–213.
2. Edson, D.A. (1982) Magnetically impelled arc butt welding of thick wall tubes. *Doc. IIW III-726–82*.
3. Takagi, K., Arashida, F. (1982) Magnetically-impelled arc butt welding of gas pipeline. *Metal Constr.*, **10**, 542–548.
4. Kachinsky, V.S., Ignatenko, V.Yu. (1997) Magnetically-impelled arc butt welding of tubular parts (equipment and technology). *Avtomatich. Svarka*, **7**, 39–41.
5. Kuchuk-Yatsenko, S.I., Krivenko, V.G., Ignatenko, V.Yu. et al. *Machine for magnetically-impelled arc butt welding*. Positive decision on appl. 94128094 Ukraine. Filed 20.12.94.
6. Kuchuk-Yatsenko, S.I., Krivenko, V.G., Ignatenko, V.Yu. et al. *Machine for magnetically-impelled arc butt welding*. Positive decision on appl. 98115957 Ukraine. Filed 21.11.98.



SOLID-STATE JOINING OF TITANIUM TO STEEL (REVIEW)

L.S. KIREEV and V.N. ZAMKOV

The E.O. Paton Electric Welding Institute, NASU, Kyiv, Ukraine

Considered are the methods for solid-state joining of titanium to steel with a different degree of the force effect: diffusion bonding, cold welding, inertia friction welding, wedge-press and vacuum press welding, explosion welding, vacuum percussion welding and magnetic-pulse welding. The ways of producing quality joints are described.

Key words: dissimilar joints, diffusion bonding, cold welding, inertia friction welding, wedge-press welding, roll welding, titanium-steel bimetal, explosion welding, vacuum percussion welding

Plastic deformation of all metals in the joining zone, and between titanium and steel in particular, is the imperative condition for formation of a joint using any method of solid-state joining. The rate of deformation determines the intensity of processes which control formation of the joint. Therefore, all the available solid-state joining methods can be conditionally subdivided into three groups by the intensity of their force effect [1].

The first group includes joining methods with a low-intensity force effect (e.g. diffusion bonding in which the rate of deformation of billets being joined is 10^{-4} – 10^{-6} s $^{-1}$). As a rule, these joining processes occur under the creep conditions, where the deformation rate depends upon the process parameters and deformation resistance of the billets.

The second group includes joining methods with a medium-intensity force effect. Such joining processes have a forced character of plastic deformation and occur during a short period of time (often they involve preheating of materials being joined). Here the deformation rate is 10^{-1} – 10^{-3} s $^{-1}$. These methods are most promising among all other solid-state joining methods, as variations of the temperature-force deformation conditions offer the possibility of producing quality joints in many combinations of materials.

The third group includes methods with a high-intensity force effect (explosion welding, vacuum percussion welding, magnetic-pulse welding). These processes are characterised by a high deformation rate (up to 10 s $^{-1}$), short duration (force pulse duration) and involve, as a rule, no preheating of materials joined. The joints usually have low impact toughness and ductility, as the short duration of the force effect restricts the possibility of development of the required processes within the joining zone. However, the short duration of the force effect becomes a positive factor in joining dissimilar metals which interact to form brittle phases. In this case it is necessary to limit or even prevent development of the diffusion processes.

Joining with a low-intensity force effect. Diffusion bonding of metals occurs at a temperature of $T \approx 0.7T_{\text{melt}}$ (T_{melt} is the metal melting temperature) [2]. This ratio is optimal not only for the case of joining commercially pure similar metals or alloys, but also for dissimilar metals and alloys.

Initial investigations on diffusion bonding of titanium to steel are described in [3]. Kinetic characteristics of variation in resistance of layers to separation and elongation of commercial titanium VT1-1 and armco-iron cylindrical samples with a diameter of 6 mm in tensile tests are described in [4]. The authors of this study conducted bonding using process parameters given in Table 1.

Increase in the bonding time (more than 10 min) at 1273 K (mode 6) is accompanied by a dramatic decrease in strength and ductility of the bond. In tensile tests all the specimens fractured in the transition zone. Moreover, after bonding at 1023 and 1173 K the fracture was localised on the contact surface between intermetallic and α -solid solution and partially in the α -phase. In the presence of the over-saturated solid solution or the α + TiFe eutectoid band the fracture occurred particularly in this layer. The bonds exhibited the highest strength with the intermetallic layer 3–5 μ m wide.

In bonding titanium alloy OT4 to steels 12Kh18N10T and 08Kh22N6T the effect of the process parameters on mechanical properties of the bonds is similar in many respects to that found for pure metals (commercial-purity titanium and armco-iron). The possibility was established of producing diffusion bonds between alloy OT4 and steel 12Kh18N10T, and OT4 and 08Kh22N6T, having the tensile strength of 420 and 550–600 MPa, respectively, under the following conditions: $T = 1123$ K, $P = 10$ – 15 MPa and $\tau = 15$ min [3]. Trials on bonding the VT5-1 alloy

Table 1. Parameters of bonding titanium VT1-1 and armco-iron cylindrical samples

Mode No.	Temperature, K	Pressure, MPa	Mode No.	Temperature, K	Pressure, MPa
1	1023	20	4	1173	5.0
2	1073	15	5	1223	2.5
3	1123	10	6	1273	1.0

**Table 2.** Tensile strength of diffusion bonds between titanium and iron (steel) made through vanadium interlayer

<i>Metals joined</i>	σ_t , MPa	<i>Carbon content of iron (steel), wt. %</i>
Fe+V+Ti	300	0.04
08Kh17T+V+Ti	300	0.08
12Kh18N10T+V+Ti	100	0.12

(Ti–Al–Sn system) in a combination with 12Kh18N10T showed the possibility of producing bonds with tensile strength of 280–330 MPa at $T = 1173$ K, $P = 15$ MPa and $\tau = 15$ min.

Diffusion bonding of titanium to steel was considered also in studies [5–7, etc.]. It was shown that direct bonding of commercially pure titanium to steel 12Kh18N10T provided bonds with tensile strength which is not more than 50 % of that of stainless steel (250–270 MPa). Metallography and electron diffraction analysis revealed intermetallics in the contact zone of these bonds. In bonding through a liquid phase [8] ($T = 1358$ K) the bonds had tensile strength of 300 MPa, which corresponds to strength of the solidified eutectic and hardly depends upon the titanium alloy and steel grades. Such bonds are characterised by a high scatter of strength properties and low ductility. The authors of study [3] think that diffusion bonding in vacuum cannot provide bonds with strength and ductility of the base metal in the presence of an intermetallic layer on the contact line, as in this case the adhesion between the layer and the base metal is not strong enough, and the intermetallic is hard and brittle. It is likely that diffusion bonding of titanium to steel through intermediate layers of other metals is more promising.

Prof. G.K. Kharchenko and his colleagues from the E.O. Paton Electric Welding Institute investigated vacuum diffusion bonding of titanium to steel through an interlayer of vanadium, which forms a continuous series of solid solutions with titanium and iron [9]. Interlayers were made from a foil not more than 0.2 mm thick. They were placed between cylindrical samples with a diameter of 12 mm and 30 mm high. Bonding was performed under the following conditions: $T = 1173$ – 1273 K, $P = 2$ – 3 MPa and $\tau = 5$ – 10 min. Results of mechanical static tensile tests of the bonded samples are given in Table 2.

In all the tests the bonds fractured by the brittle mechanism along the interface between iron (steel) and vanadium, which contained vanadium carbides. The latter can be formed even at a temperature of 823 K. Investigation of the contact zone of the Fe+V+Ti bond after diffusion bonding and annealing showed the possibility of formation of titanium carbide with a microhardness of $14.6 \cdot 10^3$ MPa also on the side of titanium [7, 9]. The vanadium interlayer is transparent for chromium which interacts with titanium to form compound $TiCr_2$ [4].

Therefore, the vanadium interlayer alone does not solve the problem of diffusion bonding of titanium to

Table 3. Mechanical properties of diffusion bonds between titanium alloy VT5-1 and steel 12Kh18N10T (with V–Cu interlayer)

<i>Relative thickness of layers*</i>		$\sigma_{0.2}$, MPa	σ_t , MPa	δ , %	ψ , %	<i>Fracture location</i>
<i>Cu</i>	<i>V</i>					
0.02	0.05	296	570	8.4	14.0	Steel
0.03	0.10	310	530	6.7	9.8	Copper
0.03	0.20	320	490	5.3	6.8	Same
0.02	0.70	310	440	5.4	10.5	Vanadium

*Layer thickness to sample diameter ratio.

steel. This problem can be solved by using an extra layer of copper between vanadium and steel [7]. Coefficient of diffusion of carbon into copper is low, and no intermetallic compounds are formed in the vanadium–copper system. Solubility of copper in vanadium at room temperature is about 6 %, while at 1800 K it is about 8 % [10]. Strength of copper ($\sigma_t = 200$ – 220 MPa) and commercial-purity vanadium ($\sigma_t = 380$ – 420 MPa) is much lower than strength of steel 12Kh18N10T ($\sigma_t = 550$ – 600 MPa) or a titanium alloy, e.g. VT5-1 ($\sigma_t = 800$ – 900 MPa). However, the strengthening effect taking place in bonding through soft interlayers [11–13] can increase strength of the bonds to a level much higher than strength of the interlayers.

Studies [5, 6, 14] indicate to a promising future of using vanadium–copper interlayers in diffusion bonding of titanium to steel. The use of the vanadium and copper layers of an optimal thickness, ensuring the contact strengthening effect, provides bonds with a sufficient strength and satisfactory toughness and ductility (Table 3). In this case impact toughness of the bonds is close to the lower limit of impact toughness of one-phase titanium alloys. The bending angle of flat specimens 2 mm thick, cut from bonded rods, amounts to 50–60°. Bonding was performed under the following conditions: $T = 1273$ K, $P = 3$ – 6 MPa and $\tau = 5$ – 15 min. The presence of the copper layer limits the bonding temperature, while the specific pressure and time of bonding are selected so that they provide a minimum deformation of the titanium part of the bond.

To increase technological effectiveness of the bonds, it was suggested that diffusion bonding of titanium to steel should be performed not through two separate layers of vanadium and copper, but through one compact multilayer insert [5–7]. Such inserts were made by rolling using a vacuum rolling mill. To avoid adhesion of copper to the mill rolls and minimise thickness of the layer, copper was placed inside the insert (it was covered with other metals on the two sides: vanadium on the side of titanium and nickel — on the side of steel). The insert was a pack consisting of alternating V–Cu–Ni layers. The pack was rolled at a temperature of 1200 K and deformation of 60–80 %. Thickness of layers of the finished insert was as follows: vanadium — 0.1–0.4, copper — 0.01–

**Table 4.** Optimal friction welding conditions for titanium to steel

Metals welded	Interlayer material	Rotation frequency, s ⁻¹	Compression force, kN		Upsetting, mm
			Initial	Final	
VT1-0 — St.20	Copper	29	17	40	4–5
VT1-0 — 12Kh18N10T	Niobium–iron	27	12	37	5

0.02 and nickel — 0.01–0.05 mm. Diffusion bonding of titanium alloy VT5-1 to steel 12Kh18N10T through such an insert provides the sufficiently high quality of the bonds ($\sigma_t = 430\text{--}560$ MPa, $\delta = 5.5\text{--}8.6$ % and $\psi = 9.8\text{--}32.1$ %). In this case the bonds tested to static tension fractured in nickel or copper.

In the cases where copper cannot be used as an interlayer, as required by conditions of operation of parts consisting of dissimilar metals, it is suggested that it should be replaced by a palladium or chromium layer [7, 15]. The use of vanadium–palladium interlayers shows more promise, as palladium forms solid solutions with vanadium, iron, nickel and chromium, does not form carbides, and has a high ductility. The bonding temperature is 1373–1473 K. Strength of the bonds is determined primarily by the degree of strengthening of palladium (the softest layer in the bond) and is at a level of strength of steel 12Kh18N10T ($\sigma_t = 480\text{--}580$ MPa), retaining satisfactory ductility (12–24 %).

The technology of diffusion bonding of titanium to steel through interlayers has the widest acceptance in manufacture of bimetal joints (transition pieces) in different-application pipelines.

Joining with a medium-intensity force effect.

The methods for joining with a medium-intensity force effect include cold welding, friction welding, low-temperature diffusion bonding, roll welding, etc.

The process of cold welding of metals (including titanium to steel) is considered in detail in studies [7, 16–18, etc.]. Therefore, here we will note only the main technological characteristics of this process.

Welded joints in titanium VT1-0 and steel 12Kh18N10T rods 3 mm in diameter, made with three upsetting operations (up to 80 % titanium is consumed per upsetting), had the following properties: $\sigma_t = 500\text{--}600$ MPa, $\delta = 8\text{--}15$ % and bend angle $\alpha = 60^\circ$. The TiFe phase was revealed in a joint after welding. Its appearance was caused by a local increase in temperature of thin layers of metal within the zone of the joint during the plastic deformation process. The cold welded joints between titanium and steel cannot work at increased temperatures even for a very short time. Thus, at a temperature of 1073 K mechanical properties of the joints dramatically decrease as early as after 10–20 s, and the joints become unserviceable.

The PWI conducted investigations of the process of inertia friction welding of titanium to steel [19].

Table 5. Results of mechanical tests of welded joints between titanium VT1-0 and steel 12Kh18N10T

Interlayer material	Interlayer thickness, mm		σ_t , MPa	Fracture location
	Before welding	After welding		
Niobium	4–6	3–4	340–360	Joint
Iron	3–5	1–2	300–410	Same
Nickel	0.01	—	480–520	Base metal
Copper	0.01	—	480–520	Same
Niobium–iron	4–8	2–5	460–520	»

The main difference of inertia friction welding from the conventional process is in heating the welding location at a decreasing spindle rotation speed, which determines operational peculiarities of the process. In formation of a joint the temperature in it is not in excess of the melting point of the base metal. The joint is formed in a solid phase, diffusion processes develop within the weld zone, and mechanical stirring of contacting metal volumes takes place [20]. Samples with a diameter of 14 mm made from titanium VT1-0 and alloys VT6 (system Ti–Al–V) and VT16 (system Ti–Mo–Al–V) were welded to steels 12Kh18N10T and 20 [19]. Welding was performed in air or argon. However, mechanical properties of the joints were identical in both cases, as the tests were conducted only on the central part of a joint which was not oxidised during welding. Upsetting was provided mostly due to plastic deformation of titanium. Table 4 gives optimal conditions of inertia friction welding of titanium to steel, and Table 5 gives strength properties of the resulting welded joints.

It follows from Table 5 that the highest quality of a joint is achieved in using thin interlayers deposited on steel by the galvanic method. A similar picture is observed in welding titanium VT1-0 to St.20 [7]. It is likely that upon reaching the temperature in the joint which exceeds the temperature of formation of eutectic titanium–copper (1143 K) or titanium–nickel (1228 K), a liquid phase layer is formed in contact, the process of formation and disruption of new bonds stops, and temperature of the joint is established at a level of the temperature of the eutectic. The liquid layer is pressed out during upsetting, and the time of cooling of the welded joint is not enough for intermetallics to form [18]. It should be noted that formation of the eutectic takes place also in welding titanium to iron (steel 12Kh18N10T) without an interlayer. However, mechanical properties of welded joints in this case are much lower (see Table 4). Here the welded joints contain remains of metal of the eutectic composition, and it is these remains that cause brittle fracture of the joints at $\sigma_t = 300\text{--}440$ MPa. In welding through niobium interlayers the zones where steel is mixed with niobium contain microcracks formed at the cooling stage because of substantial differences in linear expansion coefficients of niobium and steel. Strength of such joints is 340–360 MPa,



and fracture in testing the specimens occurs in the weld zone.

Double interlayers are most promising for friction welding of titanium to steel: niobium on the side of titanium and iron on the side of steel 12Kh18N10T, having mean values of linear expansion coefficient comparable with the base metal [19].

Wedge-press welding should also be classed with welding with a medium-intensity force effect [21]. This method of welding steel 12Kh18N10T to titanium is performed through an aluminium or copper interlayer 0.1–0.2 mm thick. The end of the steel billet is machined to a cone (15–20°), and a seat of the similar shape is made in the titanium billet. Welding is performed in argon by heating the billets to 673–723 K through an aluminium interlayer or to 1023–1123 K through a copper interlayer. Bimetal transition pieces made by this technology have strength in their welded part higher than strength in the steel part, which is attributable to a developed contact area.

Studies [22–24] substantiate the possibility of directly joining (without interlayers) titanium to steel by the diffusion bonding process in the range of relatively low temperatures and high joining pressures. A vacuum joining setup with radiation heating and pneumohydraulic mode of pressure transfer was designed and manufactured for practical realisation of this process. Here the maximum pressure applied on the parts joined is 500 kN, maximum heating temperature is 1373 K and working vacuum is $133 \cdot 10^{-4}$ Pa.

Studies [23, 24] show that choice of rational joining parameters should be based on certain peculiarities of the kinetics of processes occurring in the zone of contact of titanium to steel. The dynamic recovery or recrystallisation processes have the highest rate at the initial moment. After formation of a physical contact, they are superimposed by the processes of atomic heterodiffusion, and reactive diffusion begins only after a certain latent period. Duration of the latent period, like the rate of atomic heterodiffusion and dynamic recovery processes, depends upon the temperature. The latent period is characterised by the highest value of the temperature coefficient, and the recovery and recrystallisation processes are characterised by the lowest temperature coefficient. Therefore, decrease in the bonding temperature to 923 K provided the possibility to avoid the reactive diffusion, make the atomic heterodiffusion just to start and heal the most dangerous defects during the optimal bonding time. It was shown that the kinetics of the process considered is affected also by the deformation rate during bonding. For example, increase in the deformation rate provided by using the «free deformation» method [25] leads to a substantial acceleration of the dynamic recovery processes, atomic heterodiffusion and, to a lesser degree, reactive diffusion.

The investigations conducted resulted in the development of optimal conditions for direct joining of titanium to steels 20Kh13 and 12Kh18N10T. The joints have strength equal to that of a less strong

metal, i.e. titanium. The technology developed was employed to make transition pieces used for the manufacture of thermal-electric heaters (fire-bar elements) with a titanium sheath, intended for heating sea water. They passed the entire package of the required tests and exhibited high operational reliability.

Roll welding of titanium to steel can be performed using both vacuum and conventional mills. Low capacity of vacuum rolling mills does not always allow welding (cladding) large billets. In welding using conventional rolling mills, the plates to be welded are placed inside a sealed pack which is purged with inert gas or evacuated during heating to protect metals from oxidation and saturation with nitrogen and hydrogen. Pyrophoric materials are placed sometimes into the pack to combine oxygen and nitrogen. According to the data of [4], shear resistance of the joints between steel 9 mm thick and titanium 3 mm thick (made by rolling at a temperature of 1273 K in vacuum of 10^{-2} – 10^{-3} Pa) grows from 30 to 220 MPa with an increase in deformation from 8 to 30 % per pass. Strips rolled in low vacuum (≈ 1.5 MPa) had low strength and fractured in cutting test specimens.

Comparison of results of vacuum roll welding of titanium VT1-1 to armco-iron and steels of the 3, 5, 45, 09G2S and 12Kh18N10T grades showed a negative effect of carbon on strength of the joints. For example, increase in a carbon content from 0.028 to 0.45 %, other conditions being equal, decreased tensile strength from 260 to 140 MPa. It is likely that carbon, while diffusing to the surface of the joint, forms titanium carbide (there may be no TiFe and TiFe₂ in this case) and causes passivation of the titanium surface. No formation of metallic bonds between the mating surfaces takes place. Using an interlayer of pure vanadium (carbon content is no more than 0.02 %) for welding leads to increase in strength of the joints, and fracture in rupture tests occurs in the titanium layer. In the case of using vanadium of an insufficient purity (containing up to 0.3 % C and 0.6 % Zr) as an interlayer, vanadium carbides may be formed in the welded joint zone, and fracture of the joints will occur particularly at the carbides. Probability of their formation increases with increase in the carbon content of steel. Width of the layer of vanadium carbides in the welded joint zone increases 1.5–2 times with increase in the reduction degree from 20 to 80 %. High mechanical properties ($\sigma_t = 570$ MPa, $a_n = 3$ kJ/m²) of the joints between titanium alloy VT6s and steel 12Kh18N10T are provided by roll welding through a Nb–Cu interlayer at a temperature of 1223 K, the total reduction ratio in three passes being 45–50 %.

It should be noted that annealing for 1 h at 1073 K applied to titanium–steel bimetal produced by roll welding without interlayers leads to decrease in tensile strength to 160–180 MPa, and microhardness of the titanium–transition zone–steel regions is 2500–5000–1000 MPa. In this case the welded joint zone contains TiFe and TiC. Similar treatment of bimetal



with a Nb-Cu interlayer does not decrease and even increases to some extent the value of hardness of the region in the welded joint zone on the titanium side.

The possibility of producing bimetal strips 0.1–0.3 mm thick by cold rolling is reported in [4]. To ensure quality welding, it is required that after degreasing and brush cleaning the reduction in the first pass be 60–65 %. The gas content of titanium should be decreased: oxygen to 0.07 %, hydrogen to 0.008 % and nitrogen to 0.044 %. Both layers in this case should be uniformly reduced (iron should be annealed at 873–923 K).

Joining with a high-intensity force effect. The most typical process of joining with a high-intensity force effect is explosion welding [26–28, etc.]. This process allows production of bimetal billets and parts of almost unlimited dimensions from diverse metals and alloys, including titanium and steel. Many investigators considered the pulse character of interaction of reactive titanium with steel to be the advantage of this welding process. It was concluded on the basis of this consideration, particularly in pioneering studies, that no brittle interlayers could be formed in the explosion welded joints, as the character of interaction of titanium with steel in this case was thought to be similar to that taking place in cold welding. As it was found later on, chemical interaction and even melting at the collision with steel is a rule, rather than exception. Results of experimental studies showed that explosion welding of titanium to steel is characterised by availability of a narrow range of process parameters at which it is possible to provide strong welded joints. Three types of the joints produced at different values of the basic process parameters were revealed [28].

Joints of the first type are characterised by formation of a straight-lined or «sinusoidal interface», containing no regions with a crystallisation structure. The joints of this type are typical for «soft» welding conditions. Joints of the second type are most common, they feature pronounced wave formation and presence of eddy waves. These zones usually comprise regions of the crystallised melt with a dendritic structure, containing shrinkage cracks, discontinuities and cavities. Stirring of metals welded takes place in the eddy zones.

Under the forced conditions (third type) the cast zones are widened to form a continuous layer along the contact line. Therefore, it is necessary to ensure sufficient collision velocities and pressure to remove the surface layer and activate the steel and titanium surfaces, on the one hand, and make welding conditions sufficiently «soft» to provide the joints of the first type (without considerable melts), on the other hand.

Steel-titanium bimetal can be produced by explosion welding, avoiding transition diffusion zones and defects, the static tensile strength of the joints being 350–500 MPa. At an optimal detonation rate of an explosive equal to 1850 m/s and a welding gap of

3–4 mm, strength of the resulting joints in plates of titanium VT1-0 2 mm thick and St.3 10 mm thick was about 550 MPa [26]. In this case the joining line had a sinusoidal shape and contained no cast regions. It is noted in this study that in the case of welding by the angular method the interface has a distorted wavy shape and cast regions which contain cavities and contaminants. In addition, the welded joint zone on the titanium side has local cast regions of increased hardness, which seem to cause decrease in strength of the joints to 320 MPa.

The conclusion made in study [27] is that it is necessary to minimise the velocity of the contact point. The joints between titanium and steel produced by the angular method also comprised cast regions of inclusions with hardness of *HV* 8000–9200 MPa. Microanalysis showed that composition of the cast regions corresponded to composition of a TiFe_2 compound. The joints with cast inclusions at the wave peaks have rupture strength of 330–390 MPa. At the same time, samples with a wavy shape of the joining zone, but having no cast inclusions, exhibited rupture strength of 40–100 MPa at the absolute absence of visible intermetallic compounds. Therefore, this study did not reveal a direct relationship between the amount of intermetallic compounds and strength of the welded joints.

The effect of the velocity and energy of collision of plates on strength of welded joints was considered in study [26]. Increase in the collision velocity above an optimal value leads to formation of a brittle «white phase» (eutectic TiFe_2) and increase in wave parameters. Further increase in the collision velocity causes increase in surface area of the «white phase» regions and formation of cavities and cracks in these regions. A factor which affects formation of the «white phase» is not the velocity, but the energy accumulated in it prior to collision [29]. Thickness of the brittle layer may vary 1.5–2 times at the same collision velocity and at thickness of the titanium plate 2 and 6 mm (i.e. different energy). Composition and structure of the «white phase» do not depend upon the collision parameters. Microhardness within the range of each inclusion remains constant and ranges from 880 to 9400 MPa. The experimental studies showed that at a detonation front propagation velocity of 1800 m/s the brittle interlayer is formed in the joints at a collision velocity higher than 800 m/s [26]. At a collision velocity of 1500 m/s the relative area of intermetallic inclusions is 50 %, this exerting a substantial effect on strength characteristics of the joints between titanium VT1-0 and St.3 ($\sigma_t = 280$ MPa). Study [27] describes production of a similar joint with a high strength ($\sigma_t = 550$ MPa) at a collision velocity of about 550 m/s.

A more specific conclusion of tolerable values of the collision energy which exerts no effect on strength of the joints is made in studies [29–31], based on investigations of joining steel to titanium and zirconium to steel 08Kh18N10T (forming similar interme-



tallic compounds). A critical value of the specific kinetic energy of collision for the steel–titanium pair is 1500 kJ/m^2 , which corresponds to a collision velocity of 320 m/s [32].

Therefore, the collision velocity equal to $300\text{--}500 \text{ m/s}$, depending upon thickness of a flyer plate (so that the specific kinetic energy of collision is not in excess of its critical value), can be considered optimal for explosion welding of titanium to steel [33].

Properties of the titanium–steel bimetal produced by explosion welding are substantially affected by subsequent postweld heat treatment [28]. At heating temperatures of $373\text{--}873 \text{ K}$, rupture strength of the joints between titanium VT1-0 to steels 3 and 12Kh18N10T hardly changes, compared with its strength in the as-explosion welded condition. At heating temperatures of $873\text{--}1273 \text{ K}$ the strength of the bimetal joint dramatically decreases to $10\text{--}40 \text{ MPa}$. Investigations of welded joints showed an increased hardness ($HV 3000 \text{ MPa}$) of titanium at a depth of $0.1\text{--}0.3 \text{ mm}$ and steel at a depth of 0.1 mm , which is indicative of strain hardening of metals taking place in the welded joint zone. Tempering at a temperature of 573 K for 1 h decreases hardness to $HV 2500\text{--}2000 \text{ MPa}$. However, the character of microstructure of the joining zone hardly changes in this case. Heating to a temperature of 1123 K with holding for 1 h leads to formation of a light interlayer of increased hardness ($HV 3700\text{--}4200 \text{ MPa}$) in the titanium–steel joining zone. Thickness of the interlayer increases with increase in the annealing temperature.

Investigations conducted by different authors suggest that while the explosion welded joints between titanium and steel (without interlayers), when static tension tested, fracture in the base metal at a distance from the joint zone, they nevertheless can have a reliable operation, but only at temperatures not higher than 773 K . It is possible to use one or two interlayers in explosion welding, depending upon the application of the weldments. Single interlayers are made from silver, nickel, copper, vanadium, niobium, iron or alloys of iron with refractory metals. To decrease the probability of formation of brittle compounds at the interface, it is recommended to use the iron layer with a carbon content of not more than 0.02% [7]. Two interlayers, niobium and copper, are most often used in explosion welding. Niobium, copper or copper alloys are employed in the form of a finished composite interlayer produced by rolling. Principles of variations in mechanical properties of the titanium alloy OT4/niobium–copper alloy/steel 12Kh18N10T composite material, depending upon thickness of the copper alloy interlayer, are investigated in [34]. As shown by the test results, decrease in thickness of this layer is accompanied by increase in strength of the joint, which reaches its maximum value at a copper layer thickness below 0.1 mm . Heating of the produced welded joint to 1073 K does not change the character of its fracture, but decreases strength, as it

leads to complete elimination of hardening of metals resulting from explosion loading during welding.

The PWI developed the method for welding with a high-intensity force effect [35]. The main point of this method is that a single force pulse produced by a striker moving at a velocity of 1 to 30 m/s is transferred to the mating surfaces locally preheated to a temperature above $0.5T_{\text{melt}}$. This results in collision of the heated surfaces in vacuum, their local deformation and formation of a welded joint in hundredths or even thousandths of a second. Besides, this leads to creation of favourable conditions for joining dissimilar metals and reduces the probability of formation of intermetallics. In literature this method is described as vacuum percussion welding [36–38, etc.].

Main technological parameters of vacuum percussion welding include temperature and impact energy which provides the required high-rate deformation of metal volumes in the near contact regions. Heating of billets to a welding temperature T_w is performed at a rate of about 20 K/s to ensure local heating of the contact zone. The time of exothermic holding is chosen on the basis of uniform heating of metals through thickness of the contact zone and cleaning of the metals from oxides and contaminants. The cooling time depends upon the welding parameters, size of parts and accepted technology. Investigation into different types of the impact mechanism (powder-charge drop hammers, linear motors, etc.) showed that the free falling weight or weight falling at a forced acceleration is the most practicable type of the striker. Vacuum percussion welding is applied to advantage for the manufacture of tubular transition pieces from dissimilar materials. High performance of a tubular titanium–steel transition piece can be provided by joining two tubes heated by means of circumferential forging and creating local vacuum in the joint using a special sleeve [39]. In this case the sleeve is forged together with the titanium and steel edges to be welded. It was found using a microprobe that the diffusion transition zone up to $8 \mu\text{m}$ thick contains intermetallic compounds TiFe , TiFe_2 , Ti_2Ni , TiNi and TiCr_2 . Titanium penetrates but slightly into steel through the diffusion zone, while iron, chromium and nickel diffuse into titanium to a considerable depth.

Forge welding can be regarded as an analogue of the above method, the only difference being that in the case of percussion welding the metal is preheated to T_w only in the contact zone. Forge welding has two essential drawbacks: considerable width of the intermetallic layer leads to formation of defects in the joint, and machining is required to remove the steel sleeve after forging to produce a finished tubular transition piece.

1. Karakozov, E.S., Orlova, L.M., Peshkov, V.V. et al. (1977) *Diffusion welding of titanium*. Moscow: Metallurgiya.
2. Kazakov, N.F. (1976) *Diffusion welding of materials*. Moscow: Mashinostroenie.
3. Garukhina, K.E., Kazakov, N.F. (1964) *Vacuum diffusion welding of dissimilar metals*. Leningrad: LDNTP.



4. Charukhina, K.E., Golovanenko, S.A., Masterov, V.A. et al. (1970) *Bimetallic joints*. Moscow: Metallurgiya.
5. Gurevich, S.M., Kharchenko, G.K. (1967) Diffusion welding of titanium alloys with stainless steels. *Aviats. Promyshlennost*, **10**, 85–88.
6. Kharchenko, G.K. (1969) Problems of diffusion welding of dissimilar metals. *Avtomatich. Svarka*, **4**, 29–32.
7. (1986) *Metallurgy and technology of welding of titanium and its alloys*. Ed. by V.N. Zamkov. Kyiv: Naukova Dumka.
8. Kharchenko, G.K. (1965) Eutectic joint of titanium to steel. *Avtomatich. Svarka*, **11**, 78.
9. Kharchenko, G.K., Gordonnaya, A.A. (1966) Diffusion welding of titanium to steel with vanadium interlayer. *Ibid.*, **6**, 74–75.
10. Savitsky, E.M., Baron, V.B., Dujsemaliev, U.K. et al. (1964) Vanadium-copper constitutional diagram. *Vestnik AN Kazakh. SSR*, **7**, 37–44.
11. Bakshi, O.A., Shron, R.Z. (1962) On problem of strength evaluation of welded joints with soft interlayer. *Svarochn. Proizvodstvo*, **9**, 11–14.
12. Bakshi, O.A., Shatov, A.A. (1966) On stress state and deformation of solid material in welded joints with hard and soft interlayers. *Ibid.*, **5**, 7–10.
13. Bakshi, O.A., Shron, R.Z. (1971) On estimation of strength of welded joints with soft interlayer. *Ibid.*, **3**, 3–5.
14. Kharchenko, G.K., Ignatenko, A.I. (1968) Strength of joints with thin soft interlayer. *Avtomatich. Svarka*, **5**, 31–33.
15. Kochergin, A.K., Shestakov, A.I., Kharchenko, G.K. (1972) *Pressure welding of sealed surfaces of valves*. Leningrad: LDNTP.
16. Sakhatsky, G.P. (1979) *Technology of welding of metals in solid state*. Kyiv: Naukova Dumka.
17. Aajbinder, S.B. (1957) *Cold welding of metals*. Riga: AN Latv. SSR.
18. Kharchenko, G.K., Gursky, P.I., Gordonnaya, A.A. (1965) Cold welding of titanium to steel. *Avtomatich. Svarka*, **9**, 39–41.
19. Kharchenko, G.K., Prodan, S.K. (1983) Inertia friction welding of titanium to steel. *Ibid.*, **4**, 70.
20. Seleznyov, A.G., Khristoforov, A.I., Mozharov, M.V. et al. (1970) Examination of transition layer structure in friction welding using radioactive isotope. *Ibid.*, **1**, 21–24.
21. Kolesnichenko, V.A., Shnurev, G.D., Alyokhin, V.P. (1973) Wedge-press welding of dissimilar metals with drastically different and similar hardness. In: *Lectures on welding of dissimilar and different metals*. Moscow: MDNTP.
22. Kireev, L.S. (1985) Vacuum pressure welding of commercial titanium to 2Kh13 and 12Kh18N10T steels. *Avtomatich. Svarka*, **3**, 56–57.
23. Larikov, L.N., Belyakova, M.N., Bibikin, A.A. et al. (1984) Causes of decrease of titanium-steel welded joints strength. *Ibid.*, **4**, 17–19.
24. Zamkov, V.N., Larikov, L.N., Belyakova, M.N. et al. (1986) Diffusion processes in vacuum pressure welding of titanium to stainless steel. *Ibid.*, **3**, 21–23.
25. Larikov, L.N., Belyakova, M.N., Kireev, L.S. et al. (1982) Peculiarities of stress-strain state of diffusion welded joints in dissimilar metals. *Ibid.*, **12**, 13–17.
26. Sedykh, V.S., Kazak, N.N. (1971) *Explosion welding and properties of welded joints*. Moscow: Mashinostroenie.
27. Karpener, S. (1976) *Explosion welding of metals*. Minsk: Belarus.
28. Kudinov, V.M., Koroteev, A.Ya. (1978) *Explosion welding in metallurgy*. Moscow: Metallurgiya.
29. Lysak, V.I., Sedykh, V.S., Trykov, Yu.P. (1981) Influence of mass of explosion welded components on structure and properties of produced joints. *Svarochn. Proizvodstvo*, **6**, 15–17.
30. Lysak, V.I., Sedykh, V.S., Trykov, Yu.P. (1983) Principle of weld formation in explosion welding of sandwich-type composites. *Ibid.*, **3**, 4–6.
31. Trykov, Yu.P., Shmorgun, V.G., Epishin, E.Yu. (2001) Structure and properties of explosion welded titanium-steel bimetal after hot rolling. *Izv. Vuzov, Chyorn. Metallurgiya*, **7**, 67.
32. Lysak, V.I., Sedykh, V.S., Trykov, Yu.P. (1984) Determination of critical limits for explosion welding processes. *Svarochn. Proizvodstvo*, **5**, 6–8.
33. Konon, Yu.A., Pervukhin, L.B., Chudnovsky, A.D. (1987) *Explosion welding*. Moscow: Mashinostroenie.
34. Belousov, V.P., Sedykh, V.S., Trykov, Yu.P. (1971) Mechanical properties of titanium-steel explosion welded joints with interlayers. *Svarochn. Proizvodstvo*, **9**, 19–21.
35. Kharchenko, G.K., Ignatenko, A.I. *Pressure welding process*. USSR author's cert. 404588, Int. Cl. B 23 K 19/00. Publ. 1974.
36. Gurevich, S.M., Kharchenko, G.K., Ignatenko, A.I. (1974) Vacuum percussion welding — new process of joining materials in solid state. In: *Proc. of 4th All-Union Seminar on Welding of Refractory Metals and Alloys*. Kyiv: PWI.
37. Gurevich, S.M., Kharchenko, G.K., Ignatenko, A.I. et al. (1977) Intensification of pressure welding process. In: *Abstr. of 8th Sci.-Techn. Conf. on Diffusion Bonding of Metallic and Non-Metallic Materials*. Moscow: PNILD-SV.
38. Gurevich, S.M., Kharchenko, G.K., Ignatenko, A.I. (1983) New method of pressure welding of dissimilar materials. In: *Proc. of 8th All-Union Seminar on Welding of Dissimilar, Composite and Multilayer Materials*. Kyiv: PWI.
39. Volta, G., Perona, G. *La soudure par martelage*. Pat. 1450315 France. Publ. 19.10.65.



VACUUM DIFFUSION BONDING OF CHROMIUM TO COPPER

G.K. KHARCHENKO¹, Yu.V. FALCHENKO¹, O.A. NOVOMLINETS¹ and V.F. GORBAN²

¹The E.O. Paton Electric Welding Institute, NASU, Kyiv, Ukraine

²I.M. Frantsevich Institute for Materials Science Problems, NASU, Kyiv, Ukraine

The technology for vacuum diffusion bonding (VDB) of chromium to copper has been developed to manufacture bimetal cathodes used for making wear-resistant friction layers and decorative coatings. It has been established that VDB results in deposition of copper on chromium in the contact zone. The mechanism of deformation of the perforated copper interlayer has been studied. The use of such an interlayer is shown to hold promise for VDB of chromium to copper.

Key words: *vacuum diffusion bonding, chromium, copper, perforated interlayer, deformation*

Development of the technology for joining chromium to copper is associated with the industrial demand for bimetal cathodes up to 80 mm in diameter intended for vacuum chromium sputtering. It should be noted that no data on vacuum diffusion bonding (VDB) of chromium to copper are available in literature. These metals greatly differ in their physical-chemical and mechanical properties, are characterised by an insignificant mutual solubility and, according to constitutional diagram, form no intermediate compounds [1].

Continuous interlayers (CI) in the form of coatings, foils, screen or powder materials are used in VDB of dissimilar materials to activate mating surfaces and enhance diffusion processes [2]. In the another modification of VDB the use is made of perforated interlayers (PI) of copper or pure aluminium [3–6] to intensify the process of formation of bonds and improve strength characteristics of metal-ceramic joints.

This study considers three variants of formation of bonds in VDB of chromium to steel: without interlayer (Cr–Cu), using a continuous copper interlayer (Cr–CI–Cu) and using a perforated copper interlayer (Cr–PI–Cu).

Optimisation of the VDB conditions and investigation into peculiarities of deformation of interlayers were conducted on 2×10×10 mm samples of low chromium alloy VKh-2K and copper M1. The mating surfaces were degreased and scraped prior to bonding. The interlayers were made from annealed copper M1 0.3 mm thick. Preparation of PI consisted in deposition of a rectangular coordinate grid on the foil and drilling of holes. Perforation coefficient K_p equal to 0.2 was selected according to recommendations given in studies [4–6]: $K_p = \Sigma S_h / S_b$ (ΣS_h is the total area of the holes and S_b is the area of the bonding surface).

Deformability of chromium, copper, CI and PI, as well as kinetics of filling the holes with thickness of PI varied by upsetting were investigated on microsections using optical microscope «Neophot-32».

As established by the investigations, the degree of deformation of CI was 30 % lower than that of PI in bonding under optimal conditions.

It is shown in [4–6] that deformation of thin interlayers with the pressure–shear deformation diagram is realised on PI, rather than on CI. Compared with CI, the rate of plastic deformation of PI is 15–30 times higher, and values of shear deformations in the near-contact volumes are tens of times higher. This suggests that the regions of high concentrations of defects (vacancies, dislocations) are formed, the mass transfer has an abnormally high rate and chemical reaction rates increase in structure of the near-contact volumes of the materials during VDB through PI. The above factors lead to activation of physical-chemical processes of interaction between the materials bonded [4].

Investigations of deformability of the copper PI and kinetics of filling the holes showed that in our case the mechanism of deformation of PI differed from that described in [4–6], where PI was placed between two hard materials, and thickness of a soft PI decreased to such an extent that the material of the interlayer fully filled the holes made in it. In our case the holes in PI were filled not only with the material of the interlayer proper, but also with the material of the copper billet (Figure 1).

As established, in bonding the samples of the above sizes at $K_p = 0.2$ the major part of the volume of a hole is filled with the interlayer material, i.e. the intensive shear deformation is fixed in the near-contact volumes of the metals joined, which causes formation of a quality bond between chromium and copper (Figure 2).

Dissolution of air gases in metal is known to cause rarefaction in the sealed gap separating the mating surfaces prior to bonding [7, 8]. Study [7] established the fact of sublimation of nickel and its subsequent deposition. It can be suggested that in the case of VDB of chromium to copper using the copper PI the process of sublimation of copper or chromium followed by its deposition should occur in the sealed gaps (locations of holes in the interlayer). This coat-

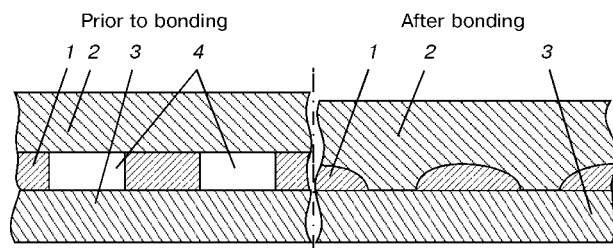


Figure 1. Schematic of filling the holes in PI: 1 – copper PI; 2 – copper; 3 – chromium; 4 – location of holes in PI

ing provides intensification of formation of the volumetric interaction zone in VDB of metals [2].

It should be noted that a marked evaporation of copper in vacuum of 1.33 Pa begins at a temperature of 946 °C, while evaporation of chromium begins at a temperature of more than 1100 °C [9, 10]. The interlayer gap in the parts to be solid-state joined, which are pressed in air prior to heating, can be considered to be a sum of sealed microvolumes filled with air. Self-cleaning of the surface from oxides, formation of vacuum and sublimation of metal take place in these microvolumes during heating [8].

The following experiments were conducted to study the processes occurring in closed sealed microvolumes of the chromium–copper vacuum diffusion bonds. Bonded were the plates of chromium and copper with a copper ring located between them. The ring provided a gap between the chromium and copper plates. After bonding ($T = 950\text{ °C}$, $P = 8\text{ MPa}$, $t = 20\text{ min}$) the samples were cut and the chromium surface was examined. Visual examination and scanning electron microscopy of the chromium surface using the JSM-840 microscope revealed the deposited copper layer on chromium.

Based on analysis of the results obtained and considering the data of studies [7–10], it can be suggested that the process of VDB of chromium to copper occurs in three stages: auto-evacuation of the sealed gaps in the bond, deposition of copper on chromium and bonding of copper to chromium through the deposited copper layer.

The copper part of the bond was shear tested and thermal conductivity of the bimetal bond was evaluated.* It was established as a result of this work that in the case of bonding using PI the shear force was a bit higher (up to 15 %) than in bonding using no interlayers, whereas thermal conductivity of the bond was 60 % of that of copper.

After optimisation of bonding conditions on model samples, these conditions, as well as the perforation coefficient were adjusted with respect to actual sizes

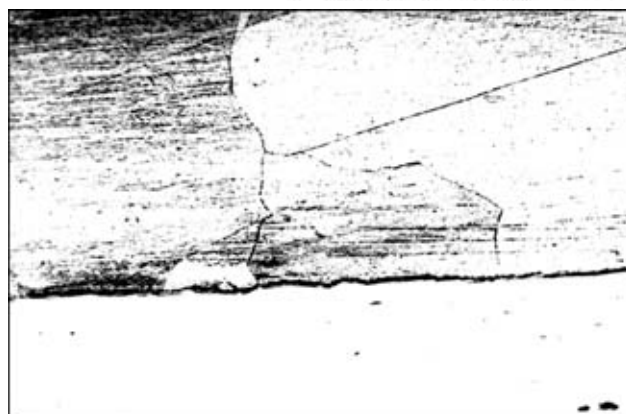


Figure 2. Microstructure of the chromium–copper bond made using the perforated copper interlayer (×100) (reduced by 2/3)

of bimetal units (up to 80 mm in diameter and up to 65 mm high). The use of the copper PI and special fixture allowed plastic deformation to be localised in the bond zone and the quality bond to be produced at a degree of deformation of the copper part of the cathode equal to no more than 5 %.

CONCLUSIONS

1. Deposition of copper on chromium was found to take place in the contact zone during VDB.
2. The use of the copper PI in VDB of copper to chromium leads to intensification of shear deformations taking place in the near-contact volumes of metals bonded.

1. Barabash, O.M., Koval, Yu.N. (1986) *Structure and properties of metals and alloys*. Kyiv: Naukova Dumka.
2. Lyushinsky, A.V. (2001) Criteria of selection of interlayers in vacuum diffusion bonding of dissimilar materials. *Svarochn. Proizvodstvo*, **5**, 40–43.
3. Lyamin, Ya.V., Karakozov, E.S., Musin, R.A. *Method of pressure joining with preheating*. USSR author's cert. 1463415, Int. Cl. B 23 K 20/16. Publ. 30.01.89.
4. Musin, R.A., Lyamin, Ya.V. (1991) Application of perforated interlayers in diffusion bonding. *Svarochn. Proizvodstvo*, **2**, 2–4.
5. Lyamin, Ya.V. (1998) *Development of methods for intensification of diffusion bonding process and increase in strength of metal–ceramic bonds*. Synopsis of Thesis for Cand. of Techn. Sci. Perm.
6. Lyamin, Ya.V., Musin, R.A. (1994) Deformability of perforated interlayers in diffusion bonding. *Svarochn. Proizvodstvo*, **6**, 24–26.
7. Tkachenko, E.V., Medovar, B.I., Bojko, G.A. et al. (1986) Sublimation of nickel in closed space in heating. *Problemy Spets. Elektrometallurgii*, **2**, 17–18.
8. Kuchuk-Yatsenko, S.I., Kharchenko, G.K., Falchenko, Yu.V. et al. (1998) Self-cleaning of solid-phase mating surfaces from oxides in heating. *Avtomatich. Svarka*, **2**, 16–24.
9. Salli, A., Brendz, E. (1971) *Chromium*. Moscow: Metallurgizdat.
10. Kabanov, N.S., Slepak, E.Sh. (1970) *Technology for resistance butt welding*. Moscow: Mashinostroenie.

*The work was performed by Dr. B.M. Rassamakhin (National Technical University «KPI»).



MASS TRANSFER PROCESSES IN PRESSURE JOINING OF DISSIMILAR METALS

L.I. MARKASHOVA, V.V. ARSENYUK, G.M. GRIGORENKO and E.N. BERDNIKOVA

The E.O. Paton Electric Welding Institute, NASU, Kyiv, Ukraine

Considered are the principles of basic physical-chemical processes (plastic deformation, mass transfer, phase formation) accompanying formation of joints in dissimilar materials (copper, titanium, aluminium and their alloys, as well as different grades of steels) characterised by a limited mutual solubility under pressure joining conditions for a wide range of external loading rates ($1 \cdot 10^{-4}$ – $1 \cdot 10^3$) s^{-1} .

Key words: strain rate, plastic deformation, stresses, segregations, diffusion, dislocations, mass transfer mechanisms, mass flows, phase formation

The field of application of joints in dissimilar metallic materials, most of which are made by different methods of pressure joining, is limited because of their decreased mechanical and a number of other service properties. The latter is usually related to susceptibility of this type of the joints to brittle phases formed during the joining process along the contact surface [1, 2]. Brittle phases may be of many types, such as eutectoid and eutectic mixtures, metastable solid solutions, intermetallics of a different degree of dispersion, etc. [3]. Formation of such phases is induced by the effect of certain thermal-deformation conditions of joining, while the kinetics and mechanism of this process are thought to be the result of mass transfer caused directly by the temperature impact [4, 5]. However, lately the mass transfer effects have been related also to the effect of joining distortions and stress field gradients formed at the front of the effective external joining stresses [6]. Unfortunately, the data on the relationship of the phase formation and mass transfer processes under the pressure joining conditions, and especially on the effect of a character of plastic deformation as the main joining process parameter on principles of mass transfer within the joining zone, are very scanty.

In this connection, it seems topical to conduct more detailed experimental studies and analyse correlation of factors which can be arranged into a cause-effect chain: plastic deformation–mass transfer–phase formation–service characteristics of the joints. This study gives some of the results of the investigations performed in the above areas.

Experimental procedure and materials. The study was performed on the joints in dissimilar metals and their alloys characterised by a limited mutual solubility, such as titanium VT1-0, copper M-0 and M-1, commercial-purity aluminium AD-1, strengthened Al–Cu alloy 1201 and different grades of iron and steel.

Peculiarities of mass transfer and phase formation in the contact zone of a joint in dissimilar metals were investigated using a set of complementary methods, such as optical microscopy to give a general idea of the structure; methods of radioactive tracers which

include layer-by-layer autoradiography and measurement of integrated activity; analytical scanning electron microscopy to investigate the general character of distribution of specific chemical elements (photography in characteristic radiation); and element analysis in local regions of the contact zone Philips microscope SEM-515). In addition, the use was made of direct investigations of a fine structure combined with microdiffraction analysis of composition of phase formations by transmission electron microscopy (JEOL microscope JEM-200CX) at an accelerating voltage of 200 kV. Besides, a special ion thinning method was developed, which allowed preparation of very large fields for investigations to be performed directly within the contact zone of dissimilar metals.

Also, peculiarities of mass transfer and phase formation were investigated in production of dissimilar joints under thermal-deformation conditions identical to those used to reveal principles of plastic deformation.

Investigation results. The investigation results obtained by the radioactive tracer methods combined with methods of analytical scanning and microdiffraction electron microscopy showed the following. Under conditions of low rates of joining deformation characteristic of diffusion bonding (DB), the radioactive tracer methods revealed a substantial increase in the rate of mass transfer taking place in the contact zone, which was proved by variations in the coefficient of diffusion of metal atoms. The effective diffusion coefficient in this zone is comparable with the grain-boundary and surface diffusion coefficients. However, diffusibility dramatically decreased through depth δ of the deformed metal zone, and at a distance of about 7–10 μm from the mating surfaces of the materials joined it decreased 150–200 times, which is described in detail in [7]. That study proves that preliminary machining of the mating surfaces favours increase in the intensity, as well as in-depth widening of the active mass transfer region, which is initially caused by an increased density of crystalline lattice defects in mechanically polished surfaces and subsequent active redistribution of these defects under thermal-deformation conditions of DB.

More detailed parallel investigations of a fine structure of the contact zone revealed relationship between the mass transfer processes and mobility of

the crystalline lattice defects, which is the case of structures of the diffusion bonds between copper and titanium, as well as the joints between steels 3 and 12Kh18N10T made by roll welding (RW) through a nickel interlayer (Figures 1 and 2). Figure 1 shows the process of formation of segregations and finely dispersed intermetallic phases at individual dislocations in the sliding systems of copper, as well as sub- and intergranular boundaries in titanium in the copper to titanium bonds. The process of phase formation in the St.3 to 12Kh18N10T joints looks the same (Figure 2). The given structure of cross sections of the contact zone in metals joined illustrates sequence of stages of formation of extended intermetallic phases. These stages include formation of segregation clusters of a different density at individual dislocations, appearance of discrete islands of the new phases and, finally, subsequent coalescence of the phase islands accompanied by growth of the extended intermetallics directed, as a rule, along the sub- and intergranular boundaries.

Revealed also were some peculiarities of mass transfer characteristic of the high-rate deformation methods under conditions of vacuum percussion (VPW), magnetic-pulse (MPW) and explosion welding (EW).

Thus, it was established that, when coming to the high-rate deformation methods, proceeding from structural, concentration and phase changes, in addition to an obvious role of dislocations being the main channel of mass transfer, this process exhibits also a bit different character. For example, electron microscopy conducted under different conditions (secondary electrons, characteristic radiation) on sections reveals displacement of metal layers in the immediate vicinity to the mating surfaces in a direction of action of external welding stresses in the magnetic-pulse welded joints between copper and aluminium (Figure 3, *a*). These layers have the form of isolated, clearly defined microvolumes. Some of them are adequate in the reflection intensity to the base metal, while others behave as regions of a transient contrast, which is attributable to changes in concentration relationships of elements in the displacing layers (Figure 4).

In addition, transfer of individual ultra dispersed (several tens of nanometres) particles of metals

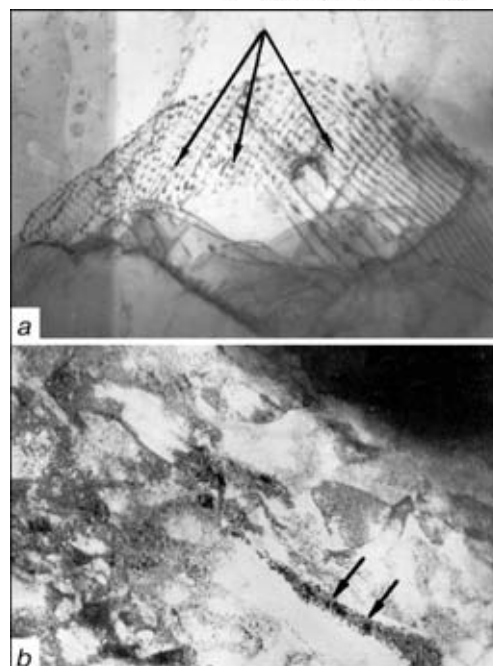


Figure 1. Mass transfer and phase formation at low deformation rates in DB: *a* — titanium-copper bond with dislocation mass transfer in copper ($\times 30,000$); *b* — same in titanium ($\times 20,000$) (arrows indicate segregation and ultra dispersed phases in dislocation sliding systems of copper along sub- and intergranular boundaries)

joined, as well as species of a cluster type to a substantial distance from the interface (to a depth of 200 μm and more) is observed in the joining zone in transmission microscopy. These dispersed particles can be watched in special modes of electron microscopy, such as the dark field mode, and at sufficiently high magnifications (about $\times 200,000$) (Figure 3, *b*).

The more pronounced processes of displacement of mass flows of the materials joined take place in EW, e.g. in welded joints between titanium and stainless steel (Figure 5).

Another distinctive feature of mass transfer with the high deformation rate methods (VPW, EW) is the effect of detachment from the interface and subsequent directed movement of particles of a harder (flyer) metal through the bulk of a material joined. For example, movement of zirconium into copper in VPW (Figure 6) and iron into aluminium in EW (Figure 7, *a, b*) was often observed in scanning electron microscopy. In this case the moving particles have

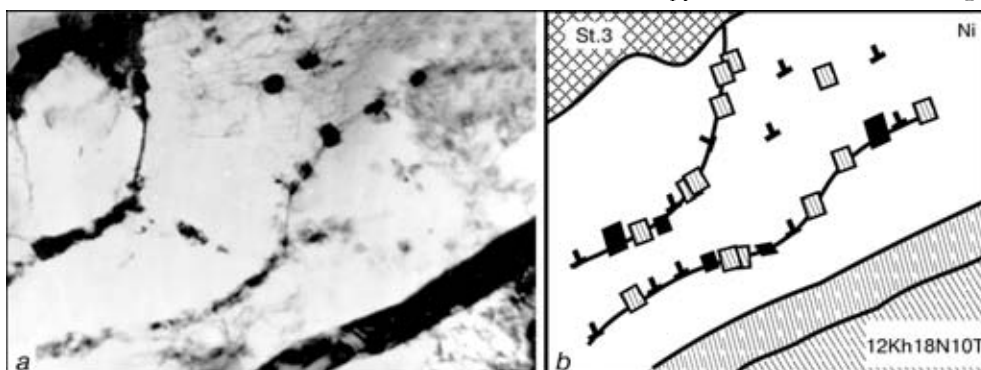


Figure 2. Structure of metal (*a*) and schematic (*b*) of St.3 + 12Kh18N10T joints made by roll welding through a nickel interlayer (arrows indicate forming intermetallic discrete phases and interlayers) ($\times 37,000$)

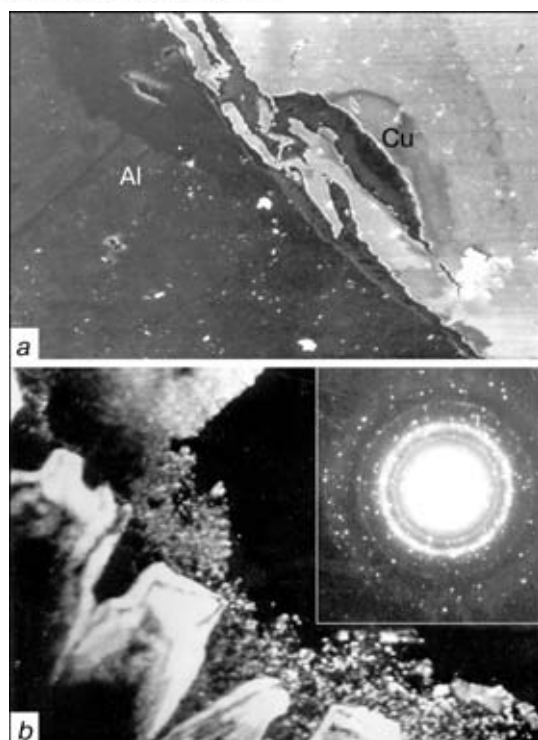


Figure 3. Mass transfer in the contact zone of dissimilar copper to aluminium joints made by MPW: *a* — mechanical transfer of layers along interface ($\times 450$); *b* — transfer of dispersed copper particles into aluminium at a distance of about $400\text{ }\mu\text{m}$ from interface ($\times 200,000$)

different sizes (up to several micrometres), and they may move to different distances from the interface. Direction of their movement has no crystallographic referencing, which is characteristic of DB, but it coincides with the direction of action of external effective stresses. Movement of such particles along tracking channels is shown in more detail in Figure 7, *a, b*.

The depth of the «drift» of the detached particles, e.g. zirconium into copper in VPW (Figure 6), is $\approx 0.5\text{ }\mu\text{m}$. Under the EW conditions, as is the case of multilayer iron + aluminium + copper joints [8, 9], this distance amounts to about several micrometres (Figure 7, *a, b*). Besides, channels via which the particles move are either collapsed cavities or cavities partially filled with a moving flow of particles of different sizes. In all cases metal in the region of the channels undergoes substantial elasto-plastic deformations, which is evidenced by the traces of deformation, fragmentation and relaxation. Thus, a characteristic diffusion trace was detected in a channel via which the particles of chemical elements move,

i.e. it seems that the channel walls are «alloyed» with elements of a moving particle. It should be noted, however, that the above phenomena were observed in scanning electron microscopy of sections.

Direct transmission examinations of thin foils of the EW joints also clearly reveal transfer of particles. The procedure for the direct examination of a fine structure made it possible to detect that displacement of particles in the case of the high-speed joining methods was associated with collective forms of movement of the crystalline lattice defects, such as shear bands (Figure 7, *c*). For example, the displacement of iron particles about $1\text{ }\mu\text{m}$ in size to a depth of about $100\text{--}120\text{ }\mu\text{m}$ from the interface was observed in the steel to aluminium joints, and the shear bands (like those observed under similar conditions of movement of particles) had no crystallographic orientation in this case [10–12].

As seen from the experimental results, various mass transfer processes occurring by different mechanisms take place in the contact zone between the dissimilar metals under the thermal-deformation pressure joining conditions. The range of the above mechanisms widens substantially with increase in the rate of external loading.

Consider the currently available literature data on the principles of the said processes revealed in metals under different thermal-deformation conditions of their treatment.

Thus, based on comparison of the energy of formation and activation of movement of spot-type defects, study [13] shows that diffusion caused by high temperatures in metals with bcc and fcc lattices in a non-deformed or slightly deformed state would occur mostly by involving the spot-type defects at vacant nodes. As noted by Messner, Reynolds and Averbach et al. [14, 15], variation in temperature in this case causes a comparatively large variation in the diffusion coefficient. Experimentally determined was the dependence of the diffusion coefficient upon the linear and 2D defects (dislocations and grain boundaries, respectively) [16–18]. It is emphasised that formation of this type of defects creates particularly favourable conditions for diffusion. It is noted in [19], however, that acceleration of diffusion along the grain boundaries takes place in the cases where the ratio of the diffusion coefficient along the boundaries to that in the bulk of the grain is $D_{\text{bound}}/D_{\text{bulk}} \geq 1 \cdot 10^5$, and where the grains are relatively small in size ($R \leq 1 \cdot 10^{-3}\text{ cm}$). In addition, Wassan and Dorn [20],

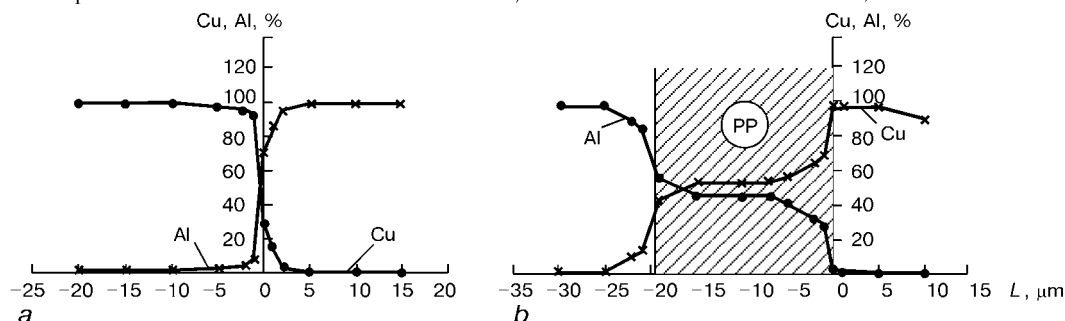


Figure 4. Concentration changes in the welding zone in regions of a variable contrast (*a*) and in regions of phase precipitates (PP) (*b*) (L — distance from the interface)

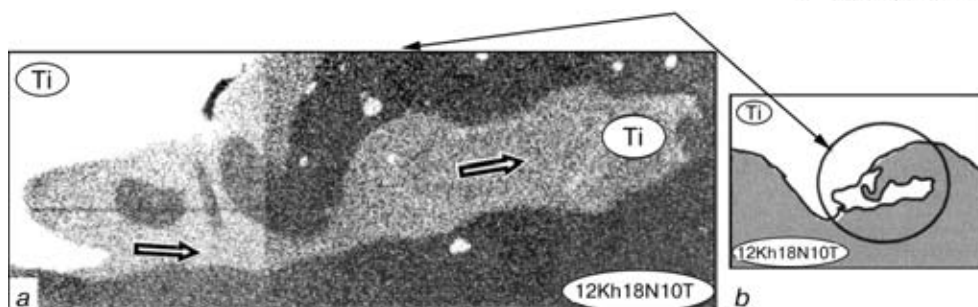


Figure 5. Example of displacement of mass flows in EW: *a* — electron microscopy picture ($\times 650$) of titanium flow in characteristic radiation (grey colour) into the internal volumes of stainless steel (dark background); *b* — schematic of the process

Messner, Reynolds, Averbach and Cohen [14, 15], and Hoffman and Turnbull [21, 22] paid attention to a substantial difference (almost 30 times) in values of the diffusion coefficients along static and moving grain boundaries. It should be borne in mind, however, that the noted principles of diffusion relate mainly to the thermodynamically equilibrium state of metal. With the commercially available methods of materials treatment, stresses induced by elastic and plastic deformations (in phase transformations, cold and high-temperature deformations, etc.) lead to formation of essential redundant (non-equilibrium) concentration of defects, which must favour a more considerable increase in diffusivity of atoms in crystals [23, 24].

It is the issue of the effect of non-equilibrium distortions of the crystalline lattices of deformed materials that has been attracting attention of a wide range of researchers. However, results of the studies performed in this area turned out to be rather ambiguous [24–33]. Thus, the calculations made by Ruoff and Balluffi [25–27], Wassan and Dorn [20] and Kimura and Maddin [28] showed that acceleration of diffusion had a different effect and occurred due to dislocations, the moving ones in particular. In addition, upon completing the comprehensive analysis, Kimura and Maddin detected a not less than 100 times increase in the diffusion rate (the diffusion acceleration effect was proportional to the deformation rate, i.e. the instantaneous concentration of defects). A still higher (more than 1000 times) increase in the

diffusion effect in deformation of nickel and copper is reported in studies by Osipov and Konobievsky [24]. These authors investigated the role of non-equilibrium distortions and sensitivity of diffusion to stresses caused by preliminary deformations. Similar phenomena were noted by Bokshtein [19], Rai and Ashby [30], and Dekhtyar and Mikhalevskiy [31].

As shown by analysis of the role of high-temperature deformation in variations of the self-diffusion coefficient of nickel [20, 23, 26], the diffusion grows with increase in the deformation degree, and rapidly asymptotically approaches the saturation value. Ruoff and Balluffi [25, 26] made a conclusion that variations in the diffusion can be roughly considered to be proportional to increase in the deformation, i.e. the diffusion enhances with increase in the deformation rate. Besides, this effect can also be observed at a lower test temperature. However, according to the data by Darby [29], in the case of deformation of silver at 800 °C the diffusion observed was not that substantial.

Decrease in the diffusion coefficient takes place, for example, under the high pressure conditions [33]. It is also shown that different metals have different susceptibility to variations in the diffusion coefficient under pressure, depending upon the compressibility coefficient of materials.

Therefore, it follows from the above-said that the principles of variations in the diffusion coefficient with different deformation methods do not always coincide (the effect may be observed or not observed

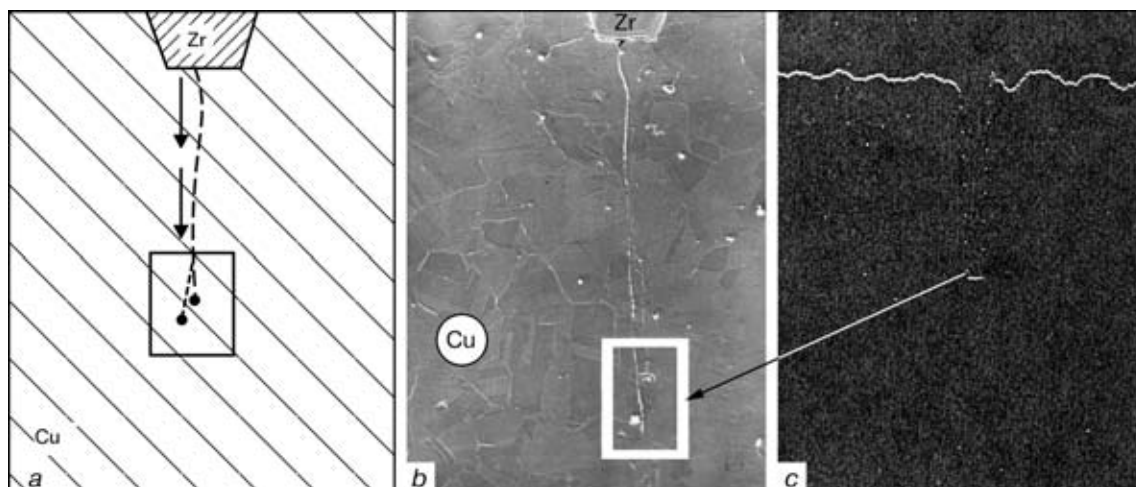


Figure 6. Peculiarities of mass transfer under the high deformation rate conditions of VPW in the copper + zirconium joint: *a*, *b* — schematic and structure of movement of the zirconium particles into copper, respectively; *c* — distribution of zirconium along the path of movement of the particles ($\times 200$)

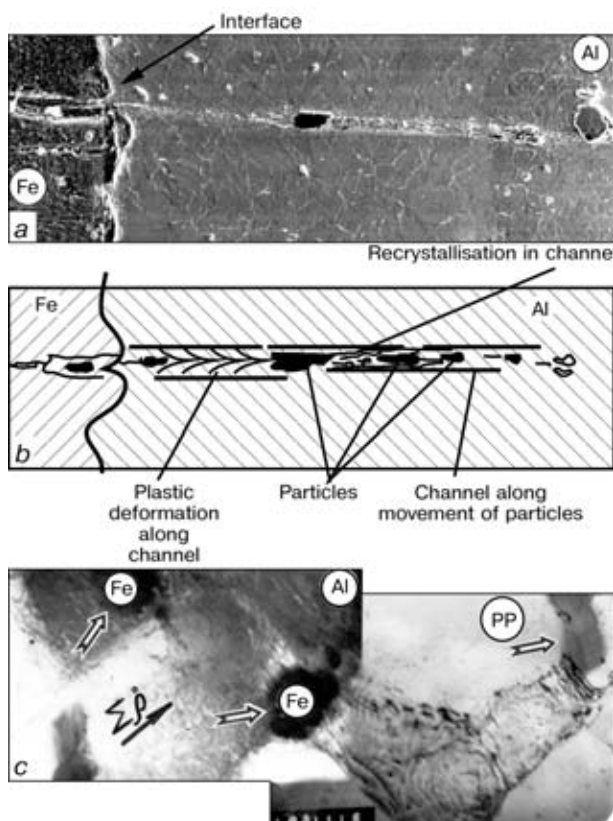


Figure 7. Peculiarities of mass transfer under the high deformation rate conditions of EW in the iron + aluminium joint: *a, b* — structure and schematic of movement of an iron particle via tracking channels in the bulk of aluminium, respectively ($\times 200$); *c* — transfer of iron particles into aluminium (scanning electron microscopy) ($\times 30,000$)

at a total deformation level of about 30 %). In addition, the diffusion acceleration effect does not always take place under the high-temperature deformation conditions. But the majority of researchers note a substantial acceleration of the processes at high rates of $\dot{\epsilon}$ and low deformation temperatures. It was established that at the low deformation rates the rate of diffusion varies with strain ϵ (at a constant test temperature), whereas with increase in the ϵ values the deformation rate grows more rapidly, compared with the case where the linear law holds.

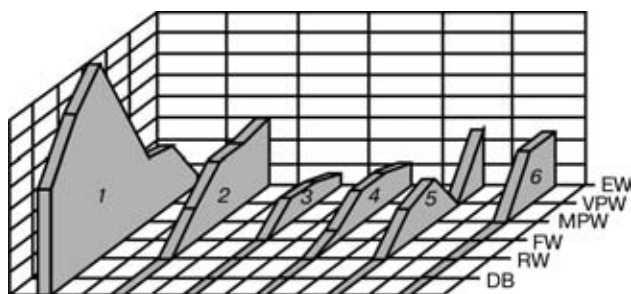


Figure 8. Diagram of changes of mass transfer mechanisms (dislocation and mechanical ones) and their volume fraction in the mass transfer process, as well as forms of realisation of mechanical mass transfer in the contact zone of dissimilar metals with increase in the deformation rate: 1 — dislocation mass transfer mechanism; 2 — collective form of movement of lattice defects; 3 — turns of volumes; 4 — ultra dispersed mass transfer; 5 — displacement of masses; 6 — coarse particles (FW — friction welding)

Mechanisms of the mass transfer process are considered in view of the fact of a dramatic change in mass transfer under different conditions of deformation of metals. Thus, analysing principles of the processes under consideration, researchers advance opinions that diffusivity of metal atoms, depending upon specific conditions, may occur by different mechanisms. In addition to the above-mentioned mechanisms of the diffusion processes which take place due to spot-type and linear lattice defects, there are also an experimentally established effect of a substantial acceleration of mass transfer showing up primarily under conditions of high loading rates, including in VPW [34–37]. However, the opinions differ concerning causes of its formation.

Thus, Vladimirov et al. [34] relate these processes to displacement of a set of vacancies, whereas Larikov, Falchenko, Mazanko et al. [35–37] relate them to the effect of the internodal mechanism, and disciples of the Prof. Lavrentiev's school [38] — to the specific features of the hydrodynamic flow. According to the concepts developed by Panin and his school, occurrence of the high-rate mass transfer can be caused by special atom-vacancy states formed in an intensive field of external effects taking place in a deformed material [39].

Coming back to the experimental results given in this study on relationship of the processes of plastic deformation and mass transfer in the joints between dissimilar metals, note that at minimum strain rates ($\dot{\epsilon} \approx 1 \cdot 10^{-4} \text{ s}^{-1}$) in the case of DB, judging from the character of the formed structures, it is primarily the dislocation mechanisms of plastic deformation that take place in the contact zone, these mechanisms being associated with displacement of individual dislocations along certain crystallographic sliding systems. Accordingly, the mass transfer processes (which is proved by comparison of the character of the formed phases and peculiarities of a fine structure) take place, as a rule, by involving the spot-type and linear lattice defects, and along the sub- and intergranular boundaries.

Increase in the deformation rate (in MPW, VPW and EW) is accompanied by realisation of plastic deformation to a substantial degree due to collective displacements of the lattice defects, i.e. intensive shear bands, which are no longer associated with crystallographic systems, but directed along the effective (external) joining stresses. The rotational mechanisms of plastic deformation (turns of material microvolumes of different sizes) are also involved here. The mass transfer processes under such conditions of the high-energy external effects also take place by involving different mechanisms, such as displacement of mass flows of one metal into the other (which occurs mostly near the contact zone), displacement of segregation clusters and particles of different sizes, as well as their complexes. Besides, realisation of different forms of accelerated mass transfer is likely to be favoured by special structural (amorphous-crystalline) states formed in the zone of localisation of deformation at the high-rate methods of external loading [40, 41]. It should be noted that displacement of microvolumes of one metal into the other (flows of masses and particles) is the process of a mechanical



mass transfer, i.e. this process takes place under the effect and in a direction of external stresses. This is proved also by comparatively straight-lined paths of the above displacements which pass through the blocks (up to several tens) of grains independently of the crystallographic orientation of the latter.

Figure 8 shows a change in the mass transfer mechanisms from the dislocation to mechanical ones, including the mass transfer due to rotational and shear mechanisms of plastic deformation, mechanical displacement of particles of different sizes and their complexes, as well as mass flows of one metal into the other in a direction of external stresses with increase in the deformation rate.

As far as the phase formation processes are concerned, here the following should be noted. While with the low-rate loading methods the formation and growth of dense continuous intermetallic phases in the joints between dissimilar metals take place in a directional and compact manner along the contact plane of the metals joined, where the processes of plastic deformation and, hence, mass transfer are primarily localised, conditions of the high rates of external loading are favourable for prevention of formation of directional continuous brittle interlayers. The latter is associated with dispersion and scatter of the formed intermetallic phases over a very wide joining zone. Therefore, the DB method under the high loading rate conditions seems more preferable in terms of ensuring quality bonds between dissimilar metals, especially in those combinations of metals which are characterised by a limited mutual solubility.

CONCLUSIONS

1. Mass transfer may take place by different mechanisms, depending upon the loading rate during joining.

2. At minimum deformation rates the displacement of masses takes place mostly via the dislocation channels of mass transfer.

3. Increase in the deformation rate is accompanied by widening of a range of different mass transfer mechanisms, which is attributable to involvement of their different forms associated with mechanical displacement of masses in a direction of effective external stresses, including displacement of masses of one metal into the other, detachment from the interface and movement of different sizes of particles and their complexes, as well as rotational mass transfer mechanisms.

1. Kazakov, N.F. (1976) *Diffusion bonding of materials*. Moscow: Mashinostroenie.
2. Gelman, A.S. (1970) *Principles of pressure welding*. Moscow: Mashinostroenie.
3. Shron, R.Z., Zelezin, V.N. (1978) *Heat treatment and properties of welded joints*. Leningrad: Mashinostroenie.
4. Bakshi, O.A. (1977) *Theory and practice of welding manufacturing*. Sverdlovsk: UPI.
5. Yoshiyasu, I., Takahiko, S., Masahiro, S. et al. (1998) Characteristics of behaviour of diffusion in the transition zone of a copper-aluminium joint in friction welding. *Transact. of Jap. Soc. Mech. Eng. A*, **618**, 494-499.
6. Kazuyuki, H., Takeshi, I., Takenobu, A. et al. (1993) Parameters of explosion welding and strength of joint in cladding stainless steel with different aluminium alloys using an intermediate stainless steel plate *J. JWS*, **1**, 16-21.
7. Markashova, L.I., Malevsky, Yu.B. (1975) Peculiarities of diffusion in joining without fusion. *Avtomatich. Svarka*, **10**, 9-11, 23.
8. Markashova, L.I., Kireev, L.S., Zamkov, V.N. et al. (1997) Peculiarities of formation of an interfacial zone in pressure

welding of dissimilar metals. In: *Welded structures*. Harwood A.P.

9. Markashova, L.I., Statsenko, V.V., Ignatenko, A.I. et al. (1993) Peculiarities of mass transfer under different conditions of pressure welding. In: *Proc. of Conf. on Advanced Technologies in Machine-Building and Instrument Making*, Saratov, May 1993. Saratov: SPU.
10. Markashova, L.I., Sergeeva, Yu.A., Statsenko, V.V. et al. (1990) Study of micromechanism of structure formation under conditions of magnetic-pulse welding. In: *Welding of dissimilar, composite and multilayer materials*. Kyiv: PWI.
11. Petushkov, V.G., Markashova, L.I., Zotov, M.I. et al. (1989) Micromechanisms and conditions of localisation of deformation in high-energy loading. In: *Proc. of 10th Int. Conf. on High-Energy Effects on Metals*, Lyublena, Sept. 18-22, 1989.
12. Petushkov, V.G., Markashova, L.I., Zotov, M.I. et al. (1989) Peculiarities of plastic deformation of aluminium in explosion welding. In: *Coll. of pap. of Int. Conf. on Special Methods of Welding*, Zagreb, March 30, 1989.
13. Shumon, P. (1966) *Diffusion in solids*. Moscow: Metallurgiya.
14. Messner, A., Benson, R., Dorn, I. (1961) Self-diffusion in nickel single crystals. *Transact. of ASM*, **53**, 227-232.
15. Reynolds, I.E., Averbach, B.L., Cohen, M.L. (1957) Self-diffusion and inter-diffusion in gold-nickel alloys. *Acta Met.*, **5**, 29.
16. Frank, F.C., Turnbull, D. (1966) Self-diffusion along edge dislocations in nickel. *Phys. Rev.*, **2**, 495-504.
17. (1973) *Processes of inter-diffusion in alloys*. Ed. by K.P. Gurov. Moscow: Nauka.
18. Shinyayev, A.Ya. (1975) *Diffusion processes in metals*. Moscow: Nauka.
19. Bokshetj, S.Z., Ginzburg, S.S., Kishkin, S.T. et al. (1984) Diffusion along grain boundaries. *Poverkhnost*, **2**, 231-234.
20. Wassan, A.R., Dorn, I.E. (1965) Analysis of enhanced diffusivity in nickel. *J. Appl. Phys.*, **1**, 222-228.
21. Hoffman, R.E., Turnbull, D.I. (1954) The effect of relative crystal and boundary orientations on grain boundary diffusion rates. *Acta Met.*, **2**, 419-426.
22. Hoffman, R.E., Pikus, F.W., Ward, R.A. (1956) Self-diffusion in solid nickel. *Transact. of AIME*, **206**, 483-485.
23. Romashkin, Yu.P. (1968) *Study of diffusion in metals at plastic deformation*. Syn. of Thesis for Cand. Techn. Sci. Degree. Moscow.
24. Osipov, K.A. (1960) *Theoretical problems of high-temperature strength of metals and alloys*. Moscow: AN SSSR.
25. Ruoff, A.L., Balluffi, R. (1963) On strain-enhanced diffusion in metals and point defect. *J. Appl. Phys.*, **34**, 1634-1647.
26. Balluffi, R.W. (1982) Grain boundary diffusion mechanism in metals. *Metallurg. Trans.*, **12**, 2069-2096.
27. Balluffi, R.W., Cahn, J.W. (1981) Mechanism for diffusion induced grain boundary migration. *Acta Met.*, **13**, 493-500.
28. Kimura, H., Maddin, R. (1954) Golden single crystal vacancies concentrations, deformed at high temperatures. *Ibid.*, **9**, 1065-1069.
29. Coodhew, P.J., Darby, T.P., Balluffi, R.W. (1976) On the dislocation structure. *Scripta Met.*, **5**, 495-499.
30. Raj, R., Ashby, M.F. (1971) On grain boundary sliding and diffusion at creep. *Met. Trans.*, **4**, 1113-1127.
31. Dekhtyar, I.Ya., Mikhalevskov, V.S. (1959) Influence of crystalline structure defects on diffusion parameters in nickel alloys. In: *Investigations on high-temperature alloys*. Moscow: AN SSSR.
32. Geguzin, Ya.E. (1984) *Physics of sintering*. Moscow: Nauka.
33. Goldstein, I.J., Hanneman, R.E., Ogilvie, R.E. (1965) Diffusion in the Fe-Ni system at 1 and 4 kbar pressure. *Transact. of Met. Soc. AIME*, **4**, 812-820.
34. Vladimirov, V.I., Kusov, A.A. (1982) Interaction of mobile avalanche dislocations with ensemble of dipoles. *Fizika Metallov i Metalloved.*, Issue 2, 367-371.
35. Larikov, L.N., Falchenko, V.M., Mazanko, V.F. et al. (1974) Peculiarities of mass transfer in welding of armco-iron in solid state. *Avtomatich. Svarka*, **5**, 19-21.
36. Arsenyuk, V.V., Gertsriken, D.S., Mazanko, V.V. et al. (1997) Migration of atoms in iron-argon metastable solid solution. *Dopovidi NANU*, **8**, 108-112.
37. Gertsriken, D.S., Mazanko, V.V., Tyshkevich, V.M. et al. (1999) *Mass transfer in metals at low temperatures under external effects*. Kyiv: G.V. Kurdyumov IMF.
38. Egorushin, V.E., Panin, V.E., Savushkin, E.V. et al. (1987) Highly excited states in crystals. *Izv. Vuzov, Fizika*, **1**, 9-33.
39. Olemskoj, A.I., Panin, V.E., Petrunin, V.A. (1988) On collective mode of highly excited state of solid. *Ibid.*, **12**, 14-18.
40. Zasmichuk, E.E., Markashova, L.I. (1990) Microbands in rolling-deformed nickel single crystals. *Mat. Sci. and Eng. A*, **127**, 33-39.
41. Markashova, L.I., Sergeeva, Yu.A., Chudakov, V.A. et al. (1991) Peculiarities of structure formation and mechanisms of plastic deformation in magnetic-pulse welding. *Avtomatich. Svarka*, **3**, 21-26.

STATE-OF-THE-ART, TENDENCIES AND PROSPECTS OF DEVELOPMENT OF HIGH-FREQUENCY WELDING CONVERTERS (REVIEW)

A.E. KOROTYNSKY

The E.O. Paton Electric Welding Institute, NASU, Kyiv, Ukraine

Main stages of evolution of high-frequency welding converters based on power transistor switches are considered. It is shown that main success in the development of welding equipment of this type is mainly due to achievements in the field of power electronics. New types of power modules based on distribution of structures and cycloconverter circuits are described. The ways for further improvement and development of welding power sources are outlined.

Key words: arc welding, inverter, high-frequency welding converter, power key, chopper-module

Volume of deposited metal, produced by arc welding, in the whole world exceeds 90 %. This method of permanent joining is the main technological process, therefore, the designers and manufacturers of welding equipment (WE) pay a special attention to it. Power sources (PS) of welding arc are one of the main elements of the technological chain, greatly influencing the quality of welded joints, as well as technico-economical characteristics of the arc welding process as a whole.

Process of PS evolution for arc welding has passed the following stages:

- reduction in material consumption due, mainly, to decrease in mass and dimensions of transformers;
- improvement of energy characteristics of power sources (efficiency and power factors) due to increasing requirements for energy saving;
- widening of functional capabilities of power sources required for further solution of problems of mechanization and automation of welding manufacturing;
- increase in requirements for electromagnetic compatibility, caused by the fact that a large amount of electronic devices, highly sensitive to electromagnetic disturbances, appeared both in industry and life.

These stages, described in details in [1], were connected with achievements in the field of a semiconductor electronics. Transition from welding transformers to rectifiers was stipulated by the appearance of reliable power diodes at the market. Development of thyristors (controlled rectifiers) made it possible to design PS with feedback control external characteristics. This greatly widened the functional capabilities of PS, as the creation of universal WE for different methods of arc welding has become real.

The further improvement of thyristors, connected with widening of their frequency range, decrease in dynamic losses, as well as improvement of reliability characteristics, made it possible to design the high-frequency inverters with low mass-dimensional char-

acteristics. Detailed analysis of works performed in this direction is described in [2]. And though the interest to the developments in this field is noticeably decreased during recent years, however, the results achieved in the design of optionally switching-off thyristors [3] enable us to assume that this phenomenon is temporary. This is proved also by achievements in the field of creation of reverse-connected dynistors [4] which could serve a perfect key element for powerful welding sources designed for currents above 1000 A. The reverse-connected dynistor is a semiconductor device of thyristor type, but unlike the latter, it has conductivity in a reverse direction. As it has no control electrode, its triggering is performed by passing a short pulse of a reverse polarity current, the so-called current pumping pulse. These peculiarities create, surely, definite difficulties in construction of control diagrams of reverse-connected dynistor, however, they can be easily overcome. Based on them the powerful high-frequency (HF) generators of continuous oscillations have already been created for the solution of problems of a HF treatment and hardening of metals. As to the field of welding, then, it can be stated, that, unfortunately, the designers of WE have not yet paid a serious attention to this type of a powerful electron key.

It should be noted that the main advantages of the recent decade in the field of manufacture of WE are mainly connected with welding high-frequency converters (HFC) made on transistor commutators. The present work is devoted to the analysis of status of main tendencies and prospects of development of this class.

Evolution of transistor HFC. The first attempts to use transistors in WE for microwelding referred to the 1960s. K.K. Khrenov and A.N. Milyakh [5] suggested a diagram of PC with a powerful control transistor in the secondary circuit. The required external characteristic is created due to arc voltage feedback control. However, in these diagrams the energy generated at transistor is occurred to be very high due to comparatively high open-circuit voltage $U_{o.c.}$. The use of these diagrams for power sources, designed for current of more than 100 A, by a parallel connection

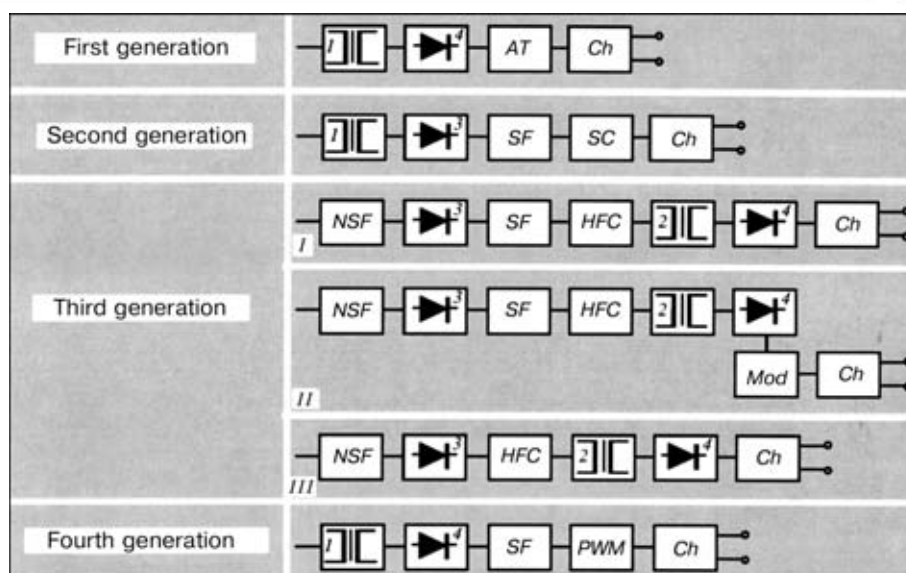


Figure 1. Evolution of transistor HFC: 1 – LF transformer; 2 – HF transformer; 3, 4 – primary and secondary rectifiers, respectively (AT – analog transistor; NSF – noise-suppression filter; SF – smoothing filter; HFC – high-frequency converter; SC – secondary converter; Mod – auxiliary modulator; Ch – choke; PWM – pulse-width modulator; I–III – see in the text)

of several transistors was not successful because of a low reliability of transistors.

The increase in reliability of HFC (transistor PS) required the creation of HF power elements capable to operate in key conditions. At the stage of creation of the second generation of transistor power sources (Figure 1), a secondary converter, operating in a key condition, appeared in the structure of the power unit. So, an analog controller is transferred into a discrete controller and, thus, eliminates losses which were observed at emitter-collector transition of a control transistor. However, these solutions did not provide also the decrease in consumption of active materials and in dimensions, as the classical welding transformer still remained.

The third generation of transistor HFC, which is due to the appearance in the market of reliable high-voltage transistors with high dynamic parameters and small losses, began to be developed intensively in the 1990s. At the same time a number of schematic technical solutions with a transformer-free input appeared [6] (Figure 1, III) that made it possible to decrease significantly the mass-dimensional characteristics of the PS. These devices were designed on HF transformers which are connected at the output of a power HFC. Mass and dimensions of these welding transformers as compared with traditional transformers are 40–50 times reduced. The use of current and voltage feedbacks promoted the design of universal welding converters for any methods of arc welding and rod electrode welding, namely TIG, MIG/MAG, MMA [7, 8]. Over the recent years the tendency in PS upgrading is observed in all the leading companies-manufacturers of WE [9–14]. To solve the problems of welding aluminium alloys the AC inverters have been designed [8, 11], being adjustable both in current and also in duration of welding current in positive and negative part of the period. Some authors are solving this problem by connection of an auxiliary modulator into the transistor converter diagram (Figure 1, II) [14, 15], which improves not only the

welding-technological properties of the power source, but also reduces the energy consumption.

Technical solutions are known [16] which have no smoothing filter capacitor. These devices (Figure 1, II) realize the method of power synchronous rectifying and are capable to operate at sufficiently low (to –30 °C) temperatures. Their experimental service in MMA welding provided good results.

The next stage in the WE development (fourth generation of PS) began at the end of the 1990s and was due to the appearance of chopper-modules [17], representing a matched diode-transistor structure (namely main diode and transistor have similar operating currents and voltages). The chopper-modules are used mainly for the creation of powerful welding PS ($I_w \geq 400$ A), and they are installed, as a rule, in the secondary circuit (Figure 1). Mass-dimensional characteristics in these sources are much higher than those in welding converters of the third generation, however, such is the price we have to pay for high reliability and dynamic properties. Multifunctional welding-technological system of BESTER Company can serve an example of interesting technical solution [18] of the use of chopper modules. Its main element is an inverter source (Inv) «Magic» with 0–500 A ranges of welding current adjustment. The source is universal due to the presence of adjustable current and voltage feedbacks in it, that makes it possible to realize HFC for different methods of welding. The above-mentioned approach is challenging in the creation of multistation welding systems with high energy characteristics. The described stages of evolution of transistor HFC coincide mainly with those indicated in [19]. Difference consists only in a comprehensive analysis of the third stage at which the important results were achieved in the creation of new types of welding PS.

To define the further ways of development and improvement of WE it is necessary to dwell on the analysis of recent achievements in the field of electrical materials, blocks and units of power electronics

and microprocessor engineering, as well as HFC and their control associated with use of algorithms based on fuzzy logic and neural networks.

It is owing to progress in power electronics, stipulated by appearance of different quick-response, reliable and powerful commutating elements, that the investigations and developments of high-frequency welding PS were carried out intensively during the recent years. A sufficiently precise, in our opinion, gradation of generations of power keys is given in [17] where it is stated that the wide application of IGBT and MosFET transistors in WE began in the 1990s. Typical time of current «on»/«off» for IGBT keys is 0.2–0.4 and 0.2–1.5 μ s. Residual voltage at a completely switched-on transistor, designed for 1200 V, does not exceed 3.5 V [20]. This is much lower than the voltage drop in an open key of MosFET type. Therefore, the further development of power electronics was going on by improvement of technology of manufacture of IGBT transistors. The fourth generation of IGBT modules of Hitachi Company [21], made on the basis of a planar technology with a self-matching, makes it possible to decrease both static and dynamic losses, to provide more effective

heat removal and, thus, to improve the service life and thermal stability of the product.

In IGBT modules, designed for 1200 V saturation voltage, it was possible to decrease the latter from 2.2 to 0.5 V, and also to reduce the commutation losses by 25 % using the new technology. Simultaneously, the performance of a recuperative diode was improved and the losses for switching were decreased. This promoted the creation of powerful key elements for currents up to 1200 A at voltage up to 3.3 kV (Tables 1–3).

Creation of chopper-modules is a rather promising direction for converting engineering, as they represent an integral design in which power transistor *T* and diode *D1*, as well as recuperative diode *D2* are arranged (Figure 3). As will be shown below, it would be possible to design WE on their base for currents up to 1000 A. There are transistor-diode modules (GAR-type) and diode-transistor (GAL-type) depending on the configuration of power elements. Owing to this arrangement they simplify significantly the processes of wiring of power circuits and also increase the reliability of their functioning.

Table 1. IGBT modules of the fourth generation of series GR

Module current, A	1700 V (single)	1200 V (single)	1200 V (double)	600 V (double)
100			MBN100GR12	
150			MBN150GR12	MBN150GR6
200			MBN200GR12	MBN200GR6
300			MBN300GR12	MBN300GR6
400		MBN400GR12		MBN400GR6
600		MBN600GR12		
800	MBN800GR17	MBN800GR12		
1200	MBN1200GR17	MBN800GR12		

Table 2. IGBT modules of the fourth generation of series GS

Module current, A	1200 V (single)	1200 V (double)	600 V (double)	1200 V (six-fold)	600 V (six-fold)
75		MBM75GS12AW		MBB75GS12AW	
100		MBM100GS12AW		MBB100GS12AW	
150		MBM150GS12AW	MBM150GS6AW		
200		MBM200GS12AW	MBM200GS6AW		MBM200GS6AW
300	MBN300GS12AW	MBM300GS12AW	MBM300GS6AW		
400	MBN400GS12AW		MBM400GS6AW		
600	MBN600GS12AW		MBM600GS6AW		
1200	MBN1200GS12AW				

Table 3. IGBT modules of the fourth generation of series «High power type»

Module current, A	3300 V (single)	2500 V (single)	2000 V (single)	1700 V (single)	3300 V (chopper)
400	MBN400D33A		MBN400C20		
600	MBN600C33A		MBN600C20		
800					MBL800D33B
1200	MBN1200D33A	MBN1200D25A			
1800				MBN1800D17C	

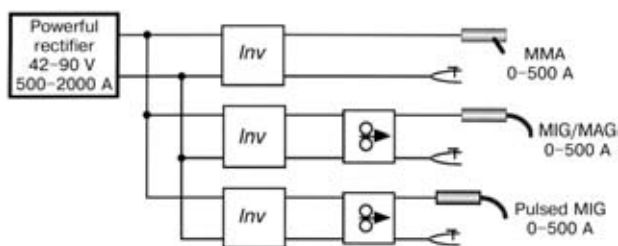


Figure 2. Multifunctional welding-technological system «Magic 500» of BESTER Company

During recent years there is a tendency in a power electronics to combine power elements, circuits of control, protection and diagnostics in a single module. As the logic functions are transferred into the module structure, these devices were named as intellectual power modules (IPM). Their application allows reduction in mass and dimensions in WE at significant widening of its functional capabilities and also increase in reliability and decrease in manufacture labour content.

The IPM are the sophisticated hybrid power devices combining a high rate of switching and low losses of transistors IGBT with built-in circuits of control, protection and diagnostics. The high efficiency of protection from overloads in current and short-circuit condition is attained by use of special chips with a separate emitter transition, being «sensitive» to current. The elementary diagrams of power units IPM of Mitsubishi Company and their technical characteristics are given in Figure 4. The application of IPM is described more in detail in [22].

Power units HFC. In technical literature a large amount of articles, manuscripts and books is devoted to the problem of HFC creation. When WE is designed, the different diagrams of HFC are used [23, 24], and they are mainly manufactured using power transistors IGBT or MosFET. Among the known diagram solutions, the single- [25] and double-action

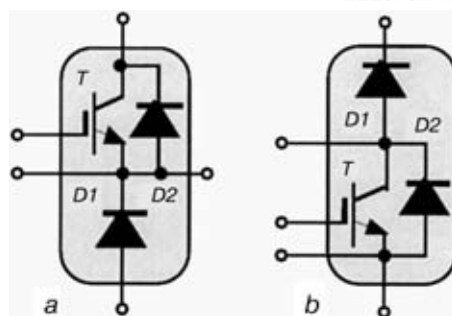


Figure 3. Diagrams of chopper-modules of GAR- (a) and GAL- types (b)

[26], half-bridge [27] and bridge converters [28] are used. Attempts to improve the energy characteristics and also to increase the frequency of converters have led to the creation of resonance HFC [29]. In author's opinion of [30] this way of the HFC development is most promising as, except higher efficiency factors and frequency of conversion, it provides the much better electromagnetic compatibility characteristics.

Not dwelling on all the known diagram-technical solutions in a wide field of converting engineering, let us consider some of them more in detail which are most suitable for designing present-day types of WE, whose simplified diagrams are given in Table 4.

Step-down PWM-converter. Transformer is not used in this type of the converter, therefore, there is no decoupling between input and output. Here, the constant input voltage is converted into a lower voltage with the help of a transistor key controlled by a PWM-modulator. Having appropriate feedbacks this device is the effective current stabilizer and can be, therefore, used effectively in designing WE for MMA and TIG. These converters are most promising as separate stations of multistation welding systems [31] when the use of ballast rheostats is eliminated completely, thus improving greatly the parameters of en-

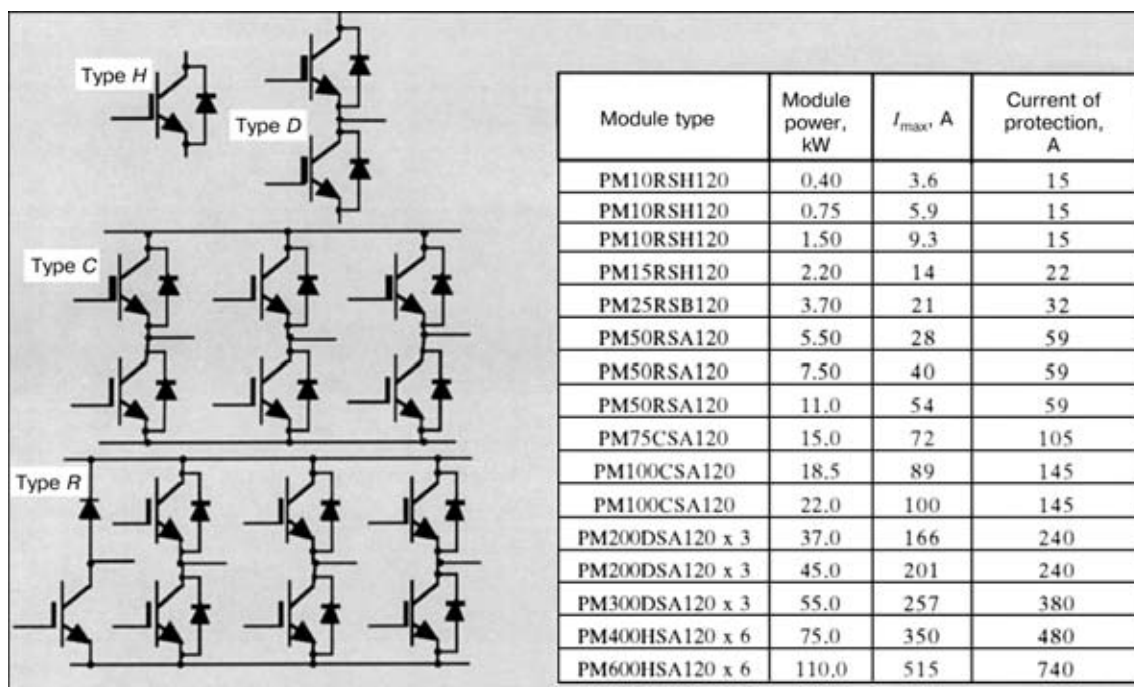
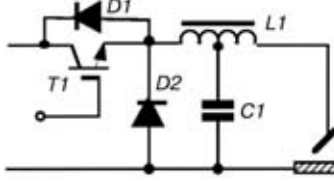
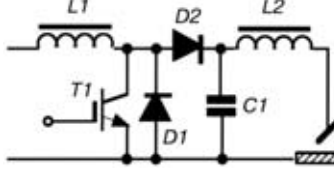
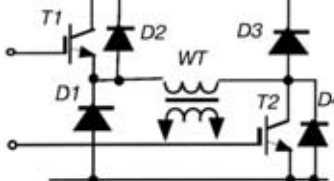
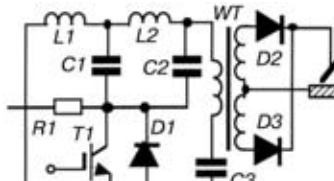
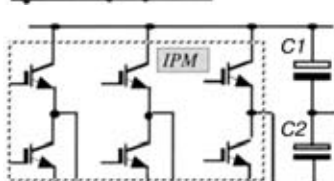


Figure 4. Power units of different types of intellectual power modules and their technical characteristics

Table 4. Schematic-technical construction of converter power unit

Type of converter	Main diagrams	Recommendations for selection of power keys
Step-down PWM-converter		Chopper-modules of GAR-type for MMA welding and GAL-type for TIG welding
Step-up PWM-converter		Chopper-modules of GAL-type are preferable
Single-cycle bridge converter		Chopper-modules of GAR- and GAL-type are preferable
ALL-based converter		Any types of IGBT and MosFET transistors, as well as chopper-modules of GAL-type can be used
Cycloconverter		IPM, equipped with built-in circuits of control and protection, for example, PM15RSSH120, are most preferable

ergy saving. If to use the chopper-module of GAR-type for their construction, when transistor *T1* and diodes *D1*, *D2* are combined, then it is possible to reach the high reliability of welding devices.

Step-up PWM-converter. This device is operating similar to the above-mentioned converter. It differs only in the fact that the output voltage in it is higher than the input voltage. In the step-up PWM-converter the arc voltage is equal to the sum of input voltage and voltage determined by commutation of transistor *T1* governed by PWM-modulator. The above-said properties of this converter make it possible to recommend it for the designing of a self-contained WE, for example, supplied from the storage batteries [32].

Single-cycle bridge converter. Diagrams of single-cycle converters on MosFET and IGBT modules found a wide spreading in designing machines for rod electrode arc welding, MIG/MAG welding, and also TIG welding operating at currents up to 300 A. In more powerful welding machines the diagrams of bridge, sometimes half-bridge, converters are used.

The diagram of one of single-cycle bridge converter variants, based on chopper-modules, is given in Figure 5. The power unit is controlled by a driver IR 2110. This device is featured by a feasibility of a recuperative release of energy into the PS with the help of diodes *D1* and *D3*. High reliability of operation of this type of welding converters is defined by the presence of protective diodes *D2* and *D4*, and also by a proper selection of design of a welding transformer [17] and output choke.

Converters based on an artificial long line (ALL). The above-described diagrams have serious drawbacks due to a wide range of frequencies of currents and voltages being converted. Naturally, this leads to the fact that a high level of electromagnetic disturbances is generated as a result of service of inverter PS, exceeding often the admissible value. Therefore, the problems of electromagnetic compatibility [33, 34] become rather actual. The radical way of elimination of this drawback of welding converters is the transition to resonance diagrams, characterized by high selective properties [35].

In this connection we made an attempt of selection of such diagram of the converter in which the pulses generated were close in their shape to harmonic oscillations that could solve more easily the problems of electromagnetic compatibility and also simplified the processes of commutation of the transistor keys. As is known [36, 37], the ALL-based converters are most suitable. Diagrams of these converters are made usually on lengths of homogeneous lines or on the base of lines with concentrated parameters, whose one of variants is shown in Figure 6. Forming links of ALL consist of n sections of $L_j C_j$ which are commutated by appropriate keys K_j . At the moments of commutation the cyclic currents I_j are formed in each of cells, whose superposition defines the output current I_0 of converter, and, consequently, the value of the rectified welding current. It is evident, that moments of switching-on of commutators K_1, \dots, K_n affect greatly the level of pulse formed in this diagram of the converter. ALL are distinguished by a simultaneous commutation, i.e. «synchronous lines» and by a successive commutation in which the operation of keys is realized according to a definite program being preset by a commutation control unit (CCU).

Analysis of transition processes in lines with a programmed commutation is quite complicated and can be made using numerical methods. Therefore, we shall deal only with a synchronous condition of the ALL operation, whose main calculated relationships were obtained by E.S. Weibel [38]. The principle of operation of this class of formers of HF oscillations is based on selective properties of ALL made on concentrated elements (L — inductance and C — capacitance). If in line, presented in Figure 7, and short-circuited at one end and connected to load (welding transformer WT) at another end, to charge preliminary capacitors $C1, C2$ up to voltage of PS, and then to close key K , then the oscillating transition process will occur. Frequency of these oscillations is defined by parameters of reactive elements $L1, L2, C1, C2$. Consequently, the pulse duration in the primary winding of WT will be determined by an «electric length» of ALL. If the parameters of line are selected so that $L1 = L2 = L$, and $C1 = C2 = C$, then the oscillations at frequency determined by expression $f = 1/2\pi\sqrt{LC}$ will be generated in the device. The device is capable to generate single pulses, close in shape to harmonic pulses, whose duration is $\tau_p = 1/f$. Values of pulse duty factor g of line operation cannot

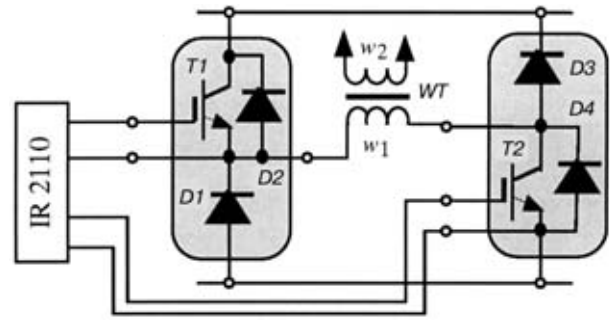


Figure 5. Diagram of power circuit of welding single-cycle bridge converter made on chopper-modules

be less than 2, as they are determined by a double time of ALL «electrical line» passing.

Let us estimate the parameters of line with allowance for preset welding current I_w and frequency of HF transformations f . In operation from industrial mains of 220 V the output voltage of PS is $U_{\max} = 310$ V. Consequently, the current of primary winding of WT should correspond to value $I_0 = I_w/k_{tr}$ (k_{tr} is the coefficient of WT transformation, determined by ratio U_{\max}/U_{o-c}), i.e. it is possible to write $I_0 = I_w U_{o-c}/U_{\max}$. As the pulses of duration τ_p and pulse duty factor g are formed in the line, then their energy can be determined by the expression

$$W_p = U_m I_0 \tau_p g = I_w U_{o-c} \tau_p g. \quad (1)$$

The level of this energy should be provided by capacitors $C1, C2$ for which it is determined by known expression $W_C = CU_{\max}^2/2$. It can be written for a perfect line without losses as

$$\frac{CU_{\max}^2}{2} = I_w U_{o-c} \tau_p g. \quad (2)$$

Hence, we shall find capacitance of the capacitor

$$C = \frac{2I_w g \tau_p}{U_{\max} k_{tr}}. \quad (3)$$

Inductance of ALL formers shall be determined by substituting capacitance C from (3) to expression $L = 1/4\pi^2 f^2 C$:

$$L = \frac{U_{\max} k_{tr}}{8\pi^2 f^2 I_w g \tau_p}. \quad (4)$$

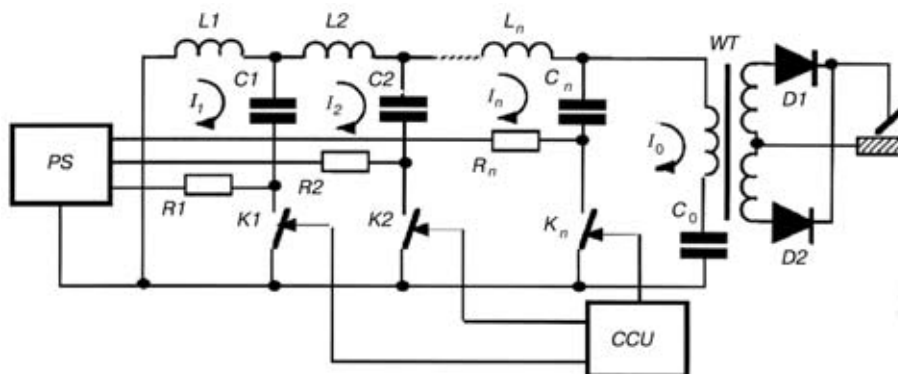


Figure 6. Diagram of ALL-based converter with concentrated parameters (R_1, \dots, R_n — charging resistance)

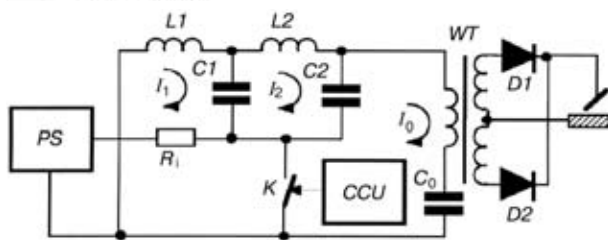


Figure 7. Converter with a synchronous commutation of ALL elements (R_i — resistance of PS)

It can be seen that expressions (3) and (4) are main for the design of welding converter made on ALL base as they describe completely its structure.

As an example, let us calculate the elements of ALL module designed for the manufacture of welding machine with the following characteristics: operating frequency is 50 kHz, $I_w = 120$ A, $U_{max} = 310$ V, $U_{o.c} = 45$ V. Consequently, the transformation coefficient is 6.9, $\tau_p = 20$ μ s, and current in WT primary winding will be 17.5 A. If to assume that $g = 2$, then the values of parameters of reactive elements of line calculated from (3) and (4) will be, respectively, $C = 4.5$ μ F and $L = 23$ μ H.

Experimental check-out of mock-up of welding source made according to diagram shown in Figure 7 was performed using a ballast rheostat as a load. Values of reactive elements corresponded to above-calculated values. Commutation was performed by a transistor key of Y25120D type (Motorola Company). To protect key from a reverse voltage the diodes KD213 were used. Current I_0 in the primary winding of WT (Figure 8, a) and current of key I_k (Figure 8, b) were measured using the Hall's wide-band generator. The oscillogram shows the presence of a negligible asymmetry of positive and negative half-waves of current I_0 (see Figure 8, a). Therefore, it is necessary to take measures to eliminate «magnetizing» of WT magnetic core. It is seen in Figure 8, b, that the amplitude of a reverse burst is 25–30 % of the basic current. It means that it is possible to use diodes with limiting values, i.e. by 3–4 times lower than those in key current.

The approach described using ALL was the basis in the designing of a power unit of the welding converter «Koral-163», developed at the E.O. Paton Electric Welding Institute (see insert in the Journal).

In some cases it is possible to use the simpler diagrams of resonance HFC. One of them is shown in Figure 9. It is based on so-called resonance key with a natural condition of commutation [29]. Device represents a somewhat changed model of a single-cycle

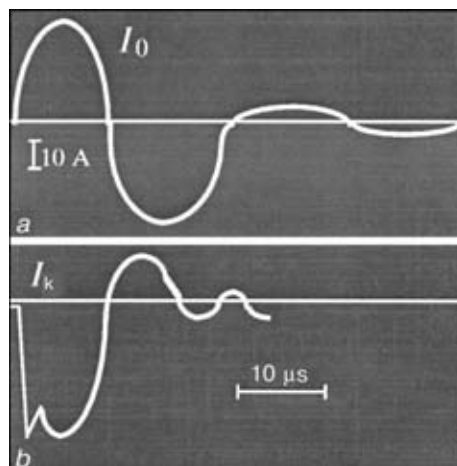


Figure 8. Oscillograms of currents I_0 (a) and I_k (b)

straight-running converter, in which the traditional transistor commutator is replaced by a «resonance» key. The latter consists of transistor $T1$, diode $D2$ and reactive elements of resonance contour L_r and C_r . It should be noted that the leakage inductance of WT can be used as L_r .

The welding unit is operated as follows. When $T1$ is closed and the magnetic field energy is stored in choke $L1$, the welding current is passing in circuit $D4-L1$. In opening of $T1$ key (this moment is defined by driver UC3875) the current begins to increment in inductance L_r that leads to the current increase in the secondary winding of WT. In this case the value of current passing through diode $D5$ is decreased, and through $D4$ is increased, while the voltage in the secondary winding is increased. Increase, and then decrease of the WT output voltage occurs by a sinusoidal law, as L_r and C_r form a resonant circuit. At the moment, when $T1$ is closed, diode $D2$ prevents the reverse current passing through the key. When current in L_r becomes equal to zero, the welding current is passing in circuit $C_r-D4-L1$. This phase of the device operation is finished by a full discharge of C_r and the circuit $D5-L1$ starts its operation again.

This operation finalizes the first resonance cycle and the next cycle is started from the moment of key $T1$ triggering. Consequently, the welding current can be adjusted by the duration of pauses between the resonance cycles.

It is seen, that the device is sufficiently simple in design, safe in operation and has also a narrow spectrum of generating interferences. Competitive commercial models of WE can be designed on its basis.

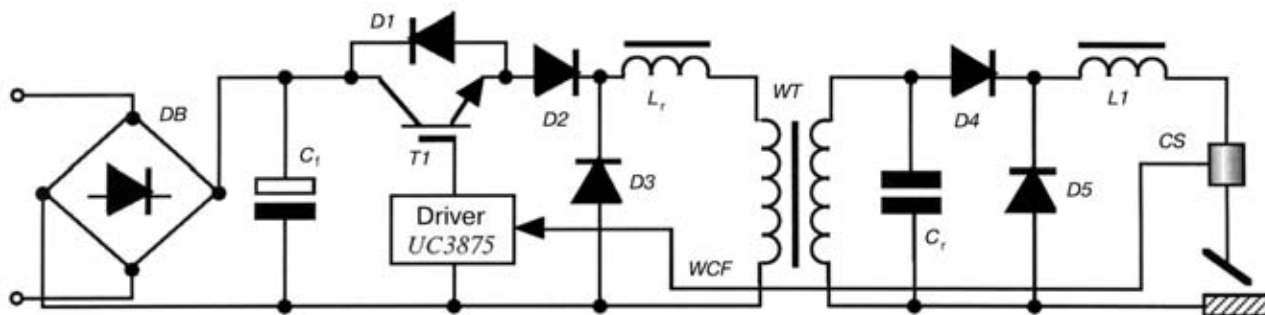


Figure 9. Simplified diagram of resonance welding HFC (DB — rectifier; C_f — filtering capacitor; WCF — welding current feedback signal; CS — current sensor)

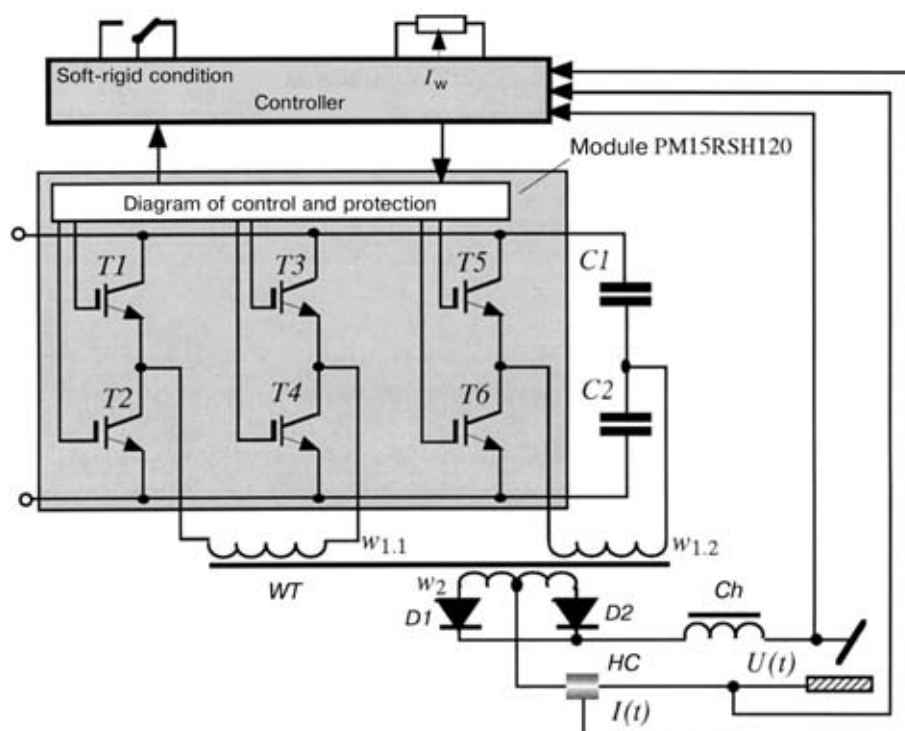


Figure 10. Welding converter of a combined type on PM15RSH120 base (HC — Hall's converter)

Converters based on IPM. As was above-mentioned, the IPM provide wide possibilities to designers of WE in the creation of highly-reliable models of power sources for different methods of welding. It refers especially to the modules of types *C* and *R* (see Figure 4).

As an example, Figure 10 shows a diagram of HFC with a combined external characteristic, which was made on the base of module PM15RSH120. The device represents a two-channel welding PS, consisting of two power units: bridge and half-bridge converters. The bridge converter contains transistor keys $T1-T4$, whose diagonal is connected to the primary winding $w_{1.1}$ of WT . The half-bridge converter is made on transistors $T5$ and $T6$, capacitors $C1$ and $C2$ and winding $w_{1.2}$. Thus, two controllable energy flows are formed and create, after their summing, a common welding current in the secondary winding w_2 . If the magnetic flow in $w_{1.1}$ provides the basic welding current, then the winding w_2 is used for conditions («hot start») and welding current modulation.

The welding PS is controlled by a controller, which includes drivers TL494. Their operation conditions are defined by signals of current and voltage feedbacks. Consequently, it is possible to form steep-falling, sloping and also rigid external characteristics.

The drawback of IPM is not sufficiently high frequency of conversion: from data of [22] it is not more than 20 kHz. If there is a task to create the welding PS with increased dynamic parameters, then it is possible to use ideas which were applied in the design of welding cycloconverters (CC) [39]. One of these diagrams of HF welding converter is given in Figure 11, *a*. The phase control in it is realized by keys of module PM15RSH120 in accordance with time diagrams shown in Figure 11, *b*. In principle, the device represents three separate half-bridge converters con-

nected to common capacitors $C1$ and $C2$. If to select the commutation frequency of each half-bridge to be equal to 18 kHz, then the welding current in the secondary winding will change at 54 kHz frequency.

The described diagrams do not describe all the possible variants of the device which can be made on IPM base. In this direction many scientific and practical tasks are to be solved.

Modular organization of HFC. At present many world leading organizations and companies pay a large attention to the research and development works connected with the creation of the multifunctioning WE [40–42]. Thus, for example, EWM High-Precision Schweisstechnik GmbH created models of WE of a modular design, intended for MIG/MAG welding, the rod electrode welding is also possible. A power module (PM) for this equipment is manufactured in three modifications of conditions for 250, 350 and 500 A currents. In welding with non-consumable electrode the module of arc exciting using a high-voltage pulse is provided. The equipment includes also a unit which realizes the welding current modulation at 8 kHz pulse frequency.

The Lincoln Electric Company is solving the problem of creation of multifunctioning welding PS in another way. Their approach is based on use of a standard inverter with 20 kHz frequency conversion, whose operation conditions are preset by a multifunctional controller. Using a five-position switch it is possible to preset conditions of manual rod electrode arc welding, non-consumable electrode argon welding, mechanized arc welding in inert and active gases, as well as flux-cored wire welding.

Taking into account the modern trends in the development of WE, connected with a wide use of electronic components of the fourth generation, we offer a sufficiently simple and reliable method of creation

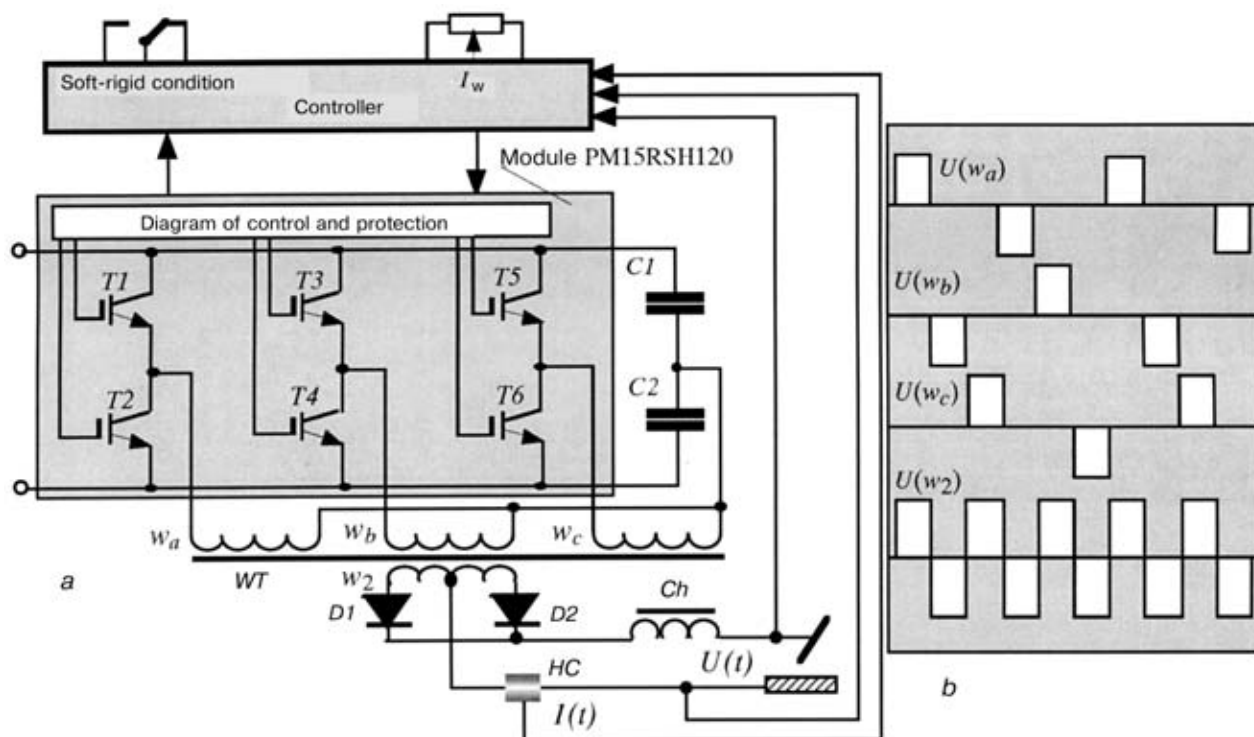


Figure 11. Welding cycloconverter of a half-bridge type on PM15RSH120 (a) and diagram of its operation (b) (w_a, w_b, w_c and w_2 — windings of primary and secondary circuit, respectively)

of the multifunctional WE, providing its structural-modular reconfiguration depending on the selected method of welding [43]. The above approach is peculiar by its feasibility to be used in WE for plasma technologies where the increased open-circuit voltage is required.

This class of WE is based on self-contained PM, which is shown in Figure 12. It is designed on the base of HF transistor converter*, whose output characteristic is formed with the help of a control unit (CU). Thus, the external characteristic of the device as a whole is defined by time parameters of CU and output choke (Ch). Control conditions of the device (Contr) can be preset both by a potentiometer and also a built-in microcontroller.

Methods of modules connection by input and output can be distinguished depending on the technological task being solved. If their input parameters are 220 V and 50 Hz, then modules can be connected in parallel to a single-phase mains (1×220 V). If the number of modules is three-fold, then the four-wire connection to the mains (3×220 V) is preferable, the three-wire connection to the mains (2×220 V) is also

admissible. In case of absence of the three-phase mains it is easy to transfer to the single-phase supply of input circuits that is, undoubtedly, advantage of these power sources. The above-mentioned device is convenient to use in combination with mini electrical stations.

Modules are connected in parallel by output almost in all methods of the arc welding, in series — in air-plasma cutting and periodically with time — in realizing the AC welding condition.

Let us consider more in detail the peculiarities of design and operation of two-module device, on the base of which it is possible to design schematic diagrams, different in configuration, of power sources of the required technological purpose. Table 5 shows separate schematic diagrams and also variants of their technological application. The practical realization of all the technological conditions mentioned in the Table is performed by two-module multifunctional PS whose diagram is given in Figure 13. This device includes two identical power modules PM1 and PM2 with control units CU1 and CU2. The latter are capable to operate both in a self-contained condition and also by commands of the common control unit (CU/C), forming control signals for the conditions commutation block (CCB). At its commands, which define the condition of power commutating elements K1, K2 and K3, the technological condition is preset from the control panel. When all the commutators are open, this device is capable to operate in the condition of two-station welding with a full decoupling of welding circuits. In closing of commutator K3 the

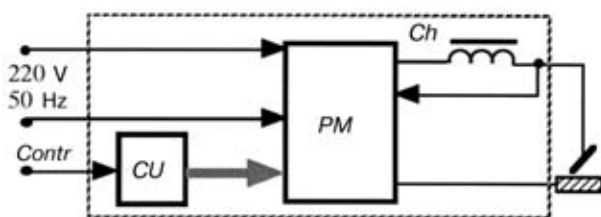


Figure 12. Schematic diagram of power module

* In the present work the authors used HF transistor converters of Company «EP Systems» (Italy), and also modules made on the ALL base, developed at the PWI.

Table 5. Methods of modules connection

Schematic diagram	Condition of commutators	Condition of outputs	Technological application
	K1:1 K2:1 K3:0	A:0 B:1 C:0	Parallel connection (in MMA welding and mechanized MIG/MAG welding at $I_w = 10-300$ A)
	K1:0 K2:0 K3:1	A:0 B:1 C:0	Series connection (in air-plasma cutting under conditions $U_a = 150$ V and $I_w = 100$ A)
	K1:0 K2:0 K3:0	A:1 B:0 C:1	Separate connection (at two-station MMA welding and mechanized MIG/MAG welding at $I_w = 5-150$ A)

Note. The given data correspond to module with parameters $U_{0,c} = 75$ V and $I_w = 150$ A.

device is transferred into the air-plasma cutting condition at which the current of up to 100 A is provided.

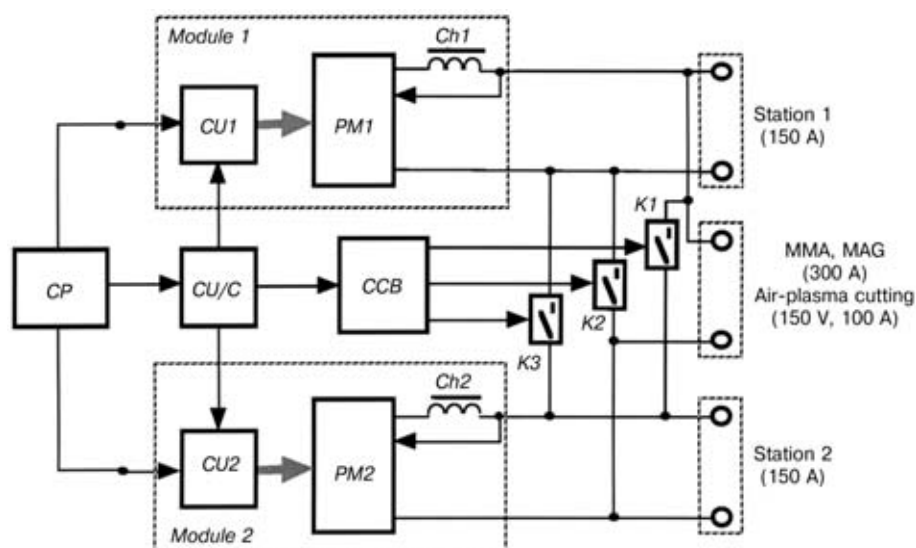
Great difficulties are encountered in the condition of parallel connection of modules that is due to the fact that within the wide ranges of adjustment it is necessary to keep the equality of their output voltages with an error of not worse than $\leq 5\%$. This is attained by a comparison diagram which is included into CU/C . The root-mean-square value values of voltage, acting on $Ch1$ and $Ch2$ are used as feedback signals.

The described device can be used at a negligible modification for AC welding. Variant of structure of welding power source with indicated functional purpose is shown in Figure 14. Additionally, a device of thyristors control (TCD) and two power commutators $TK1$ and $TK2$, when each of them is operating, respectively, in formation of pulses of positive and negative half-waves of welding current, are included.

Algorithm of device operation can be explained using time diagrams presented in Figure 15. At the moment t_1 the module $PM1$ is excited at $CU1$ command and thyristor commutator $TK1$ is open simul-

taneously. At the output the pulse of welding current at a positive polarity is beginning to form. At the moment t_2 the $PM1$ is first switched off and then $TK1$ is closed. In time interval t_2-t_3 there is no welding current at the PS output. The value of this interval is selected from the condition of time necessary for damping the transition processes associated with commutation of power elements of the welding PS. At the moment t_3 the phase of current pulse formation is started at negative polarity. $PM2$ is started in succession and commutator $TK2$ is open. Negative pulse of welding current is interrupted at the moment t_4 . Further, the processes are repeated in periodicity which is set by the operator. Time intervals t_1-t_2 and t_3-t_4 are preset from the control panel and can be set within the 5–500 ms range. Amplitudes of current pulses both at positive and negative polarity are set independently within 5–150 A ranges. Thus, the described device is sufficiently convenient for welding aluminium alloys and other non-ferrous metals.

Taking into account the present-day requirements for electromagnetic compatibility, the PS is equipped

**Figure 13.** Diagram of two-module multifunctional welding power source with a reconfigured design

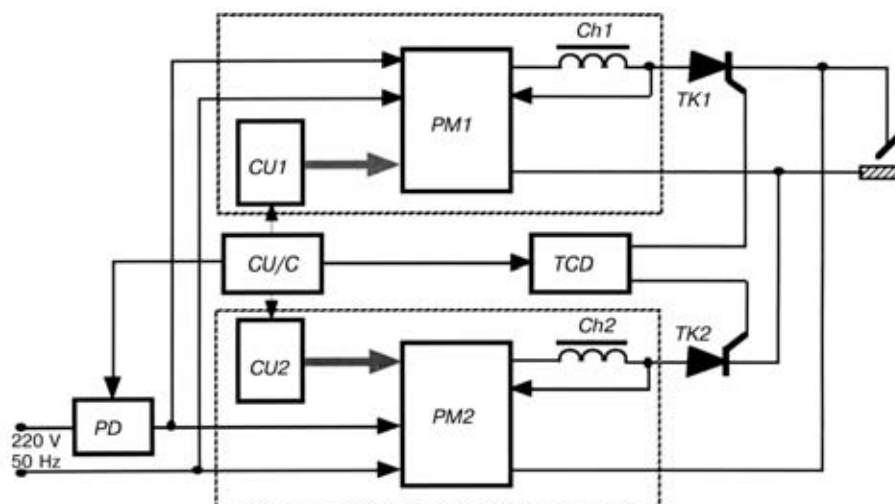


Figure 14. Variant of design of welding power source in AC conditions

with a protection device (PD) of mains, which represents a combined filter of lower and higher frequencies. The first filter suppresses the low-frequency interferences, the second filter — the interferences created by HFC of power modules.

In creation of a modular design of the welding machine a selection of the main unit, i.e. PM, is one of the actual problems. If, for example, to select the standard modules of Company «EP Systems» of W100E, W130E and W150E type, then, the mentioned conditions by welding current can be attained, as is seen from Table 6, for two- and three-module structures of welding equipment.

However, as the experience gained showed the creation of a specialized power module, whose functioning purpose could meet task requirements most completely, is more preferable. In this connection it seems to us that HFC, made on the base ALL elements with a synchronous commutation, are most challenging (see Figure 7).

Control of arc welding process using HFC. Problems of control of welding HFC are described comprehensively in [17]. Therefore, we dwell only on the results obtained during recent years, and not included into it.

First of all, this refers to the control by the method STT [44], based on use of surface tension forces for a controllable drop transfer in MIG/MAG welding. This algorithm was suggested and developed by specialists of the Lincoln Electric Company and has an adaptive nature which makes it possible to improve the energy characteristics of welding and also to re-

duce drastically, that is very important, the amount of spattering metal.

The great achievements were attained in use of algorithms based on the theory of fuzzy sets [45], the so-called fuzzy algorithms. Conception, based on fuzzy algorithms, states that the control algorithm, developed in a proper way, is similar to a highly-skilled welder [46]. It means that it increases quality of its functioning, and consequently, of produced welded joints from one process of welding to another, as it contains a process of a self-teaching. In other words, power sources with a such control system have quality feedback in making welded joints.

Some authors [47, 48] are searching for optimum algorithms based on neural network approaches. Capabilities to teach of neural networks are similar to capabilities of a high-skilled welder, that allows their use for an operative control of the welding process. The mentioned networks [48] are suitable for control of a penetration depth in welding thin-sheet materials, searching for a gap and trajectory of welding and control of a torch movement over it, as well as for construction of a mathematical model of a pool to calculate the optimum welding conditions. Combined approaches are possible when neuroalgorithms, based on a fuzzy logic, are used simultaneously.

Table 6. Variants of modular structures

Duration of load, %	Welding current, A	Two-module design	Three-module design
W100E			
100	60	120	180
60	80	160	240
35	100	200	300
W130E			
100	85	170	255
60	100	200	300
35	130	260	390
W150E			
100	100	200	300
60	120	240	360
35	150	300	450

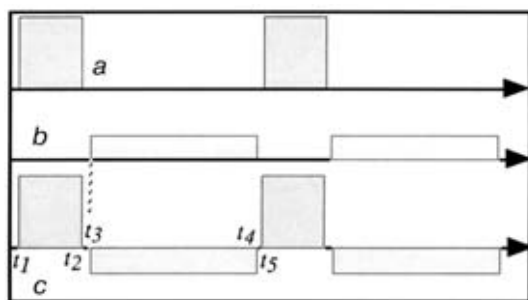


Figure 15. Temporary diagrams of device operation: a, b — pulses, respectively; c — output current of power source

Even now, the above-mentioned algorithms, based on methods of artificial intellect (AI), lead to quite new results as regards to providing the high quality of welded joints. Taking into account a continuous updating of microcontroller systems and growth of their efficiency it is possible to state with a confidence that the AI methods will be successfully implemented in WE for increasing its quality and reliability.

Appearance and technical characteristics of models of welding HFC, developed at the PWI and based on the above-mentioned principles, are given in inserts of the Journal.

Prospects of development of equipment, based on transistor HFC, for arc welding. Based on above information about the works in the field of welding HFC, made at the PWI over the recent years, and also analysis of modern tendencies in the development of HFC-based WE, it is possible to speak about a wide application of highly reliable power commutators of the third and fourth generations, equipped with means of a built-in intellect. New schematic technical solutions of power units have appeared which are characterized by high efficiency and power factors. Their control systems are made on the base of microcontrollers, which realize the adaptive algorithms, for example STT, and also the works are carried out on use of the AI-based algorithms. The main directions of future investigations can be as follows.

The leading companies, manufacturers of WE, continue, probably, their works connected with a search and updating of new solutions of diagrams of welding current power units of HFC for different methods of arc welding. The investigations will be directed to the increase in efficiency and power factors, widening of temperature range ($-40 - +50\text{ }^{\circ}\text{C}$) of operation, increase in reliability (faultless operation should not be less than 5000 h), reduction in level of electromagnetic interferences in accordance with European and world standards.

Consequently, there are grounds to assume that the further development will refer to resonance methods of welding current conversion, which allow the operation frequency of power modules to be increased significantly [49]. This will lead to the further decrease in mass and dimensional characteristics. If to use such index as a ratio of welding machine mass to maximum current, then it will be equal, evidently, to $0.01\text{--}0.015\text{ kg/A}$, i.e. inverter for up to 150 A current will have mass of 1.5–2.0 kg. For power sources operating at very low (down to $-50\text{ }^{\circ}\text{C}$) temperatures the methods of a synchronous power rectifying of welding current [16] can be recommended, which exclude the application of high-capacity ca-

pacitors with an oxide dielectric, not capable to operate at the above-mentioned temperatures.

Using the achievements of the recent years in the field of creation of molecular accumulators [50], the methods of a transformer-free conversion of welding current can find a wide spreading [51]. Hypothetic diagram of this welding power source is given in Figure 16. The power source consists of three main units: a former of a constant voltage (*FCV*), a pulsed converter of voltage (*PCV*) and welding current converter (*WCC*). *FCV* includes a rectifier *DB*, charging unit (*ChU*), whose level of operation is preset by a potentiometer *R1* and a filtering capacitor *C_f*. A pulsed voltage converter consists of a molecular accumulator *C_{MA}* and a block of keys *K1–K4*, whose algorithm of commutation is preset by *CU*. The condition of functioning the latter is determined by a welding current feedback (*WCF*) signal. In *PCV* a known condition of «flying» capacitor is realized, with the help of which a quasi-galvanic decoupling between input circuit and welding circuit is provided. The operation of *WCC* block is similar to the operation of a converter, decreasing voltage (see Table 2), therefore, we do not present its description.

Methods of designing welding HFC will change significantly. For example, units of welding transformers will be made on printed-circuit boards alongside with electron blocks, that will eliminate the effect of parasitic parameters of the unit operation. Here, the primary winding turns can be made by etching on the board itself, while the turns of the secondary, the more powerful winding, will be made by using technology of spraying on isolating gasket. Magnetic cores of such transformers can also be made by spraying of amorphous iron powder.

The further intellectualizing of WE will be realized on the basis of a wide application of single crystal computers with a calculating service life and efficiency equal to personal computers. In some cases special processors can be used. In the field of software an appearance of integrated media and expert systems for different methods of welding, oriented on use of AI algorithms, is expected.

Competitiveness in the field of WE market will require the solution of problems of its reliability. These problems can be solved not only by design solutions and selection of moderate conditions of functioning of power units, but also providing most critical elements, and also creation of means of diagnostic support [52]. In this connection, the modular welding machines will find the further development.

Great changes will be expected in a service of WE. New devices of remote control and control of welding

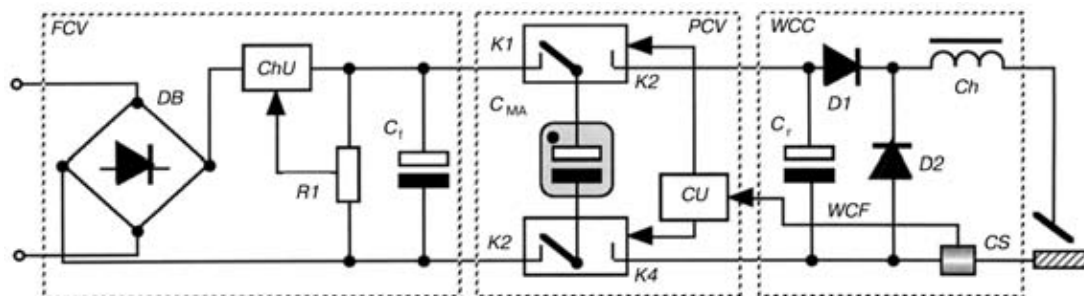


Figure 16. Transformer-free welding HFC (for designations see the text and Figure 9)

current sources on the basis of a radio signal will be created [53, 54]. Probably, the devices of a vocal input of commands of welding conditions control will be implemented.

To increase the level of electric safety of WE the detectors of current leakage have been already developed [55] and implemented with the help of which the power circuits are disconnected in critical conditions. Role of these current sensors (CS) is especially important in use of the transformer-free diagrams.

Thus, 90 % of the up-to-date welding machine with HFC represents an intellectual electron device. Components of the electrical engineering amount to 5–10 %. Therefore, it is not surprising that the leading companies in the field of a power electronics, such as Panasonic, Hitachi, Kawasaki, etc., make now a serious and more growing competition at the world market of WE. If now they occupy successfully the most part of markets by power sources for different methods of arc welding, designed for currents of up to 500 A, operating under normal conditions, then it is necessary to suppose that they are carrying out developments of WE for currents of 1000 A and higher, as well as for operation at low (down to -40°C) temperatures and service under tropic conditions. Tendency in the development of electronics and achievements in the field of development of new materials, for example, amorphous iron, prove that these problems will be solved in the nearest future.

1. Lebedev, V.K. (1995) Tendencies of development of arc welding power sources. *Avtomatich. Svarka*, **5**, 3–6.
2. Pentegov, I.V., Meshcheryak, S.N., Kucherenko, V.A. et al. (1982) Inverter arc welding power sources. *Ibid.*, **7**, 29–35.
3. Carroll, E., Klaka, S., Linder, S. (1998) IGBT thyristors. New approach to super-power electronics. *Elektrotehnika*, **7**, 46–53.
4. Grekhov, I.V. (1991) Main principles of construction of powerful pulse and high-frequency oscillators based on reverse-connected dynistors. *Ibid.*, **11**, 26–29.
5. Paton, B.E., Lebedev, V.K. (1966) *Electric equipment for arc and slag welding*. Moscow: Mashinostroenie.
6. Pilinsky, V.V. (1985) *Secondary power sources with transformer-free input for electronics*. Kyiv: KPI.
7. Ioffe, Yu.E., Mozhaitsky, V.A. (1998) General-purpose universal welding inverter power source Invertex V300-1. *Svarochn. Proizvodstvo*, **1**, 44–46.
8. Paton, B.E., Lebedev, A.V. (1988) Control of fusion and electrode metal transfer in CO_2 welding. *Avtomatich. Svarka*, **11**, 1–5.
9. (2001) *SELCO: General Catalog*.
10. (2002) *STEL: General Catalog*.
11. (2001) *CEBORA: Inverter TIG DC*.
12. (2001) *CLOOS: Innovation aus Tradition*.
13. (2001) *KEMPPPI: Schweißmaschinen MIG-Bunner, WIG-Bunner, Austrues Eng. Roboter*.
14. Ushio, M., Nakata, K., Tanaka, M. et al. (1994) Fume generation in Al–Mg alloy welding with AC-pulsed GMA welding method. *Transact. of JWRI*, **1**, 21–26.
15. Hadara, S., Tong, H., Ueyama, T. et al. (2001) Progresso della qualità e della produttività nella saldatura di lamiere sottili con il procedimento MIG pulsato in corrente alternata. *Rivista Italiana della Saldatura*, **4**, 453–459.
16. Rudyk, S.D., Turchaninov, V.E., Florentsev, S.N. (1998) Perspective welding current sources. *Elektrotehnika*, **7**, 8–13.
17. Vereshchago, E.N., Kvasnitsky, V.F., Miroshnichenko, L.N. et al. (2000) *Circuit technique of inverter power sources for arc welding*. Nikolaev: UGMTU.
18. (2001) *BESTER: Product Catalog*.
19. Kaulich, G., Killing, R. (2000) Entwicklung der Schweißstromquellen zum Lichtbogenschweißen. *Praktiker*, **12**, 458–461.
20. Florentsev, S.N., Savkin, A.I. (1991) Hybrid power integral circuits and modules. *Elektronika*, **6**, 5–9.
21. Nakano, E. (2000) New IGBT-modules of Hitachi Company. *Chip News*, **1**, 21–24.
22. (1997) *Handbook on application of insulated gate bipolar transistors (IGBT) and intellectual power modules (IPM) of third generation*. Ed. by V.A. Pavlovsky. Kyiv.
23. Romash, E.M., Drabovich, Yu.I., Yurchenko, N.N. et al. (1988) *High-frequency transistor converters*. Moscow: Radio i Svyaz.
24. Mallett, Ch. (1992) Recommendations on application of DC module converters. *Elektronika*, **3/4**, 86–92.
25. Polikarpov, A.G., Sergienko, E.F. (1989) *Single-cycle converters in power source devices of electronics*. Moscow: Radio i Svyaz.
26. Kobzev, A.V., Mikhailchenko, G.Ya., Muzychenko, N.M. (1990) *Modulation power sources of electronics*. Tomsk: Radio i Svyaz.
27. Bas, A.A., Milovzorov, V.P., Musolin, A.K. (1987) *Secondary power sources with transformer-free input*. Moscow: Radio i Svyaz.
28. (1990) *Functional devices of power source systems of ground electronics*. Ed. by V.G. Kostikov. Moscow: Radio i Svyaz.
29. Ivanov-Tsyganov, A.I. (1991) *Electric converter devices of RES*. Moscow: Vysshaya Shkola.
30. Li, F.K. (1990) The future with resonance power sources. *Elektronika*, **2**, 71–72.
31. Bunkin, P.Ya., Donskoj, A.V. (1985). *Multi-operator welding systems*. Leningrad: Sudostroenie.
32. Paton, B.E., Dudko, D.A., Korotynsky, A.E. (1999) Accumulator-based power sources for arc welding. *Avtomatich. Svarka*, **1**, 29–34.
33. Lucas, W. (1995) Electromagnetic emission from DC and AC TIG welding system. *Welding & Metal Fabr.*, **7**, 261–265.
34. Anisimov, Ya.F., Vasiliev, E.P. (1990) *Electromagnetic compatibility of semiconductor converters and marine electric systems*. Leningrad: Sudostroenie.
35. Korotynsky, A.E. (1999) Peculiarities of operation of high-frequency welding inverters on the basis of an artificial long line. *The Paton Welding J.*, **1**, 76–77.
36. Lietti, A. (1969) Transmitting lines with concentrated parameters as the pulsed oscillators of very high-powerful sinusoidal vibrations. *Pbistory dlya Nauchn. Issledovan.*, **3**, 78–87.
37. (1971) *Handbook on pulsed technique*. Ed. by V.N. Yakovlev. Kyiv: Tekhnika.
38. Weibel, E.S. (1964) High-power HF pulsed oscillator. *Pbistory dlya Nauchn. Issledovan.*, **2**, 27–29.
39. Gelenidze, M.N. (1988) *Welding cycloconverters and inductance-capacitance converters*. Syn. of Thesis for Dr. of Techn. Sci Degree. Kyiv.
40. Dzelnitzki, D. (1997) Modulare Mehrproceß-Stromquellen ermöglichen verschiedene Schweißverfahren. *Maschinenmarkt*, **51**, 24–27.
41. Mecke, H., Fischer, W., Merfert, I. et al. (1998) Kombiniert primär und sekundär getaktete, computergesteuerte Schweißstromquelle mit hoher Dynamik. *Schweißen und Schneiden*, **4**, 224–228.
42. Vereshchago, E.N., Kvasnitsky, V.F., Bibik, V.A. et al. (1999) Inverter multifunctional module for welding arc supply. *Avtomatich. Svarka*, **11**, 29–33.
43. Paton, B.E., Korotynsky, A.E. (1999) Wielozadaniowe urządzenie spawalnicze o przekształcalnej strukturze. *Biuletyn Instytutu Spawalnictwa w Gliwicach*, **5**, 33–35.
44. Kvasov, F.V. (1999) Peculiarities of mechanized welding with a controllable electrode metal transfer. *Svarochn. Proizvodstvo*, **8**, 27–31.
45. Herold, H., Neubert, G., Puder, F. (1994) FUZZY — eine vielversprechende Methode zur Fehlerüberwachung während des Schweißens. *DVS*, **170**, 40–44.
46. Rehfeldt, D., Schmitz, Th. (1995) Fuzzy logic in monitoring of arc welding. In: *Proc. of Int. Conf. on Joining of Materials*, Denmark.
47. Gladkov, E.A. (1996) Problems of prediction of quality and control of weld formation during welding with use of neural network models. *Svarochn. Proizvodstvo*, **10**, 36–41.
48. Fakuda, T., Shibata, T. (1992) Theory and application of neural networks for industrial control system. *IEEE*, **6**, 472–489.
49. (2002) Welding and allied technologies at the Essen Fair. *The Paton Welding J.*, **1**, 27–41.
50. Ivanov, A.M., Gerasimova, A.F. (1991) Molecular electric energy stores on the base of double electric layer. *Elektrichestvo*, **8**, 16–19.
51. Soprunyuk, P.M., Vashchenko, L.E., Korepanov, V.E. et al. *Transformer-free stabilized power source*. USSR author's cert. 1614010, Int. Cl. G 05 F 1/56. Publ. 15.12.90.
52. Korotynsky, A.E. (2001) Functional and test diagnostics of welding equipment. *The Paton Welding J.*, **11**, 36–39.
53. Grebenko, Yu., Shchukin, A. (2001) Radio channel system of state remote monitoring. *Chip News*, **4**, 48–49.
54. Yablokov, D. (2001) Modules of radio channel of «Telecontrolli» Company. *Ibid.*, **5**, 36–37.
55. Kirilenko, V.A. (2001) Leakage current detector. *Ibid.*, **6**, 54–56.